IN MEMORIAM MATRIS

POSITRON ANNIHILATION

THEORY OF POSITRON ANNIHILATION IN SODIUM, ALUMINUM AND ARGON

By

ANTONIO SALVADORI, M.Sc.

A Thesis

Submitted to the Faculty of Graduate Studies

in Partial Fulfilment of the Requirements

for the Degree

Doctor of Philosophy

McMaster University

October 1968

DOCTOR OF PHILOSOPHY (1968) McMASTER UNIVERSITY,

(Physics) Hamilton, Ontario.

TITLE: Theory of Positron Annihilation in Sodium, Aluminum and Argon.

AUTHOR: Antonio Salvadori, B.Sc., M.Sc. (N.U.I.)

SUPERVISOR: Professor J.P. Carbotte

NUMBER OF PAGES: v, 119

SCOPE AND CONTENTS:

This work is concerned with the calculation of the angular correlation curves and the lifetime of positrons annihilating in Sodium, Aluminum and Argon. The Carbotte-Kahana theory is developed using orthogonalized plane waves to represent conduction states. The theory is put in a computational form and techniques, which reduce the computational labour to a manageable level are developed for its practical evaluation. Results are obtained for the electron core contribution in Sodium and Aluminum whilst for Sodium a lattice contribution is also attempted. The core theory is applied to Argon with a limiting approximation and results are obtained in a first order perturbation theory approximation. The calculations are compared to experiment with a satisfactory result.

ACKNOWLEDGEMENTS

I wish to thank my research director, Professor J.P. Carbotte, for his very valuable guidance, encouragement and assistance.

Further I wish to thank Professors S.H. Vosko, D.J. Geldart, S. Tinney and R. Coyle S.J., for introducing me to solid state physics, computing, theoretical physics and mathematics respectively.

Thanks are also expressed to Professor D.J. Kenworthy for assistance in computing; to Professor T.D. Newton for reading and making valuable suggestions in the manuscript; and my wife Mary for her encouragement.

I am deeply indebted to the Dublin County Council, University College Dublin, McMaster University, and the Ontario Government for scholarships without which I would have been unable to reach and complete my graduate studies.

TABLE OF CONTENTS

INTRODUCTION

In 1932 Anderson [1], while studying cosmic rays, experimentally demonstrated the existence of the positron, thus verifying a prediction of Dirac's relativistic quantum theory of the electron. Even before the positron's experimental discovery Dirac[2] had already derived the theoretical transition rate for the process in which an electron and its antiparticle, the positron, disappear simultaneously, their energy being emitted in the form of two γ-rays. This process electron-positron annihilation is now well known.

Beringer and Montgomery[3], using standard counting techniques, were among the first to measure the angular distribution of the emitted γ-rays. Since then many experiments have been performed and the properties of many solids particularly metals[3,4] have been studied. Most of these are described in a recent review by Stewart[4] and also in earlier reviews by Wallace[5] and Ferrel[6].

In a typical experiment a high energy positron from a β^+ decay source, for instance Na^{22}, sandwiched between two thin aluminum foils, penetrates deep into the sample and quickly becomes thermalised[7]. More recently Carbotte and Arora[8] have calculated that at liquid Helium temperatures - but as high as $100^{\circ}K$ for Aluminum - the positron annihilates before

thermalisation. However since all of the experimental results to be considered in this thesis were obtained at room temperature this point does not arise here. After thermalisation the low energy positron migrates through the sample and eventually annihilates with one of the electrons with subsequent emission of two γ-rays. In particular since the thermal energy of the positron (0.025 eV) is very small compared with the Fermi energies of metals (1.6 - 7 eV), it can be assumed that the positron has zero momentum when it annihilates. Each of the emitted γ-rays has an energy of approximately ½ MeV and they emerge in opposite directions from the sample relatively unattenuated and unscattered. This radiation is finally detected and analysed by conventional means.

The experimental analysis of the γ-rays falls into two distinct experiments. The first type of experiment measures the angular distribution of the γ-ray radiation as a function of the angle between the two outgoing γ-rays[9]. These observed distributions are also of two types. In one type the distribution is characterised by a central inverted parabola with a tail at large angles, the parabola displaying a fairly sharp cutoff at an angle corresponding to the Fermi momentum, as illustrated by the alkali metals, the alkaline earths and aluminum. The other type of distribution extends well past the expected Fermi momentum cutoff, exhibiting a Gaussian character as in, for example, the noble metals.

The second type of experiment measures the lifetime of the positron which is proportional to the reciprocal of the total annihilation rate. Total rate experiments make use of delayed coincidence methods and obtain a prompt curve with the sample out and a delayed curve with the sample in place. The mean life τ of the positrons entering the sample generally is identified with the displacement of the centroid from the prompt curve to the delayed curve[10].

From a theoretical standpoint reference 6 gives an excellent summary of the early theories. Naturally the first theory to evolve was a Sommerfeld or free electron theory. This gave a generally good result for the inverted parabola of the angular correlation experiments but failed totally where total rates were involved by a factor of an order of magnitude. The first real step in the right direction was the theoretical analysis of Berko and Plaskett[11]. They assumed an independent particle model (I.P.M.) and computed the positron wave function in Al and Cu in the Wigner-Seitz approximation, using a potential produced by the positive ion and by a uniform charge distribution of the approximate number of valence electrons per atom. The angular correlation result for Al yielded an inverted parabola with small tails in good agreement with experiment. Unfortunately however this agreement was probably accidental as the tails in Al are very small, while in the case of Cu too much of a contribution was obtained from the core electrons. As regards the total rates

these were still wrong by factors of an order of magnitude. The above procedure while simple ignores much of the important correlations and accounts for the direct Coulomb force between the positron and annihilating electron only in an average and trivial way. This attractive force certainly influences significantly the relative motion of the pair in their centre of mass system and must lead to a significant increase of the electronic density at the positron over that computed on the I.P.M. for after all the annihilation rate is directly proportional to the electronic density at the positron site[12]. What is required is the exact solution of the Schrodinger equation for the wavefunction of the pair coupled through their Coulomb field. However since many electrons are present one should more appropriately use a screened Coulomb force. Further because of the existence of an electron sea, all the plane wave states below the Fermi surface are occupied and therefore cannot be employed in building up the electron part of the effective-pair wave-function; hence the Pauli exclusion principle should also be incorporated.

Kahana[13] was the first to realize this. He reasoned that in order to get sensible results the multiple scatterings of the annihilating electron off the positron must be included in the sense of perturbation theory. Kahana did this by solving a Bethe-Goldstone equation for the annihilating pair. Using modern Green's function techniques he summed the ladder diagrams, i.e. the multiple scattering mentioned above, to all orders but left out all other diagrams which enter the theory

in a rather arbitrary way. It is clearly impossible to analyse in detail all the remaining graphs, although Carbotte and Kahana[14] were able to show that, up to second order in the Coulomb potential, such corrections are small and many of the diagrams systematically cancelled. This can be taken as an indication that the ladder graphs represent the dominant contribution to the total rate and should describe quite well the angular correlation experiments. This was indeed found to be so.

As mentioned previously, the total rate R depends only on the electronic density at the positron which is given by the limiting value of the electron-positron pair distribution function $g_{ep}(\underline{X}_e - \underline{X}_p)$ as $\underline{X}_e - \underline{X}_p \to 0$, where $\underline{X}_e$ and $\underline{X}_p$ are the electron and positron coordinates respectively. From a knowledge of $g_{ep}(\underline{X}_e - \underline{X}_p)$ for all values of the relative coordinate $\underline{X}_e - \underline{X}_p$ the total displaced charge about the positron can be computed. To have a consistent theory one must insist that this be exactly one unit. Bergersen[15] pointed out that in the ladder approximation, the total displaced charge can actually be considerably greater than one e.g. 1.25 for sodium. On this basis he argued that Kahana's rates should be reduced by a corresponding amount. This might not necessarily be so because total rates depend only on the value of the pair distribution function for $\underline{X}_e - \underline{X}_p = 0$ whilst on the other hand serious errors in this function for finite $\underline{X}_e - \underline{X}_p$ may be responsible for most of the unphysical accumulation of charge

about the positron. Recently Carbotte[12] has shown quite clearly that in order to make the charge displacement equal to one a summation of certain third and higher order diagrams have to be added to the ladder approximation. This modified ladder approximation however only lowers the total rates by small amounts ranging from 10% in Aluminum to about 3% in Sodium. Hence this thesis will evolve in the spirit of the simple ladder approximation.

Returning to the Kahana-Carbotte theory it should be noted that their calculations considered only the conduction electrons taken in a plane wave approximation. They made two comparisons with experiment. For the angular correlation they obtained an inverted parabola with a slight bulge which fitted the experimental points very well. For the total rate a result lower than the experimental one was obtained but of the right order of magnitude. This was indeed a significant achievement because it pointed out for the first time that the inclusion of correlation effects in the annihilating pair could increase the contribution to the annihilation rate by an order of magnitude. Also it was quite understandable why the results were lower than the experimental ones since no core calculations had been done and also the lattice, which can give rise to Umklapp processes had as yet not been treated. This, of course, is of tantamount importance as has been experimentally shown by Berko[16], since the lattice produces anisotropies in the annihilation rate,

particularly in Lithium and Beryllium.

The next significant step was taken by Carbotte[17]. In his paper he derived a general theory for positron annihilation in metals showing how the Green's function expression for the partial annihilation rate $R(\underline{p})$, i.e. the angular correlation, can be rewritten as the square of a generalized Bethe-Goldstone type amplitude which must, however, first be weighed by an appropriate overlap integral of an electron and a positron single-particle Bloch state. The contribution to $R(\underline{p})$ was written as the square of the sum of two distinct terms. The first is simply the $\underline{p}$th Fourier component of the familiar electron-positron product wave-function i.e. the I.P.M. contribution. The second involves matrix elements which describe virtual transitions of the electrons to unoccupied states with subsequent annihilation. At this point Carbotte purely looked at the core contribution and found that the evaluation of these latter matrix elements was difficult and a complete numerical calculation was not attempted. Instead, a simplified model was studied in the hope of getting some understanding of the physics of the problem.

It is at this point that this thesis begins. Since the theory of Carbotte[17] is crucial to its development the principal results of reference 17 are re-derived in appendices A and B. The thesis consists of three chapters, outlining the three main pieces of work done: core annihilation in metals with specific reference to sodium and aluminum; the effect of

the lattice on the conduction band contribution in sodium; and finally positron annihilation in solid argon.

Each chapter is further subdivided into sections. In chapter one, section one the general theory of annihilation is reduced to a formula describing core annihilation in simple metals. In section two this is further reduced using a single orthogonalized plane wave (O.P.W.) to describe the conduction states and an angular average over the O.P.W. is done due to computational difficulties. The error introduced is computed and discussed in section three. The numerical evaluation for sodium and aluminum follows in section four where the various computational techniques are elaborated on and the natural units are introduced. Finally in section five comparison is made to experiments for the two metals. It is found that significant enhancement factors are obtained with only a weak momentum dependence. Thus except for a multiplicative constant, the results are nearly the same as obtained on the I.P.M. model.

Chapter two begins with a derivation of a theory for conduction electron annihilation with the inclusion of the lattice. The Umklapp processes that are thus picked up are explained. This leads quite naturally to a beautiful geometrical interpretation, which is discussed at length in section two. Section three describes the Monte Carlo and other random processes that were required and used to finally compute the expression derived in section one. Next the computations are

carried out and are followed by a discussion of the results in the final section. Due to the approximations that were necessary in order to make the calculation tractable a quantitative comparison with experiment was not attempted. Qualitatively the results are quite reasonable.

The last chapter deals solely with solid Argon. In a brief introduction the reason why Argon was chosen is given. In section one the state of the theory to the present is discussed. Next the limitations in the application of the simple metal core theory are treated in some detail as these seriously affect the results. However this application is quite reasonable as Argon, an inert gas, has complete electron shells thus resembling the inner core of a metal. An explanation of the details of the calculations follows in section three. Finally the results are computed and comparison is made with experiment. Excellent results are obtained for the angular correlations as well as reasonable agreement for the total rate.

CHAPTER ONE

CORE ANNIHILATION IN SODIUM AND ALUMINUM

A calculation of the core contribution to the angular distribution of the two quantum radiation emitted when a positron and electron annihilate and the total annihilation rate will be performed for the simple metals sodium and aluminum.

The calculation includes electron-positron correlations which are due to the screened Coulomb potential and significantly alter the electronic density about the positron. Further details of these correlations are given in Appendix A. This large density increase is expected on purely physical grounds since correlations appreciably alter the I.P.M. picture. This increase is called the average enhancement factor and for the conduction electrons it was found to be of the order of 10 by Kahana[13] and by Carbotte and Kahana[14].

The large enhancement factor of course is partly due to the fact that conduction electrons are nearly free and hence their motion can easily be disturbed. However the core electrons are not so free since their motion is dominated by the screened nuclear field of their respective ions and hence the positron Coulomb field, in the core case, represents a much weaker disturbance or perturbation. From this it follows

that smaller, but significant, enhancement factors should result for the core case.

The general mathematical expression for annihilation, (A-49) is next rewritten bearing core annihilation directly in mind i.e.

$$R^{n\ell ms}_{\underline{s}}(\underline{p}) = \frac{\lambda}{V} \left| I_{\underline{m}',o}(\underline{p}) + \sum_{\underline{m},\underline{n}} I_{\underline{m},\underline{n}}(\underline{p})\, \chi^{o}_{\underline{m},\underline{n};\underline{m}',o}(E^{p}_{o} + E^{e}_{\underline{m}'}) \right|^{2} . \qquad (1)$$

The various symbols have the same meaning as given them in the appendix, except that now $R^{n\ell ms}_{\underline{s}}(\underline{p})$ gives the contribution to the partial rate $R(\underline{p})$ arising from a core electron in the state $(n,\ell,m,\underline{s})$ where the $n\ell$ index refers to the core band, m is the magnetic quantum number, and $\underline{s}$ is the crystal momentum restricted to the first Brillouin zone. The $\underline{m}'$ in equation (1) refers to all the occupied core states. Hence the first term in the square, being a simple transform of the overlap between a core wavefunction and the positron wavefunction gives the I.P.M. result of Berko and Plaskett[11]. The summations over $\underline{m}$ and $\underline{n}$ are for unoccupied states of the electron and positron respectively. For the electrons these would mean all the states above the Fermi sea and for the positron any state with non-zero momentum.

Before discussing the second term of the square further, a simplification due to Carbotte[17] can be carried out. This simplification replaces all conduction-conduction overlap

integrals by delta functions i.e. it treats all such conduction states as plane waves. This no doubt is a good approximation in simple metals where the conduction states are not complex and have little or no band structure. However for elements such as Argon where conduction states are not so simple this approximation is not valid. Further detailed explanation is given in Appendix B.

As explained in Appendix B expression (1) is rewritten as

$$R^{(n\ell m\underline{s})}(\underline{p}) = \frac{\lambda}{V} \left| I_{n\ell m\underline{s}}(\underline{p}) + \frac{1}{V} \sum_{\underline{k}} E_{\underline{p}}^{n\ell}(\underline{k}) [\underline{k}|\underline{p}-\underline{k}|n\ell m\underline{s}]^{e} \right|^2 \qquad (2)$$

where once more all the symbols have the same meaning as defined in the appendices. Now it can be clearly seen that the second term is proportional to the overlap between a single particle core state and an unoccupied conduction state. From a physical point of view this matrix element represents virtual transitions from a core state to an unoccupied state above the Fermi surface with subsequent annihilation. These transitions are due to the excitation by the positron force which is contained in the enhancement factor $E_{\underline{p}}^{n\ell}(\underline{k})$. This factor further includes (cf B-16) the Pauli exclusion principle term $P^{+}_{\underline{k},\underline{p}-\underline{k}}$ which only allows scattering into the unoccupied states and a term $\chi_{\underline{p}}(\underline{k};-\Delta_{n\ell})$ which describes all the further multiple scatterings contained in the ladder

approximation.

The most difficult part in the evaluation of (2) is the calculation of the core-conduction matrix element since as figure 1 shows the core functions are largest where conduction states are smallest and vice cersa.

For the core functions the tight binding sum

$$\Psi_{n\ell m\underline{s}}(\underline{x}) = \frac{1}{\sqrt{N}} \sum_{\underline{a}} e^{i\underline{s}.\underline{a}}\, u_{n\ell m}(\underline{x}-\underline{a}) \tag{3}$$

is used where N is the number of primitive cells in the crystal and the $\underline{a}$'s are vectors giving the various lattice sites. The atomic wavefunction $u_{n\ell m}(\underline{x})$ centred about $\underline{x} = 0$ is given by

$$u_{n\ell m}(\underline{x}) = (P_{n\ell}(x)/x)\; Y_{\ell m}(\Omega_{\underline{x}}) \tag{4}$$

where $Y_{\ell m}(\Omega_{\underline{x}})$ is the $(\ell m)^{th}$ spherical harmonic, referred for the present to some general coordinate system by the angle $\Omega_{\underline{x}}$ and $P_{n\ell}(x)/x$ is the radial part of the core wavefunction. In particular for the computations the $P_{n\ell}(x)$ were taken from the Hartree-Fock-Slater calculations of Taylor[19] for sodium and aluminum and are given in table 1.

The substitution of the tight binding sum (3) into (2) gives

$$R^{n\ell m\underline{s}}(\underline{p}) = \frac{\lambda}{V} \left| \sqrt{\frac{N}{V}}\, \delta_{\underline{s}-\underline{p},\underline{a}} \int d^3\underline{x}\; u_{n\ell m}(\underline{x})\; e^{-i\underline{p}.\underline{x}} \right.$$
$$\left. \{v_o(x) + \frac{1}{V} \sum_{\underline{k}} E^{n\ell}_{\underline{p}}(\underline{k})\; u^*_{\underline{k}}(\underline{x})\} \right|^2 \tag{5}$$

where $\underline{a}$ is a reciprocal lattice vector; the positron wave-

function is given by

$$\Phi_o(x) = \frac{1}{\sqrt{V}} v_o(x) \tag{6}$$

and the electron wavefunction by

$$\Psi_{\underline{k}}(\underline{x}) = \frac{1}{\sqrt{V}} e^{i\underline{k}\cdot\underline{x}} u_{\underline{k}}(\underline{x}) \ . \tag{7}$$

Summing all the core electrons in the $(n\ell)$ band and denoting the contribution to the partial annihilation rate by $R^{n\ell}(\underline{p})$ yields

$$R^{n\ell}(\underline{p}) = \sum_{m=-\ell}^{+\ell} R^{n\ell m s}_{-}(\underline{p})$$

$$= \frac{\lambda}{V} \frac{1}{\Omega_o} \sum_{m=-\ell}^{+\ell} \left| \int d^3\underline{x}\, u_{n\ell m}(\underline{x})\, e^{-i\underline{p}\cdot\underline{x}} \right.$$

$$\left. \{v_o(x) + \frac{1}{V} \sum_{\underline{k}} E^{n\ell}_{\underline{p}}(\underline{k})\, u^*_{\underline{k}}(\underline{x})\} \right|^2 \tag{8}$$

where Ω_o is the volume of a primitive lattice cell.

$R(\underline{p})$ ON A ONE O.P.W. MODEL

In order to evaluate the expression

$$\frac{1}{V} \sum_{\underline{k}} E^{n\ell}_{\underline{p}}(\underline{k})\, u^*_{\underline{k}}(\underline{x})$$

a knowledge of the conduction and excited states of the electrons is needed. For sodium and aluminum a single O.P.W. has been shown to be a reasonable description of these Bloch

states[21]. The O.P.W. basically is the distortion of plane waves so as to make them orthogonal to all core wavefunctions in order to try to give the electron wavefunctions their ideal behaviour i.e. far from the core they should look like plane waves and near the core they should behave like core wavefunctions but be orthogonal to them. They can be written as

$$\chi_{\underline{k}} = \frac{A(k)}{\sqrt{V}} \left[e^{i\underline{k}.\underline{x}} - \sum_{n,\ell,m} A_{n,\ell,m}(\underline{k}) \, \Psi_{n\ell m;\underline{k}}(\underline{x}) \right] \qquad (9)$$

where A(k) is the normalization coefficient obtained in the usual manner i.e.

$$< \chi_{\underline{k}} \mid \chi_{\underline{k}} > = 1 \qquad (10)$$

The orthogonalization coefficients, $A_{n,\ell,m}(\underline{k})$, as their name implies are obtained by orthogonalizing (9) to the core states i.e.

$$< \Psi_{n\ell m;\underline{k}} \mid \chi_{\underline{k}'} > = 0 \quad . \qquad (11)$$

On performing the integration[21] it is found that

$$A_{n,\ell,m}(\underline{k}) = \int d^3\underline{x} \; u^*_{n\ell m}(\underline{x}) \; e^{i\underline{k}.\underline{x}} \quad . \qquad (12)$$

Equation (12) can be further reduced by making use of the well known expansion

$$e^{i\underline{k}\cdot\underline{x}} = \sum_{\ell m} 4\pi i^{\ell}\, Y^*_{\ell m}(\Omega_{\underline{k}})\, Y_{\ell m}(\Omega_{\underline{x}})\, j_{\ell}(kx) \qquad (13)$$

where the spherical harmonics $Y_{\ell m}$ are referred to the same general coordinate system as that used in writing the core wavefunctions $u_{n\ell m}(\underline{x})$. The substitution of equation (13) into (12) yields

$$A_{n,\ell,m}(\underline{k}) = \int d^3\underline{x} \sum_{\ell' m'} P_{n\ell}(x)\, Y^*_{\ell m}(\Omega_{\underline{x}})\, 4\pi i^{\ell}$$

$$Y^*_{\ell' m'}(\Omega_{\underline{k}})\, Y_{\ell m}(\Omega_{\underline{x}})\, j_{\ell}(kx)/x \,. \qquad (14)$$

Using the fact that

$$\int Y^*_{\ell' m'}(\Omega)\, Y_{\ell m}(\Omega)\, d\Omega = \delta_{\ell\ell'}\, \delta_{mm'} \qquad (15)$$

equation (14) becomes

$$A_{n,\ell,m}(\underline{k}) = 4\pi i^{\ell} \int_0^{\infty} dx\, x P_{n\ell}(x)\, j_{\ell}(kx)\, Y^*_{\ell m}(\Omega_{\underline{k}}) \,. \qquad (16)$$

Introducing

$$A_{n\ell}(k) = \int dx\, x\, j_{\ell}(kx)\, P_{n\ell}(x) \qquad (17)$$

equation (16) can be re-written as

$$A_{n,\ell,m}(\underline{k}) = 4\pi i^{\ell}\, Y^*_{\ell m}(\underline{k})\, A_{n\ell}(k) \,. \qquad (18)$$

It should be noted quite clearly that, unlike other authors, the orthogonalization coefficients are dependent on the angles of $\underline{k}$. This fact is of some importance and cannot be avoided here. Using these results (10) can easily be evaluated in terms of (17) to give

$$A(k) = [1 - \frac{1}{\Omega_o} \sum_{n,\ell} 4\pi(2\ell+1) \mid A_{n\ell}(k) \mid^2]^{-\frac{1}{2}} \quad . \qquad (19)$$

These coefficients are easily computed using a Simpson's rule, with a Hermann Skillmann type mesh, to perform the integrals[22]. The $A_{n\ell}(k)$, which characterise the behaviour of the O.P.W., and the normalisation coefficient A(k) are plotted in figures 2 and 3 for sodium and aluminum respectively. Results are only shown for $k \geq k_F$ since the electrons can only be excited into this region, due to the Pauli exclusion principle.

Removing the exponential and $\sqrt{V}$ factors in equation (9) the $u_{\underline{k}}(\underline{x})$ part of the O.P.W. is written as

$$u_{\underline{k}}(\underline{x}) = A(k)[1-4\pi \sum_{\underline{a}} \sum_{n\ell m} i^{\ell} e^{-i\underline{k}.(\underline{x}-\underline{a})} Y^*_{\ell m}(\Omega_{\underline{k}}) A_{n\ell}(k) u_{n\ell m}(\underline{x}-\underline{a})] \quad . \qquad (20)$$

In equation (20) the $u_{n\ell m}(\underline{x})$ are of very limited range, i.e. they are well localized functions in the Wigner-Seitz cell,

and hence the assumption of retaining only the first term in the $\underline{a}$ summation can be made. Thus

$$u_{\underline{k}}(\underline{x}) = A(k)\left[1 - 4\pi \sum_{n,\ell,m} i^{\ell} e^{-i\underline{k}\cdot\underline{x}} Y^*_{\ell m}(\Omega_{\underline{k}}) A_{n\ell}(k)\, u_{n\ell m}(\underline{x})\right] . \qquad (21)$$

The correlation term of expression (8) can now be further reduced using (21) i.e.

$$\frac{1}{V}\sum_{\underline{k}} E^{n\ell}_{\underline{p}}(\underline{k})\, u^*_{k}(\underline{x}) = \frac{1}{V}\sum_{\underline{k}} E^{n\ell}_{\underline{p}}(\underline{k})\, A(k) \left[1 - 4\pi \sum_{n,\ell,m} (-i)^{\ell} e^{i\underline{k}\cdot\underline{x}} Y_{\ell m}(\Omega_{\underline{k}})\, A^*_{n\ell}(k)\, u^*_{n\ell m}(\underline{x})\right]. \qquad (22)$$

This expression as it stands cannot be put in a readily computable form but the difficulty can however be simply overcome by noting that the enhancement factor $E^{n\ell}_{\underline{p}}(\underline{k})$ is not expected to be strongly dependent on the direction of $\underline{k}$. Hence an angular average over $\underline{k}$ suggests itself and this greatly simplifies the orthogonalization part. However its effect on the calculation should be considered as indeed it will in a later section.

Performing this angular average over $\underline{k}$, equation (22) becomes

$$\frac{1}{V}\sum_{\underline{k}} E_{\underline{p}}^{n\ell}(\underline{k})\, u^*_{\underline{k}}(\underline{x}) = \frac{1}{V}\sum_{\underline{k}} \bar{E}_{\underline{p}}^{n\ell}(\underline{k})\, A(k)$$

$$\left[1 - 4\pi \sum_{n,\ell,m} (-i)^{\ell} \int d\Omega_{\underline{k}}\, e^{i\underline{k}\cdot\underline{x}}\, Y_{\ell m}(\Omega_{\underline{k}})\, A^*_{n\ell}(k)\right.$$

$$\left. u^*_{n\ell m}(\underline{x})\right] \qquad (23)$$

where

$$\bar{E}_{\underline{p}}^{n\ell}(\underline{k}) = \int \frac{d\Omega_k}{4\pi} E_{\underline{p}}^{n\ell}(\underline{k}) \quad .$$

By defining

$$G(k;x) = x - 4\pi x \sum_{n,\ell,m} (-i)^{\ell} \int d\Omega_{\underline{k}}\, e^{i\underline{k}\cdot\underline{x}}\, Y_{\ell m}(\Omega_{\underline{k}})$$

$$A^*_{n\ell}(k)\, u^*_{n\ell m}(\underline{x}) \qquad (24)$$

equation (23) can be written as

$$\frac{1}{V}\sum_{\underline{k}} \bar{E}_{\underline{p}}^{n\ell}(\underline{k})\, u^*_{\underline{k}}(\underline{x}) = \frac{1}{V}\sum_{\underline{k}} \bar{E}_{\underline{p}}^{n\ell}(\underline{k})\, A(k)\, G(k;x)/x \quad . \qquad (25)$$

Expression (24) can be further reduced by employing the aid of equation (13) to give

$$G(k;x) = x - 4\pi x \sum_{n,\ell,m} (-i)^{\ell} \int d\Omega_{\underline{k}} \sum_{\ell'm'} 4\pi i^{\ell'} Y^*_{\ell'm'}(\Omega_{\underline{k}})$$

$$Y_{\ell'm'}(\Omega_{\underline{x}})\ j_{\ell}(kx)\ Y_{\ell m}(\Omega_{\underline{k}})\ A^*_{n\ell}(k)\ u^*_{n\ell m}(\underline{x}) \qquad (26)$$

Using (15), equation (26) reduces to

$$G(k;x) = x - 4\pi x \sum_{n,\ell,m} 4\pi\ Y_{\ell m}(\Omega_{\underline{x}})\ j_{\ell}(kx)\ A^*_{n\ell}(k)\ u_{n\ell m}(\underline{x}). \qquad (27)$$

Writing the $u_{n\ell m}(\underline{x})$ out explicitly and using the fact that

$$\sum_{m=-\ell}^{+\ell} Y^*_{\ell m}(\Omega_{\underline{k}})\ Y_{\ell m}(\Omega_{\underline{k}}) = \frac{2\ell + 1}{4\pi} \qquad (28)$$

equation (27) becomes

$$G(k;x) = x - 4\pi \sum_{n,\ell} (2\ell + 1)\ j_{\ell}(kr)\ A^*_{n\ell}(k)\ P_{n\ell}(x) \qquad (29)$$

which can readily be evaluated.

Substituting (25) into (8) and again using the explicit form of $u_{n\ell m}(\underline{x})$ yields

$$R^{n\ell}(\underline{p}) = \frac{\lambda}{V}\frac{1}{\Omega^o} \sum_{m=-\ell}^{+\ell} \Big| \int d^3\underline{x}\ P_{n\ell}(x)/x\ Y_{\ell m}(\Omega_{\underline{x}})\ e^{-i\underline{p}.\underline{x}}$$

$$[v_o(\underline{x}) + \frac{1}{V}\sum_{\underline{k}} \bar{E}^{n\ell}_{\underline{p}}(\underline{k})\ A(k)\ G(k;x)/x]\Big|^2 \ . \qquad (30)$$

The function $v_o(\underline{x})$ is the positron Bloch state at the bottom of the 1s band and is needed only in the Wigner-Seitz sphere about $\underline{R}_\nu = 0$. Hence it can be taken to be spherically symmetric and written as $R^+(x)/x$. Next an expansion of the exponential can be performed using (13) i.e.

$$R^{n\ell}(\underline{p}) = \frac{\lambda}{V}\frac{1}{\Omega^o}\sum_{m=-\ell}^{+\ell}\Big|\int d^3\underline{x}\, P_{n\ell}(x)/x\, Y_{\ell m}(\Omega_{\underline{x}})$$

$$\sum_{\ell' m'}(-i)^{\ell'} 4\pi\, Y_{\ell' m'}(\Omega_{\underline{p}})\, Y^*_{\ell' m'}(\Omega_{\underline{x}})\, j_{\ell}(px)$$

$$[R^+(x)/x + \frac{1}{V}\sum_{\underline{k}} \bar{E}^{n\ell}_{\underline{p}}(\underline{k})\, A(k)\, G\,(k;x)/x]\Big|^2 \quad . \quad (31)$$

Since the only $\underline{x}$ angular dependence is contained in the spherical harmonics the angular integration $d\Omega_{\underline{x}}$ can simply be done with the use of (15) to give

$$R^{n\ell}(\underline{p}) = \frac{\lambda}{V}\frac{1}{\Omega^o}\sum_{m=-\ell}^{+\ell}\Big|\, 4\pi\,(-i)^{\ell}\, Y_{\ell m}\,(\Omega_{\underline{p}})$$

$$\int_o^\infty dx\, j_{\ell}\,(px)\, P_{n\ell}\,(x)\,[R^+(x) +$$

$$\frac{1}{V}\sum_{\underline{k}} \bar{E}^{n\ell}_{p}\,(\underline{k})\, A(k)\, G\,(k;x)]\Big|^2 \qquad (32)$$

which can be simplified to

$$R^{n\ell}(\underline{p}) = \frac{\lambda}{V}\frac{1}{\Omega^o}\, 2(2\ell+1)\, 4\pi \left| \int_o^\infty dx\, j_\ell\,(px)\, P_{n\ell}(x)\right.$$

$$\left.[R^+(x) + \frac{1}{V}\sum_{\underline{k}} \bar{E}^{n\ell}_{\underline{p}}(\underline{k})\, A(k)\, G\,(k;x)]\right|^2 \qquad (33)$$

where use was made of the sum rule (28) and the factor 2 was introduced for spin degeneracy in the core levels.

AN ESTIMATION OF THE ERROR IN $\bar{E}^{n\ell}_{\underline{p}}(\underline{k})$

In making the spherical assumption in equation (23) i.e. using $\bar{E}^{n\ell}_{\underline{p}}(\underline{k})$ instead of $E^{n\ell}_{\underline{p}}(\underline{k})$, it should be noted that all the error arises in the orthogonalization part and not in the plane wave part. To estimate this error the two expressions

$$E^{n\ell}_{\underline{p}}(\underline{k}) = \frac{\chi_{\underline{p}}\,(\underline{k};-\Delta_{n\ell})\; U_s\;(\underline{p}-\underline{k})\;\theta_e^{u.o.}\;(\underline{k})}{(\underline{p}-\underline{k})^2 + k^2 + \Delta_{n\ell}} \qquad (34)$$

and

$$\bar{E}^{n\ell}_{\underline{p}}(\underline{k}) = \int \frac{d\Omega_{\underline{k}}}{4\pi}\, \frac{\chi_{\underline{p}}(\underline{k};-\Delta_{n\ell})\; U_s\;(\underline{p}-\underline{k})\;\theta_e^{u.o.}\;(\underline{k})}{(\underline{p}-\underline{k})^2 + k^2 + \Delta_{n\ell}} \qquad (35)$$

have to be computed for several random values of $\underline{p}$ and $\underline{k}$,

where $|\underline{p}| < 3p_F$ and $|\underline{k}| \geq p_F$.

As it stands however expression (35) cannot be computed as the dependence of $\chi_{\underline{p}}^{n\ell}(\underline{k};-\Delta_{n\ell})$ on the vectors $\underline{p}$ and $\underline{k}$ complicates matters considerably. However since only a rough estimate of the error is required, the function $\chi_{\underline{p}}^{n\ell}(\underline{k};-\Delta_{n\ell})$ will be restricted to depend only on $|\underline{k}|$ and $|\underline{p}|$. It might be pointed out that this assumption renders equation (B11) i.e.

$$\chi_{\underline{p}}^{n\ell}(\underline{k}) = 1 + \int \frac{d^3\underline{k}'}{(2\pi)^3}\,\theta(k' - k_F)\,\frac{U_s\,(\underline{k} - \underline{k}')}{k'^2+(\underline{p}-\underline{k}')^2+\Delta_{n\ell}}\,\chi_{\underline{p}}^{n\ell}(\underline{k}') \qquad (36)$$

inconsistent. However this inconsistency can be overcome by averaging the integrand over $\underline{p}$ or over $\underline{k}$. Both results yield the same answer which shows consistency.

Making this assumption it is immediately obvious that for $\underline{p} = 0$ the spherical approximation is perfectly correct as expression (35) then depends only on the magnitude of the vector $\underline{k}$. For other $\underline{k}$ and $\underline{p}$ it is not a trivial comparison but the integral can be easily done numerically and a comparison made with the true value of $E_{\underline{p}}^{n\ell}(\underline{k})$. The integral was done using a Simpson's rule on the IBM 360/30 computer of the University of Guelph.

The results show that as $\underline{p}$ increases from zero the error in the spherical approximation increases from zero to

20% at $|\underline{p}| = 3$. This increase in error is uniform and is approximately 8% at $|\underline{p}| = 1$ and 15% at $|\underline{p}| = 2$. One result that is of importance however is that in the computations $E_{\underline{p}}^{n\ell}(\underline{k})$ always came out to be greater than $\bar{E}_{\underline{p}}^{n\ell}(\underline{k})$. This means that the angular average does not subtract a sufficient amount from the right hand side of equation (23) and thus leads to too great a contribution in equation (33). The 20% factor however cannot be simply extrapolated to estimate the error due to this angular average in (33) since in order to obtain the final form (33) many averages are taken. This points to the fact that the final result should be too great as indeed is found to be the case.

NUMERICAL EVALUATION

The averaging over the angles of $\underline{k}$ in the enhancement factor was done by taking the $\underline{p}$ direction as the polar axis. This in no way restricts the argument as this $\underline{p}$ direction could be chosen in any general way. Substituting the enhancement i.e.

$$\int d\Omega_{\underline{k}}\, E_{\underline{p}}^{n\ell}(\underline{k}) = 2\pi\theta(k-k_F)\chi_p^{n\ell}(k)\int_{|\underline{p}-\underline{k}|}^{p+k} \frac{z\,dz}{k^2+z^2+\Delta_{n\ell}} \frac{U_s(z)}{pk} \qquad (36)$$

into equation (33) and taking the limit of infinite volume

gives

$$R^{n\ell}(\underline{p}) = \frac{\lambda}{V}\frac{4\pi}{\Omega^o} 2(2\ell+1)\Big| \int_o^\infty dx\, j_\ell(px)\, P_{n\ell}(x)\, [R^+(x)$$

$$+ \int_{k_F}^\infty \frac{k^2 dk}{(2\pi)^3}\, \chi_p^{n\ell}(k)\, A(k)\, G(k;x)$$

$$\int_{|\underline{p}-\underline{k}|}^{p+k} \frac{2\pi\, z dz}{k^2+z^2+\Delta_{n\ell}} \frac{U_s(z)}{pk} \Big]\Big|^2 \quad . \tag{37}$$

To streamline this equation a function $S^{n\ell}(p,x)$ is introduced defined by

$$S^{n\ell}(p,r) = \int_{k_F}^\infty \frac{k^2\, dk}{(2\pi)^3}\, \chi_p^{n\ell}(k)\, A(k)\, G(k;x)$$

$$\int_{|\underline{p}-\underline{k}|}^{p+k} \frac{2\pi\, z dz}{k^2+z^2+\Delta_{n\ell}} \frac{U_s(z)}{pk} \tag{38}$$

and thus (37) becomes

$$R^{n\ell}(\underline{p}) = 2(2\ell+1)\, \frac{4\pi}{V}\frac{R^o}{Z} \Big| \int_o^\infty dx\, j_\ell(px)\, P_{n\ell}(x) [R^+(x)+S^{n\ell}(p,x)]\Big|^2 \tag{39}$$

where Z is the valence of the element under consideration, and R^o, the Sommerfeld annihilation rate given by $R^o = \lambda Z/\Omega^o$. A transformation to Fermi momentum units $\underline{\gamma} = \underline{p}/p_F$ is made, since these units are the natural units of the system. Thus

equation (39) becomes

$$R^{n\ell}(\gamma p_F) = 2(2\ell + 1)\,\frac{4\pi}{V}\,\frac{R^o}{Z}\,\Big|\int_o^\infty dr\; j_\ell\,(\gamma p_F r)\; P_{n\ell}(r)$$

$$[R^+(r) + S^{n\ell}\,(\gamma,r)]\Big|^2 \qquad (40)$$

where $S^{n\ell}(\gamma,r)$ is now defined as

$$S^{n\ell}(\gamma,r) = \int_1^\infty \frac{k\,dk}{\gamma}\,\chi_1^{n\ell}\,(\gamma,k)\;A\;(kk_F)\;G\;(kk_F,r)$$

$$\int_{k-\gamma}^{k+\gamma} \frac{2\pi\; z\,dz\;\; \alpha U(z)}{k^2 + z^2 + \Delta^{n\ell}} \qquad (41)$$

where $\Delta^{n\ell} = \Delta_{n\ell}/p_F^2$ (23)

$$\alpha \;\; = r_s/(1.919\pi^2)$$

with r_s the usual electron gas density parameter and the potential function

$$U(z) = [z^2 + 2\pi\alpha\,\{1 - \frac{1}{2z}(1 - \tfrac{1}{4}z^2)\,\ell n(\frac{z-2}{z+2})^2\}\,]^{-1} \quad . \qquad (42)$$

The integral equation satisfied by $\chi_1^{n\ell}(\gamma,k) \equiv \chi^{n\ell}(p_F\gamma,p_Fk)$ is, doing the $\Omega_{\underline{k}}$ integration in (35)

$$\chi_1^{n\ell}(\gamma,k) = 1 + \int_1^{\infty} \frac{dk_1}{2\gamma k} K_\gamma^{n\ell}(k,k_1)\ \chi_1^{n\ell}(\gamma,k_1) \qquad (43)$$

with the kernel given by

$$K_\gamma^{n\ell}(k,k_1) = \int_{|k-k_1|}^{k+k_1} zdz\ \alpha U(z)\pi\ell n\left[\frac{k_1^2+(\gamma+k_1)^2+\Delta^{n\ell}}{k_1^2+(\gamma-k_1)^2+\Delta^{n\ell}}\right] . \qquad (44)$$

This ends the algebraic development and next the results of the computations are discussed for the sample metal sodium which, as is well known, is one of the simplest metals. Equation (43) can easily be solved for $\chi_1^{n\ell}(\gamma,k)$ by turning it into a set of linear equations and solving for these by a standard method e.g. the Gauss pivotal technique. This was done using a 41 point mesh with linear interpolation for large k values. The results for the 2p and 2s core electrons with four values of γ are shown in figure 4.

The 1s core state was never computed since its contribution is negligible due to the fact that the energy parameter $\Delta^{n\ell}$ appearing in the denominators is very large. This is also the reason why the 2p contribution for a given γ as a function of k is always greater than the corresponding 2s contribution. As expected from equations (43) and (44) for large k values $\chi_1^{n\ell}(\gamma,k)$ tends to one, hence it might be stressed once more that in this asymptotic region the $\underline{k}$ angular dependance would certainly play little or no role.

The complex structure of $G(kk_F,x)$ is shown in figure 5, where it is plotted as a function of x for various characteristic

values of k. The first value plotted, namely k = 0, was not used but served as a check on the calculations. The comparison was made with Callaway's[24] result since at the bottom of the 3s band the O.P.W. almost reduces to the Wigner Seitz wavefunction which Callaway quotes. The graphs in figure 5 also bring out the physical characteristics of the G function. As can be seen the oscillations get weaker and weaker as both r and k increase and especially for large r the graphs become a straight line with slope one. This can be interpreted physically by noting that in (29) as r and k increase the orthogonalization coefficients play less and less of a role till finally the plane wave part completely takes over and the function G becomes independent of any k dependence. Further figure 5 brings out the limitations of the model discussed in reference 17. It can be seen that the difference between $G(kk_F,x)$ at k = 0 and k = 2.5 is not great and hence if the only transitions of importance in (41) were those about the Fermi surface, i.e., k = 1 the model of reference 17 would be recovered. This results because it would then be justified to fix $G(kk_F,x)$ in (41) at $G(k_F,x)$ and take it outside of the integration. But $G(k_F,x)$ is nearly equal to $G(o,x)$ which in turn reduces to the Callaway wavefunction $R_o(x)$ [24] so that

$$S^{n\ell}(\gamma,x) \simeq R_o(x) \quad m^{n\ell}(\gamma) \tag{43}$$

with

$$m^{n\ell}(\gamma) = \int_1^{\infty} \frac{kdk}{\gamma} \chi_1^{n\ell}(\gamma,k) \int_{|k-\gamma|}^{k+\gamma} \frac{2\pi\ zdz\ \alpha U(z)}{k^2 + z^2 + \Delta^{n\ell}} \tag{44}$$

where $m^{n\ell}(\gamma)$ is essentially the same quantity as that plotted in figure 5 of reference 17. This procedure is not justified since as was pointed out the amplitude $\chi_1^{n\ell}(\gamma,k)$ does not have a strong k variation. Further the quantity

$$k \int_{|k-\gamma|}^{k+\gamma} \frac{2\pi\ zdz\ \alpha U(z)}{k^2 + z^2 + \Delta^{n\ell}} \tag{45}$$

is not a rapidly damping function about the Fermi surface. This means that $G(kk_F,x)$ for many values of k gets averaged in the expression for $S^{n\ell}(\gamma,x)$. Since for large k's the $G(kk_F,x)$ are nearly straight lines the oscillation at $x \simeq .5$ atomic units occurring in $G(kk_F,x)$ for k around 1. will clearly be considerably smoothed out in $S^{n\ell}(\gamma,x)$ [25] and indeed this is precisely what figures 6 and 7 show. Figure 6 simply shows the S^{2p}, S^{2s} curves for $\gamma = 0$ whilst figure 7 shows the development of S^{2p} as γ increases and it can be clearly seen that the oscillations die out. Thus with all of this smoothing the correlation part of the partial rate tends more and more to have a similar γ dependence as the I.P.M.

In order to bring out this very important point the functions J^+ and J^- of reference 17 are plotted in figure 8 and 9. They are

$$J^+_{n\ell}(\gamma) = \int_0^{\infty} j_\ell(\gamma p_F x)\ P_{n\ell}(x)\ R^+(x)\ dx \tag{46}$$

and

$$J^{-}_{n\ell}(\gamma) = \int_0^\infty j_\ell\ (\gamma p_F x)\ P_{n\ell}(x)\ S^{n\ell}\ (\gamma,x)\ dx \qquad (47)$$

where

$$R^{n\ell}(\gamma p_F) = 2(2\ell + 1)\ \frac{4\pi}{V}\ \frac{R^o}{Z}\ |\ J^{+}_{n\ell}(\gamma) + J^{-}_{n\ell}(\gamma)\ |^2. \qquad (48)$$

The similarity between (46) and (47) is clearly seen and so the neglect of the correlation term (47) would lead to incorrect rates. However it should be stressed that whilst the rate would be out by a factor of approximately 4 the general shape of the correlation curves would be unaltered by considering (46) only.

Finally since the computations involved were rather lengthy it was fortunate to have been able to put a simple check on them. For arbitrary k and in the region of x around the Wigner Seitz cell edge the functions $G(kp_F,x)$ behave very nearly like a straight line of slope 1. Hence in this region $S^{n\ell}(\gamma,x)$ should go like a straight line of slope $m^{n\ell}(\gamma)$ provided the O.P.W. normalization factor $A(kk_F)$ is set equal to one. This can be verified with the help of figure 7 and the value of $m^{n\ell}(\gamma)$ given in reference 17.

DISCUSSION AND CONCLUSION

In ordinary two slit annihilation experiments the

quantity that is measured is $R(\gamma_z)$, where γ_z is a direction defined by the geometry of the apparatus. The quantity calculated in this chapter is $R^c(\gamma_z)$ given by

$$R^c(\gamma_z) = \sum_{n,\ell} \int d\gamma_x \, d\gamma_y \, R^{n\ell}(\gamma p_F) \, p_F \qquad (49)$$

where $R^c(\gamma_z)$ stands for the core contribution. A direct experimental comparison cannot be made for this expression since experimental procedures do not differentiate between core contributions and other contributions. However the quantity $R^c(\gamma_z)$ can be added to the conduction electron contribution as given in reference 14 and satisfactory comparison with experiment can then be made.

In (49) the sum over all core electrons was performed, the units being such that the counting rate $R^c(\gamma_z)$ integrated over γ_z gives the total rate. This quantity as well as the I.P.M. result is plotted in figure 10 for both sodium and aluminum. The close correlation between the full curve and the I.P.M. result is now obvious. For sodium it is approximately a factor of 4 while for aluminum it is a factor of 3 with somewhat more of a variation. These same factors occur in the total rate i.e. the area under the curves in figure 10. The Berko-Plaskett result is 0.97 R^o and 0.49 R^o while this result is 3.5 R^o and 1.4 R^o for sodium and aluminum respectively. It should be noted however that all elements do not have the same enhancement factor and hence in general the I.P.M. could not be

simply multiplied by a factor to give an approximately correct result. If the complete numerical calculations are either too involved or too bothersome to be done, for after all experimentalists are not too interested in doing lengthy calculations, a method of choosing the correct enhancement factor would be to take the best one that fits the lifetime and correlation curves correctly. In fact this has been attempted by Berko and Terrell[26] for certain ferromagnetic metals in the transition series but discrepancies arise. In particular, they conclude that such a procedure overestimates the high momentum tails. The experiments favour momentum dependent enhancement factors decreasing with increasing angle. These present calculations show no evidence of such a tendency, at least in region 0 to $3p_F$. However ferromagnetic materials are not as simple to deal with as sodium and aluminum and thus the theory developed in this chapter cannot be readily applied. The lack of momentum dependence could be due to several causes. The first of course is the angular average approximation made. The region lying between zero and large p is where it is weakest but a more accurate calculation seems to be too difficult. Secondly positron self-energy corrections have been neglected. Woll and Rose[27] have pointed out that these could play a significant role; however without a proper systematic treatment of other diagrams no prediction could be made in this respect. Further it is felt that the experimental tails might not be of a high

accuracy. For low momenta the experimental counts are of the order of 2×10^4, while for the tails they are of the order of 10^2, which would lead to less accuracy in this region i.e. a greater statistical variance. Doppler broadening experiments would test the theory much more rigorously and would yield more accurate experimental tails[28].

In figure 11 a least square fit[29] of R(p) to the experimental data of Kim and Stewart[30] in sodium is presented. Only half the angular correlation curve is shown although the data from both sides of the distribution was used in the comparison. The general agreement is good; however in the tails there is still some discrepancy. For regions beyond $3p_F$ it seems that the theory is as yet limited but, for the discrepancy between p_F and $2p_F$ it should be remembered that lattice effects in the conduction bands have as yet to be treated. These will constitute the topic for chapter 2.

For the lifetime of the positron, which is equal to the reciprocal of the total rate, excellent agreement has been obtained with the experimental work of Berko and Weisberg[31]. Their result is 2.94×10^9 sec^{-1}, while this work gives 3.0×10^9 sec^{-1}.

A better result holds for aluminum in the angular correlation curves as shown in figure 12, where the theoretical data is compared to the experimental work of Kusmiss and Stewart[32]. In particular in the tails the data remains above the computed curve. Part of this discrepancy is certainly

due to lattice effects but the curve on the whole shows that the angular correlation data can at least be qualitatively understood. However in comparison to the Aluminum lifetime the theoretical result is too low by a factor of approximately 25%. This is not discouraging since recent work by Berko and Erskine[38] and MacKenzie, McKee and Bird[39] indicates that rates in plastically deformed Aluminum are generally higher than in well annealed samples. The theory developed here of course only applies to this latter case for which the lifetime may well be 20% to 25% lower than the experimental number quoted to date.

CHAPTER TWO

CONDUCTION ELECTRON THEORY WITHIN THE LATTICE FRAMEWORK

In their derivation of a theory for conduction electron annihilation, Kahana and Carbotte[14] used plane waves to describe the electron wavefunctions in the conduction band. Plane waves were used in order to keep the calculations simple. Such a theory can in fact explain experiments to good accuracy. However, it is well known that due to the presence of the periodic crystal lattice, the conduction electrons are more appropriately described by means of Bloch wavefunctions. For Sodium, which is the only element considered in this chapter, a single orthogonalized plane wave (O.P.W.) as was pointed out previously, has been shown to describe these Bloch states very well[21]. The following is an extension of the Kahana-Carbotte theory incorporating this lattice effect.

DERIVATION OF THE THEORY

As is shown in appendix A equation (A-49) for the partial annihilation rate $R(\underline{p})$ reads

$$R(\underline{p}) = \frac{\lambda}{V} \sum_{\underline{m}'} \theta_e^o(\underline{m}') \left| I_{\underline{m}',o}(\underline{p}) + \sum_{\underline{m},\underline{n}} I_{\underline{m},\underline{n}}(\underline{p}) \right.$$

$$\left. \chi_{\underline{m},\underline{n};\underline{m}',o} \left(E_o^p + E_{|\underline{m}'|}^e\right) \right|^2 \qquad (1)$$

where each term has the same meaning as given in the appendix. The summation over $\underline{m}'$ is now a summation over all occupied electron states in the conduction band. As has been seen in the previous chapter, the contribution arising from the core electron annihilation does not describe the momentum dependence of the experimental tails. Also in the region between p_F and $2p_F$ a greater overall increase of these tails is desired. Hence the aim in this chapter is to see by how much the I.P.M. tails get enhanced, expecially in the region p_F to $2p_F$ and to examine their momentum dependence. If such a contribution or dependence is supplied by the lattice it should be seen in a lesser degree to any order of perturbation theory and hence to simplify calculations it is looked for only in the first order of perturbation theory.[33] Hence expression (1) can now be written to first order as

$$R(\underline{p}) = \frac{\lambda}{V} \sum_{\underline{m}'} \theta_e^o(\underline{m}') \left| I_{\underline{m}',o}(\underline{p}) + \right.$$

$$\left. \sum_{\underline{m},\underline{n}} I_{\underline{m},\underline{n}}(\underline{p}) \chi^B_{\underline{m},\underline{n};\underline{m}',o} \left(E_o^p + E_{\underline{m}'}^e\right) \right|^2 \qquad (2)$$

where

$$\chi^{B}_{\underline{m},\underline{n};\underline{m}',o}(E^{p}_{o} + E^{e}_{\underline{m}'}) = P^{+}_{\underline{m},\underline{n}}\ (E^{p}_{\underline{n}} + E^{e}_{\underline{m}'})\ H_{\underline{m},\underline{n};\underline{m}',o} \quad . \qquad (3)$$

Equation (2) represents the graphs:

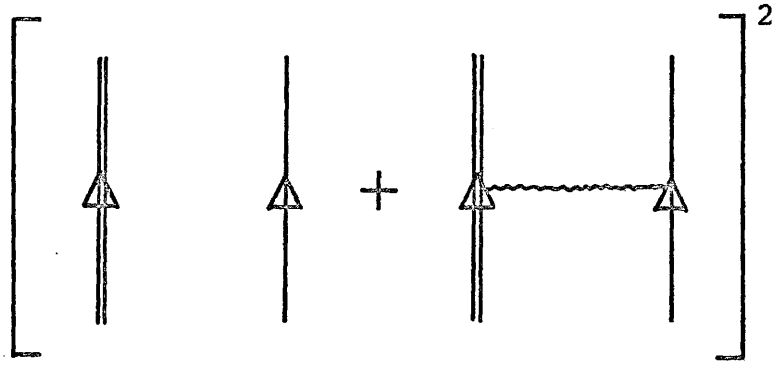

where ⫫ represents free positron propagation, ⫽ represents free electron propagation and ∿∿ is the interaction between the pair. In $P^{+}_{\underline{m},\underline{n}}\ (E^{p}_{\underline{n}} + E^{e}_{\underline{m}})$ the $\underline{m}$ and $\underline{n}$ indeces refer to excited states; consequently the energies $E^{e}_{\underline{m}}$ and $E^{p}_{\underline{n}}$ appearing in its denominator can be approximated by m^2 and n^2 respectively. This quadratic approximation is identical to that previously introduced in chapter one. Incorporating this into equation (3) yields

$$\chi^{B}_{\underline{m},\underline{n};\underline{m}',o}(E^{p}_{o} + E^{e}_{\underline{m}'}) = \frac{1}{V}\sum_{\underline{q}} U_{s}(\underline{q})\ [\underline{m}|\underline{q}|\underline{m}']^{e}[\underline{n}|-\underline{q}|o]^{p}\ \cdot$$

$$\frac{\theta^{u.o.}_{e}\ (\underline{m})\ \theta^{u.o.}_{p}\ (\underline{n})}{n^2 + m^2 - m'^2} \quad . \qquad (4)$$

Equation (2) is next simplified. For the conduction electrons the single O.P.W., as described in detail in the previous chapter, is now employed, namely,

$$\Psi_{\underline{k}}(\underline{r}) = \frac{1}{\sqrt{V}} e^{i\underline{k}.\underline{r}} u_{\underline{k}}(\underline{r})$$

i.e.

$$\Psi_{\underline{k}}(\underline{r}) = \frac{1}{\sqrt{V}} e^{i\underline{k}.\underline{r}} A(k) \left[1 - \sum_{\nu} \sum_{n,\ell,m} e^{-i\underline{k}.(\underline{r}-\underline{R}_{\nu})} u_{n\ell m}(\underline{r} - \underline{R}_{\nu}) A_{n\ell m}(\underline{k})\right] \qquad (5)$$

where

$$A_{n\ell m}(\underline{k}) = 4\pi Y^*_{\ell m}(\Omega_{\underline{k}}) i^{\ell} \int_0^{\infty} j_{\ell}(kr) P_{n\ell}(r) r\, dr$$

and

$$A(k) = \left[1 - \frac{1}{\Omega^o} \sum_{n,\ell,m} |A_{n\ell m}(\underline{k})|^2\right]^{-\frac{1}{2}} .$$

The positron wavefunction

$$\Phi_{\underline{k}}(\underline{x}) = \frac{1}{\sqrt{V}} e^{i\underline{k}.\underline{x}} v_o(\underline{x}) \qquad (6)$$

is used and as before the $\underline{k}$ dependence in $v_{\underline{k}}(\underline{x})$ is suppressed i.e. it is used in a Wigner-Seitz approximation.

The matrix elements

$$I_{\underline{m},\underline{n}}(\underline{p}) = \int \Psi_{\underline{m}}(\underline{x})\ e^{-i\underline{p}.\underline{x}}\ \Phi_{\underline{n}}(\underline{x})\ d^3\underline{x} \tag{7}$$

$$[\underline{m}|\underline{q}|\underline{m}']^e = \int \Psi_{\underline{m}}(\underline{x})\ e^{i\underline{q}.\underline{x}}\ \Psi^*_{\underline{m}'}(\underline{x})\ d^3\underline{x} \tag{8}$$

$$[\underline{n}|-\underline{q}|o]^p = \int \Phi_{\underline{n}}(\underline{x})\ e^{-i\underline{q}.\underline{x}}\ \Phi^*_{o}(\underline{x})\ d^3\underline{x} \tag{9}$$

which are defined in appendix A are now developed.

Substituting equations (5) and (6) into equation (7) gives

$$I_{\underline{m},\underline{n}}(\underline{p}) = \frac{1}{V} \int e^{i\underline{m}.\underline{x}}\ u_{\underline{m}}(\underline{x})\ e^{-i\underline{p}.\underline{x}}\ e^{i\underline{n}.\underline{x}}\ v_o(\underline{x})\ d^3\underline{x}$$

$$= \frac{1}{V} \int e^{i(\underline{m}-\underline{p}+\underline{n}).\underline{x}}\ u_{\underline{m}}(\underline{x})\ v_o(\underline{x})\ d^3\underline{x}\ . \tag{10}$$

Since $u_{\underline{m}}(\underline{x})$ and $v_o(\underline{x})$ are periodic in reciprocal space with the same period, it is possible to expand the product of the two of them in reciprocal space i.e.

$$u_{\underline{m}}(\underline{x})\ v_o(\underline{x}) = \sum_{\underline{a}} \omega_{\underline{m}}(\underline{a})\ e^{i\underline{a}.\underline{x}} \tag{11}$$

where the sum extends over all reciprocal lattice vectors $\underline{a}$, and $\omega_{\underline{m}}(\underline{a})$ is given by

$$\omega_{\underline{m}}(\underline{a}) = \frac{1}{\Omega^o} \int_{\substack{\text{atomic} \\ \text{polyhedron} \\ \text{(a.p.)}}} d^3\underline{x}\ e^{-i\underline{a}.\underline{x}}\ u_{\underline{m}}(\underline{x})\ v_o(\underline{x}) \qquad (12)$$

the evaluation of which will be explained later.

The substitution of equation (11) into (10) yields

$$I_{\underline{m},\underline{n}}(\underline{p}) = \frac{1}{V} \int e^{i(\underline{m}-\underline{p}+\underline{n}).\underline{x}} \sum_{\underline{a}} \omega_{\underline{m}}(\underline{a})\ e^{i\underline{a}.\underline{x}}\ d^3\underline{x}$$

$$= \sum_{\underline{a}} \omega_{\underline{m}}(\underline{a})\ \delta_{\underline{m}-\underline{p}+\underline{n}+\underline{a},o} \qquad (13)$$

Equations (8) and (9) are developed in a similar manner

$$[\underline{m}|\underline{q}|\underline{m}']^e = \frac{1}{V} \int e^{i\underline{m}.\underline{x}}\ u_{\underline{m}}(\underline{x})\ e^{i\underline{q}.\underline{x}}\ e^{-i\underline{m}'.\underline{x}}\ u_{\underline{m}'}(\underline{x})\ d^3\underline{x}$$

$$= \frac{1}{V} \int e^{i(\underline{m}+\underline{q}-\underline{m}').\underline{x}}\ u_{\underline{m}}(\underline{x})\ u_{\underline{m}'}(\underline{x})\ d^3\underline{x} \qquad (14)$$

Expanding $u_{\underline{m}}(\underline{x})\ u_{\underline{m}'}(\underline{x})$ i.e.

$$u_{\underline{m}}(\underline{x})\ u_{\underline{m}'}(\underline{x}) = \sum_{\underline{b}} f_{\underline{m},\underline{m}'}(\underline{b})\ e^{i\underline{b}.\underline{x}} \qquad (15)$$

where the summation extends over reciprocal lattice space and

$$f_{\underline{m}\underline{m}'}(\underline{b}) = \frac{1}{\Omega^o} \int_{a.p.} d^3\underline{x}\ e^{-i\underline{b}.\underline{x}}\ u_{\underline{m}}(\underline{x})\ u_{\underline{m}'}(\underline{x}) \qquad (16)$$

hence

$$[\underline{m}|\underline{q}|\underline{m}']^e = \frac{1}{V} \int e^{i(\underline{m}+\underline{q}-\underline{m}').\underline{x}} \sum_{\underline{b}} f_{\underline{m}\underline{m}'}(\underline{b})\ e^{i\underline{b}.\underline{x}}\ d^3\underline{x}$$

$$= \sum_{\underline{b}} f_{\underline{m}\underline{m}'}(\underline{b})\ \delta_{\underline{m}+\underline{q}-\underline{m}'+\underline{b},o} \qquad (17)$$

Finally

$$[\underline{n}|-\underline{q}|o]^p = \frac{1}{V} \int e^{i\underline{n}.\underline{x}}\ v_o(\underline{x})\ e^{-i\underline{q}.\underline{x}}\ v_o(\underline{x})\ d^3\underline{x}$$

$$= \frac{1}{V} \int e^{i(\underline{n}-\underline{q}).\underline{x}}\ v_o(\underline{x})\ v_o(\underline{x})\ d^3\underline{x}$$

expanding $v_o(\underline{x})\ v_o(\underline{x})$ i.e.

$$v_o(\underline{x})\ v_o(\underline{x}) = \sum_{\underline{c}} g(\underline{c})\ e^{i\underline{c}.\underline{x}} \qquad (18)$$

where again the summation extends over reciprocal lattice space and

$$g(\underline{c}) = \frac{1}{\Omega^o} \int_{a.p.} d^3\underline{x}\ e^{-i\underline{c}.\underline{x}}\ v_o(\underline{x})\ v_o(\underline{x}) \qquad (19)$$

hence

$$[\underline{n}|-\underline{q}|o]^p = \frac{1}{V}\int e^{i(\underline{n}-\underline{q})\cdot\underline{x}} \sum_{\underline{c}} g(\underline{c})\ e^{i\underline{c}\cdot\underline{x}}$$

$$= \sum_{\underline{c}} g(\underline{c})\ \delta_{\underline{n}-\underline{q}+\underline{c},o} \quad . \tag{20}$$

These rather lengthy algebraic manipulations were put in for completeness and the numerical evaluation of these equations will next be given. The equations (12),(16) and (19) will be dealt with together. The type of expression to be evaluated is

$$s_{\underline{n},\underline{m}}(\underline{a}) = \frac{1}{\Omega^o}\int_{a.p.} d^3\underline{x}\ e^{-i\underline{a}\cdot\underline{x}}\ q_{\underline{n},\underline{m}}(\underline{x}) \tag{21}$$

where $q_{\underline{n},\underline{m}}(\underline{x})$ is a periodic spherically symmetric function in space with period $\underline{a}$. Expanding the exponential by means of plane waves as given in (1-13) yields

$$s_{\underline{n},\underline{m}}(\underline{a}) = \frac{4\pi}{\Omega^o}\int_{a.p.} d^3\underline{x} \sum_{\ell=o}^{\infty} \sum_{m'=-\ell}^{\ell} (-i)^{\ell}\ j_{\ell}(ax) Y^*_{\ell m'}(\Omega_{\underline{k}})$$

$$Y_{\ell m'}(\Omega_{\underline{x}})\ q_{\underline{n},\underline{m}}(\underline{x}) \quad .$$

Since $q_{\underline{n},\underline{m}}(\underline{x})$ is spherically symmetric the integration over the angles of $\underline{x}$ gives

$$s_{\underline{n},\underline{m}}(\underline{a}) = \frac{4\pi}{\Omega^o}\int_{a.p.} x^2 dx\ j_o(ax)\ Y_{oo}(\Omega_{\underline{k}})\ q_{\underline{n},\underline{m}}(x)\ \sqrt{4\pi}$$

$$= \frac{4\pi}{\Omega^o a}\int_{a.p.} x\ dx\ \mathrm{Sin}\ ax\ q_{\underline{n},\underline{m}}(x) \quad . \tag{22}$$

This can be written as

$$s_{\underline{n},\underline{m}}(\underline{a}) = \frac{4\pi}{\Omega_o a} \int_{a.p.} x\, dx\, \text{Sin}\, ax[q_{\underline{n},\underline{m}}(x) - q_{\underline{n},\underline{m}}(r_s)] + q_{\underline{n},\underline{m}}(r_s)\, \delta_{\underline{a},o} \qquad (23)$$

where r_s is the Wigner Seitz cell radius. In the first term on the right hand side it is possible to replace, with very little error, the atomic polyhedron by the Wigner Seitz sphere since around $|\underline{x}| = r_s$ the integrand should almost vanish. It should be noted that $s_{\underline{n},\underline{m}}(\underline{a})$ can depend only on $|\underline{a}|$ and not on its direction. With a knowledge of $q_{\underline{n},\underline{m}}(x)$ the $s_{\underline{n},\underline{m}}(a)$ can easily be evaluated numerically. In their evaluation a Simpson's rule with a Herman-Skillman mesh was used[22]. Table II gives the results for zero momenta i.e. $f_{oo}(a)$ gives the O.P.W. of momentum o - O.P.W. of momentum o reciprocal transform; g(a) gives the positron-positron reciprocal transform; and $\omega_o(a)$ gives the positron-O.P.W. of momentum o reciprocal transform.

As can easily be seen all the transforms oscillate and hence an extremely accurate calculation involves the consideration of many terms. However it was found, on looking at several possible products, that taking the first twelve shells gave sufficient accuracy for the present work. To show the variation with $|\underline{x}|$ of the ω function relevant results for various momentum values were plotted in figure 13.

Returning to the main line of argument equations (13), (4), (17) and (20) are substituted into equation (2) to yield

$$R(\underline{p}) = \frac{\lambda}{V} \sum_{\underline{m}'} \theta_e^o(\underline{m}') \Big| \sum_{\underline{a}} \omega_{\underline{m}'}(a)\ \delta_{\underline{m}'-\underline{p}+\underline{a},o} +$$

$$\frac{1}{V} \sum_{\underline{m},\underline{n}} \sum_{\underline{a}} \omega_{\underline{m}}(a)\ \delta_{\underline{m}-\underline{p}+\underline{n}+\underline{a},o} \sum_{\underline{q}} \frac{U_s(\underline{q})\,\theta_e^{u.o.}(\underline{m})\,\theta_p^{u.o.}(\underline{n})}{n^2 + m^2 - m'^2}$$

$$\sum_{\underline{b}} f_{\underline{m}\underline{m}'}(b)\ \delta_{\underline{m}+\underline{q}-\underline{m}'+\underline{b},o} \sum_{\underline{c}} g(c)\ \delta_{\underline{n}-\underline{q}+\underline{c},o} \Big|^2 .$$

Summing over $\underline{q}$ yields

$$R(\underline{p}) = \frac{\lambda}{V} \sum_{\underline{m}'} \theta_e^o(\underline{m}') \Big| \sum_{\underline{a}} \omega_{\underline{m}'}(a)\ \delta_{\underline{m}'-\underline{p}+\underline{a},o} +$$

$$\frac{1}{V} \sum_{\underline{a},\underline{b},\underline{c}} \sum_{\underline{m},\underline{n}} \theta_e^{u.o.}(\underline{m})\,\theta_p^{u.o.}(\underline{n}) \frac{U_s(\underline{n}+\underline{c})}{n^2+m^2-m'^2}$$

$$\omega_{\underline{m}}(a)\ f_{\underline{m}\underline{m}'}(b)\ g(c)\ \delta_{\underline{m}-\underline{p}+\underline{n}+\underline{a},o}\ \delta_{\underline{m}+\underline{n}-\underline{m}'+\underline{c}+\underline{b},o} \Big|^2 .$$

Summing over $\underline{n}$ gives

$$R(\underline{p}) = \frac{\lambda}{V} \sum_{\underline{m}'} \theta_e^o(\underline{m}') \Big| \sum_{\underline{a}} \omega_{\underline{m}'}(a)\ \delta_{\underline{m}'-\underline{p}+\underline{a},o} +$$

$$\frac{1}{V} \sum_{\underline{a},\underline{b},\underline{c}} \sum_{\underline{m}} \theta_e^{u.o.}(\underline{m})\ \frac{U_s(\underline{p}-\underline{m}-\underline{a}+\underline{c})}{(\underline{p}-\underline{m}-\underline{a})^2+m^2-m'^2}$$

$$\omega_{\underline{m}}(a)\ f_{\underline{m}\underline{m}'}(b)\ g(c)\ \delta_{\underline{p}-\underline{a}-\underline{m}'+\underline{c}+\underline{b},o}\Big|^2 \quad .$$

In order to symmetrise things the coordinate transformation

$$\underline{a}' = \underline{a} \qquad \underline{b}' = \underline{a} - \underline{c} \qquad \underline{c}' = \underline{a} - \underline{c} - \underline{b}$$

is made, which is permissible as the Jacobian is equal to one. Hence

$$R(\underline{p}) = \frac{\lambda}{V} \sum_{\underline{m}'} \theta_e^o(\underline{m}') \Big| \sum_{\underline{a}} \omega_{\underline{m}'}(a)\ \delta_{\underline{m}'-\underline{p}+\underline{a},o} +$$

$$\frac{1}{V} \sum_{\underline{a},\underline{b},\underline{c}} \sum_{\underline{m}} \theta_e^{u.o.}(\underline{m})\ \frac{U_s(\underline{p}-\underline{m}-\underline{b})}{(\underline{p}-\underline{m}-\underline{a})^2+m^2-m'^2}$$

$$\omega_{\underline{m}}(a)\ f_{\underline{m}\underline{m}'}(|\underline{b}-\underline{c}|)\ g(|\underline{a}-\underline{b}|)\ \delta_{\underline{p}-\underline{c}-\underline{m}',o}\Big|^2 \quad .$$

Interchanging $\underline{a}$ and $\underline{c}$ in the second term the equation becomes

$$R(\underline{p}) = \frac{\lambda}{V} \sum_{\underline{m}'} \theta_e^{o}(\underline{m}') \sum_{\underline{a}} \delta_{\underline{m}'-\underline{p}+\underline{a},o} \left| \omega_{\underline{m}'}(a) + \right.$$

$$\frac{1}{V} \sum_{\underline{b},\underline{c}} \sum_{\underline{m}} \theta_e^{u.o.}(\underline{m}) \frac{U_s(\underline{p}-\underline{m}-\underline{b})}{(\underline{p}-\underline{m}-\underline{c})^2+m^2-m'^2}$$

$$\left. \omega_{\underline{m}}(c)\ f_{\underline{m}\underline{m}'}(|\underline{b}-\underline{a}|)\ g(|\underline{c}-\underline{b}|) \right|^2 .$$

Summing over $\underline{m}'$

$$R(\underline{p}) = \frac{\lambda}{(2\pi)^3} \sum_{\underline{a}} \theta(p_F-|\underline{p}-\underline{a}|) \left| \omega_{\underline{p}-\underline{a}}(a) + \right.$$

$$\frac{1}{V} \sum_{\underline{b},\underline{c}} \sum_{\underline{m}} \theta_e^{u.o.}(\underline{m}) \frac{U_s(\underline{p}-\underline{m}-\underline{b})}{(\underline{p}-\underline{m}-\underline{c})^2+m^2-(\underline{p}-\underline{a})^2}$$

$$\left. \omega_{\underline{m}}(c)\ f_{\underline{m},\underline{p}-\underline{a}}(|\underline{b}-\underline{a}|)\ g(|\underline{c}-\underline{b}|) \right|^2$$

is obtained. As pointed out in chapter one the quantity that is of physical interest and experimentally measured is R_{p_z} which is obtained from $R(\underline{p})$ by simply integrating over all values of p_x and p_y. Hence on taking the limit of infinite volume

$$R_{p_z} = \frac{\lambda}{(2\pi)^3} \sum_{\underline{a}} \int dp_x \int dp_y \; \theta(p_F - |\underline{p}-\underline{a}|) \, |\omega_{\underline{p}-\underline{a}}(a) +$$

$$\frac{1}{(2\pi)^3} \sum_{\underline{b},\underline{c}} \int_{|\underline{m}|>p_F} d^3\underline{m} \; \frac{U_s(\underline{p}-\underline{m}-\underline{b})}{(\underline{p}-\underline{m}-\underline{c})^2+m^2-(\underline{p}-\underline{a})^2}$$

$$\omega_{\underline{m}}(c) \; f_{\underline{m},\underline{p}-\underline{a}}(|\underline{b}-\underline{a}|) \; g(|\underline{c}-\underline{b}|)\,|^2 \quad . \qquad (24)$$

GEOMETRICAL INTERPRETATION

The geometrical interpretation of (24) may be considered by looking at reciprocal space as shown below.

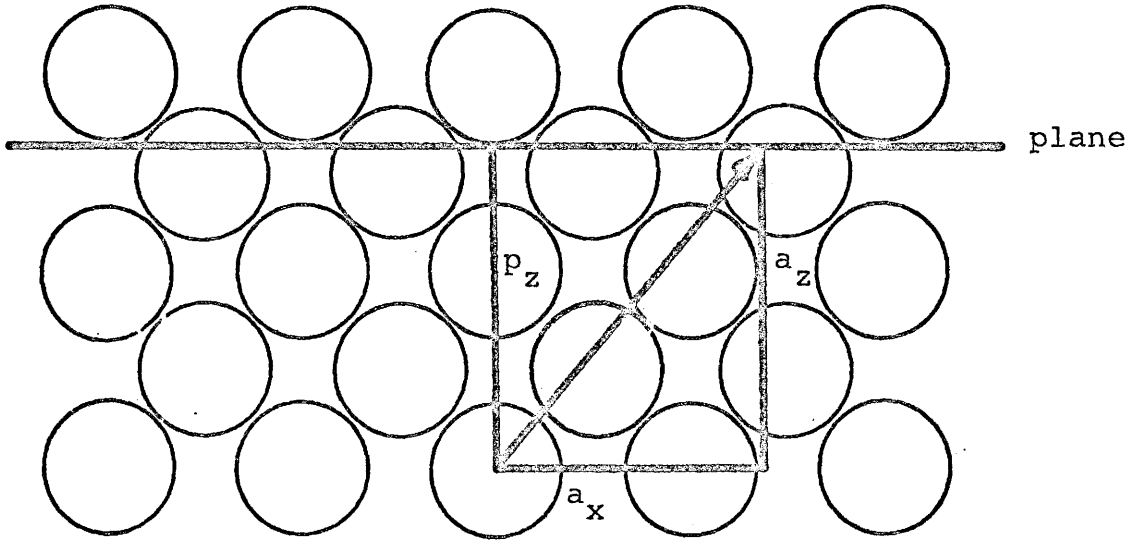

The integral is taken over a plane perpendicular to the p_z axis at a height p_z. The only portion of the plane, entering the calculations, lies inside each respective Fermi sphere of reciprocal space. The summation $\underline{a}$ is taken over all such spheres that are cut by this particular plane. The contribution is proportional to the square of the sum of two matrix elements. The first is purely the Fourier transform of the $(\underline{p}-\underline{a})^{th}$ plane wave matrix element taken between the positron wavefunction and the conduction electron wavefunction in the I.P.M. The plane wave term $e^{i(\underline{p}-\underline{a}).\underline{x}}$, expresses the fact that the two γ-rays emerge not with momentum $\underline{p}$ but with momentum $|\underline{p}-\underline{a}|$, the additional amount $\underline{a}$ coming from Umklapp type processes. These processes arise from the fact that the lattice transfers an amount $\underline{a}$ of momentum to the electron prior to annihilation. (Note that if $\underline{a}$ is set equal to zero, it follows that the first term gives the contribution solely from the single central Fermi sphere with no momentum transfer.) From table 2 it can be seen that this term gives a maximum contribution at the central sphere and then slowly converges in an oscillatory manner as one goes out into reciprocal space. The second term is basically a correction for correlations and ranks in importance with the first because the relative motion of the annihilating pair is highly correlated as indeed was seen in chapter one. It consists of the Fourier transforms of electron-electron, positron-positron, positron-electron matrix

elements describing particle excitations with subsequent annihilation. Due to the summation over $\underline{b}$ and $\underline{c}$ i.e. a complex coupling of all the spheres, it is hard to estimate what terms will dominate. This makes the calculation very lengthy as no set of terms can be neglected beyond those which have been mentioned previously. In addition a screened Coulomb potential with the relevant energy denominators is also included in equation (24).

COMPUTATION OF R_{p_z}

Referring expressly to the physical and geometrical aspects of the problem the simplification of expression (24) now follows. Performing the coordinate transformations

$$\underline{p} = \underline{p}' + \underline{a} \qquad \underline{a}' = \underline{a} \qquad \underline{b}' = \underline{a} - \underline{b} \qquad \underline{c}' = \underline{a} - \underline{c}$$

(which are allowed since the Jacobian is equal to one) gives

$$R_{p_z} = \frac{\lambda}{(2\pi)^3} \int dp'_x \, dp'_y \sum_{\underline{a}} \theta(p_F - |\underline{p}'|) \, |\omega_{\underline{p}'}(a') +$$

$$\frac{1}{(2\pi)^3} \sum_{\underline{b}',\underline{c}'} \int_{|\underline{m}|>p_F} d^3\underline{m} \, \frac{U_s(|\underline{p}'-\underline{m}+\underline{b}'|)}{(p'-m+c')^2+m^2-p'^2}$$

$$\omega_{\underline{m}}(|\underline{a}'-\underline{c}'|) \, f_{\underline{m},\underline{p}'}(b') \, g(|\underline{c}'-\underline{b}'|)|^2 \quad .$$

It should now be noticed that the coordinate transformation has reduced the integral in (24) to an integral in each separate Fermi sphere and to a summation over all spheres. From a physical point of view it is a reasonable assumption that the angular variation of the expression in each sphere is small. Therefore the assumption can be made that the expression is spherically symmetric in $\underline{p}'$. Making p_z the axis of integration and introducing a factor of 2 for spin degeneracy the result may be written as

$$R_{p_z} = \frac{4\pi\lambda}{(2\pi)^3} \sum_{\underline{a}'} \int_{|p_z-a'_z|}^{p_F} p'dp' \; | \; \omega_{p'}(a') +$$

$$\frac{1}{(2\pi)^3} \sum_{\underline{b},\underline{c}} g(|\underline{c}'-\underline{b}'|) \int_{|\underline{m}|>p_F} d^3\underline{m} \, \frac{U_s(|\underline{p}'-\underline{m}+\underline{b}'|)}{(\underline{p}'-\underline{m}+\underline{c}')^2+m^2-p'^2}$$

$$\omega_{\underline{m}}(|\underline{a}'-\underline{c}'|) \, f_{\underline{m},\underline{p}'}(b')|^2 \quad . \qquad (25)$$

Measuring all momenta in units of the Fermi momentum p_F i.e. $p' = \gamma p_F$, introducing the factor $3/4\ R^o = 2\pi\lambda p_F^3/(2\pi)^3$ and remembering that $R_{\gamma_z} = p_F R_{p_z}$, equation (25) becomes

$$R_{\gamma_z} = 3/4\ R^o\ 2 \sum_{\underline{a}} \int_{|\gamma_z - \frac{a_z}{p_F}|}^{1} \gamma d\gamma \mid \omega_{\underline{\gamma}}(a) +$$

$$\sum_{\underline{b}',\underline{c}'} g(|\underline{c}'-\underline{b}'|) \int_{|\underline{m}|>1} d^3\underline{m}\ \omega_{\underline{m}}(|\underline{a}-\underline{c}'|)\ f_{\underline{m},\underline{\gamma}}(b')$$

$$\frac{\alpha\ U\ (|\underline{\gamma}-\underline{m}+\underline{b}'|)}{(\underline{\gamma}-\underline{m}+\underline{c}')^2 + m^2 - \gamma^2} \Big|^2 .$$

Due to the slow convergence of the Fourier coefficients ω and f with respect to their arguments the summations over $\underline{b}'$ and $\underline{c}'$ have to be extended to many reciprocal lattice vectors. Taking several particular values of $\underline{a}$ and looking at

$$\sum_{\underline{b}',\underline{c}'} g(|\underline{c}'-\underline{b}'|)\ \omega_o(|\underline{a}'-\underline{c}'|)\ f_{o,o}(b')$$

it was found that 12 shells in reciprocal space are sufficient for adequate convergence. However, even by doing this, the

computation of the expression is so lengthy that the subscripted momentum dependence in the Fourier transforms had to be neglected i.e.

$$R_{\gamma_z} = 3/4\ R^o\ 2 \sum_{\underline{a}} \int_{o \le |\gamma_z - \frac{a_z}{p_F}|}^{1} \gamma d\gamma \mid \omega(a') +$$

$$\sum_{\underline{b}',\underline{c}'} \omega(|\underline{a}'-\underline{c}'|)\ f(b')\ g(|\underline{c}'-\underline{b}'|)$$

$$\alpha \int_{|\underline{m}|>1} d^3\underline{m}\ \frac{U\ (|\underline{\gamma}-\underline{m}-\underline{b}'|)}{(\underline{\gamma}-\underline{m}+\underline{c})^2 + m^2 - \gamma^2} \Big|^2 \qquad (26)$$

where the Fourier transforms are those of table II. This assumption destroys the quantitative correctness of the result but nevertheless it will still be qualitatively correct and at worst it will be a model calculation and indicative of the correct result. This approximation is certainly good for $\omega_{\underline{x}}(a)$ as can be seen from figure 13, but for the $f_{\underline{x},\underline{y}}(a)$ there is quite a momentum variation and the approximation is poor. Indeed this is the weakest point in this theory. To get an estimate of the error made the calculations for two distinct cases were performed.

The first case was the Wigner Seitz model in which all the subscripts are set equal to zero. The second case was based on the fact that for very large momentum the O.P.W. tend to plane waves; hence plane waves were used in the evaluation of the Fourier coefficients. It was found on performing the computations that both cases were equivalent to within five per cent - thus indicating that the assumptions might not be as bad as might be expected.

Furthermore the potential chosen was not the static limit of the screened Coulomb potential but a Fermi Thomas potential was used. The reason for this was purely technical since the logarithmic term in the screened Coulomb potential (cf equation I-42) would have taken too long to be evaluated on the computer.

COMPUTATIONAL TECHNIQUES

Before presenting the results, the techniques used in the computation of equation (26) will be discussed. The integral over $\underline{m}$ was carried out using a stratified sampling Monte Carlo type method[34]. In order to get an even sampling over all space the mesh was chosen in an unusual way. A vector was taken with several points randomly distributed on it. This vector was rotated in the first octant to give a

randomly distributed set of points totalling 738. The points in the first octant were then rotated to give the full remaining seven octants. In this way one can economise on the number of times the integrand has to be evaluated but in actual fact one performs a Monte Carlo calculation with 5904 points. To ensure that a satisfactory job was being done a comparison was made to a Simpson's rule evaluation of the integral

$$\int_{|\underline{m}|>1} d^3\underline{m} \frac{U\,(|\underline{\gamma}-\underline{m}-\underline{b}|)}{(\underline{\gamma}-\underline{m}+\underline{c})^2 + m^2 - \gamma^2} \qquad (27)$$

for a couple of fixed vectors $\underline{c}$ and $\underline{b}$. Agreement was obtained to within 3-5%.

In the evaluation of (26) random sample vectors $\underline{b}$ and $\underline{c}$ were taken out of each shell and they were used as the representative vectors of the whole shell. This was justified by the fact that on taking several random samples and evaluating the whole of the correlation term in (26) a variation of less than 2% resulted. Anyway this random sampling conforms to the general spirit of a Monte Carlo approach. The computer time saved by doing this is enormous. This reduces the evaluation of a 225 x 225 matrix to an evaluation of a 12 x 12 matrix. Table 3 gives a typical matrix for $p = 1$, $p_x = 0.866$ and $p_z = 0.5$. The table shows that (27) assists convergence but is not in itself sufficient

for convergence. This must be sought in the Fourier coefficient products. The rest of the computation was done exactly using the I.B.M. 7040 computer of McMaster University.

RESULTS AND DISCUSSION

Firstly the result for the independent particle model or the first term of the square in equation (24) is plotted in figure 14. This shows an inverted parabola for momentum less than p_F which reflects the spherical surface of the Fermi sea. For momentum values greater than p_F the "tails" due to Umklapp type processes are obtained. The full evaluation of expression (24) is shown in figure 15. It can be clearly seen that the central parabola is enhanced by a factor of approximately four. As was pointed out earlier this is due to correlations between the annihilating pair. However the shapes are not identical - a slight bulging out of the parabola takes place as indeed was found by Carbotte and Kahana[14] in their plane wave summation of the ladder diagrams. This furthers the evidence which shows that the Born approximation is sufficient to give a good qualitative description of the total result i.e. the summation of all the ladder diagrams which have only been carried out to first order.

The tail is also enhanced in a similar way as the main parabola. The momentum variation of the tails was not found. The calculation seems to indicate that the complete summation of all the ladders would give too much of a contribution in the region of momentum greater than two p_F; however on a brighter note it would correct the discrepancy between theory and experiment in the region between one and 2 p_F.

A detailed graphical comparison to experiments is not included here since, as was pointed out earlier this calculation is of a qualitative nature, and in a detailed quantitative way it is not too reliable.

As a final remark it might be stressed that this calculation implies that the Berko-Plaskett theory is sufficient to explain experimental results. This theory has to be multiplied by a constant factor varying from element to element to obtain reasonable results in agreement with experiment. This factor is the one referred to in the last section of chapter one.

CHAPTER THREE

POSITRON ANNIHILATION IN SOLID ARGON

The experimental angular correlation curves are of two types; an inverted parabola with tails at large angles, and a Gaussian type distribution. In chapter 1 and 2 the former type were examined. The parabolas displayed a fairly sharp cut off at an angle corresponding to the Fermi momentum as characterized by the alkali metals and by aluminum. However the distribution in the noble metals and in insulators extends well past the expected Fermi cut off, exhibiting the Gaussian character. This momentum spread is characteristic of highly localized electron states and it is expected in an insulator because all the atomic shells are filled and all the electrons are, in effect, core electrons. Indeed a Gaussian distribution was obtained in the core calculations of both sodium and aluminum as given in chapter 1 and in figure 10. The core theory of Carbotte[17], expanded in chapter 1, is now applied with certain limitations to solid argon.

Since argon is an insulator with a simple structure, it was chosen as the most suitable example for the calculations. Furthermore, in the argon crystal the atoms are bound solely by Van Der Waal's forces so that, to a first approximation,

each cell, centred at an atomic site, is electrically neutral. Thus no complications arise due to 1) positron - ion core correlation effects as would be expected in substances with ionic binding, and 2) the sharing of electrons by neighbouring atoms as in the case of crystals with covalent bonding.

PRESENT STATE OF THE THEORY

Two recent papers[35, 27] have tried to explain the theory of angular correlation and lifetime experiments. Rose and De Benedetti[35] have applied a simple Berko-Plaskett theory to their experiments. Their results, like all of the I.P.M. calculations, explain the angular distribution curves very well but, when it comes to the positron lifetime, they highly overestimate the experimental results. This overestimation of the lifetime is of course now fully understood i.e. the correlation terms are equivalent in importance to the I.P.M. terms.

Woll and Rose[27] went a little further. Instead of assuming that the positron sees a simple Hartree field due to the outer electrons, they also included an attraction due to the virtual polarization of the outer electrons. As might be expected this gave rise to a highly distorted positron

wavefunction with a peak about halfway along the Wigner Seitz cell and as a consequence the positron penetrated the core to a greater extent i.e. the core is sampled better than in the I.P.M. Their result was very good for the lifetime of the positron but their angular distribution curve is totally wrong. But since both the angular distribution and lifetime measurements should be explained simultaneously their theory is unsatisfactory.

LIMITATIONS OF THE CORE THEORY

In the derivation of the core formula (B-14) in appendix B a plane wave approximation was made. In other words wherever a conduction-conduction matrix element entered the theory it was replaced by a delta function. But Argon is more complex than the alkali metals and the single O.P.W.'s are now more complicated with more structure than in the simple metals for which the theory was derived. Figure 16 shows the momentum dependence of these O.P.W. Hence overlap matrix elements have now to be treated much more carefully than was done in appendix B as band effects play a major role. The theoretical derivation leading to equation (I-2) is only valid for Argon if it is evaluated to first order. This will of course, as in the last chapter,

be only qualitatively correct. However, in sodium 80% of our theoretical contribution came from a first order calculation so that now the first order calculation for Argon is carried out bearing in mind the fact that the final result might only be approximately 80% of the true result. This suffices as indeed the scope of this work is not to derive a theory that will explain Argon but rather to apply the already developed theory to see what type of results it gives.

This is done chiefly for two reasons. Firstly by applying this theory to other elements a better understanding of the theory itself in general might be obtained with resultant improvement. Secondly by its application to Argon it might suggest a way in which Argon and other molecular insulators could be properly treated in a diagrammatic way. This would be the next step in the general development of the theory.

APPLICATION OF THE THEORY

A knowledge of the atomic core wavefunctions and the positron wavefunction is basic to these calculations. The electron core wavefunctions used were those derived in

Hartree and Hartree[20]. No better wavefunctions were derived as these were thought to be sufficiently accurate for the present calculation. As in the case of Sodium and Aluminum it was assumed that the positron sees a simple Hartree field due to all the other electrons, taken in a Wigner Seitz approximation. The result is shown in figure 17, and it is very similar to the wavefunction of Rose and De Benedetti[35].

The O.P.W. representing the excited states were constructed in a similar manner to that described in chapter 1. As already mentioned these are plotted in figure 16 for various momentum values. The extra oscillation in the wavefunctions as compared to Sodium should be noted. This, although it seems to be a trivial point is very important since now the O.P.W. only approximate to a plane wave for very large momenta. As a result the fact is stressed once more that the core calculation is not carried out to all orders but merely to the first order in the ladder approximation. This difficulty must not however be thought to be of a physical nature; it is purely a mathematical one and no attempt was made to remove it as it was felt that agreement to 80% would be sufficient. Developing the present theory further makes the calculations too long and involved to be practical.

DERIVATION OF THE PARTIAL ANNIHILATION FORMULA

Equation (I-37) can be carried over to the Argon case very simply by remembering the fact that no Fermi momentum arises in insulators. Hence the contribution to the partial rate $R(\underline{p})$ arising from an electron in the state $n\ell$ is

$$R^{n\ell}(\underline{p}) = \frac{\lambda}{V}\frac{1}{\Omega^o}\, 2(2\ell+1)\; 4\pi \;\Big|\; \int dx\; j_\ell(px)\; P_{n\ell}(x)\; R^+(x) +$$

$$\frac{2i^\ell}{\pi} \int \frac{j_\ell(px)\; A(k)\; P_{n\ell}(x)}{[\Delta_{n\ell}+2k^2+p^2-2pk\mu_k]} \quad U_s(|\underline{p}-\underline{k}|)$$

$$G(kx)\; k^2 dk\; d\mu_k\; dx \;\Big|^2 \qquad (1)$$

$$= \frac{\lambda}{V}\frac{1}{\Omega^o}\, 8\pi(2\ell+1) \;\Big|\; J^+ + J^- \;\Big|^2$$

where the various symbols are explained in chapter 1. One major change has occurred which at first may seem trivial but actually complicates matters considerably. The Coulomb potential $U_s(|\underline{p}-\underline{k}|)$ is no longer given by (I-42) but by

$$U_s(|\underline{p}-\underline{k}|) = \frac{8\pi}{|\underline{p}-\underline{k}|^2} \quad . \qquad (2)$$

This introduces a removable singularity in the correlation term of expression (1). This can best be seen by doing the integration over μ_k in this term to yield

$$J^- = \frac{-i^\ell}{\pi p} \int_0^\infty j_\ell(px)\ A(k)\ \frac{P_{n\ell}(x)}{k^2+\Delta_{n\ell}}\ G(kx)$$

$$\ell n \left| \frac{(\ p^2+k^2-2pk\ )}{(2k^2+p^2-2pk+\Delta_{n\ell})} \quad \frac{(\Delta_{n\ell}+2k^2+p^2+2pk)}{(\ p^2+k^2+2pk\ )} \right| \ kdkdx \quad . (3)$$

The singularity is now obvious in the logarithmic term for $p = k$. In evaluating the integral care has to be taken since there are the added singularities at the integral limits. This can easily be done by using a counterterm method and with the aid of the auxiliary function

$$g(p;k) = [1 + p - k]^2 \qquad (4)$$

(3) can be written as

$$J^{-} = \frac{i^{\ell}}{\pi p} \int_0^{\infty} dk \; [g(p;k)F(p;k;\Delta_{n\ell}) - F(p;p;\Delta_{n\ell})]$$

$$\frac{1}{g(p;k)} \; \ell n \left| \frac{(p-k)^2}{(p+k)^2} \quad \frac{(p+k)^2+\Delta_{n\ell}}{(p-k)^2+\Delta_{n\ell}} \right| +$$

$$\frac{i^{\ell}}{\pi p} F(p;p;\Delta_{n\ell}) \int_0^{\infty} \frac{dk}{g(p;k)} \; \ell n \left| \frac{(p-k)^2}{(p+k)^2} \quad \frac{(p+k)^2+\Delta_{n\ell}}{(p-k)^2+\Delta_{n\ell}} \right| \qquad (5)$$

where

$$F(p;k;\Delta_{n\ell}) = \int_0^{\infty} dr \; j_{\ell}(pr) \; P_{n\ell}(r) \; G(kr) \; A(k) \; \frac{k}{k^2 + \Delta_{n\ell}} \; . \qquad (6)$$

The function $g(p;k)$ had to be introduced to obtain convergence at both limits.

COMPUTATION OF THE PARTIAL RATE AND LIFETIME

The computation of (1) is now trivial. In particular to do the integrals the Hartree-Hartree[20] mesh was used in a Simpson's rule evaluation. This mesh might be criticized as being too rough but the accuracy and speed achieved was thought to be sufficient for the

present limited purposes. The only levels evaluated were the 3s and 3p since, due to the large band gap $\Delta_{n\ell}$ [23], the other levels give an insignificant contribution.

Figures 18 and 19 give the $J^{\pm n\ell}$ functions for the 3s and 3p levels. These show the same characteristic behaviour as in the Sodium core i.e. figures 8 and 9. The theoretical and experimental [36] partial annihilation result is shown in figure 20. As can be seen agreement is remarkably good. This is very encouraging; however the lifetime calculation is a more sensitive comparison. For this the theoretical result is 0.5×10^{-8} sec compared with the experimental value of 0.43×10^{-8} sec given by Liu and Roberts [37]. This agreement is very good considering the 80% accuracy of the theory.

From this it may be inferred that a better treatment of Argon is certainly worthwhile. However in such a treatment not only should the complete ladder approximation be used but the diagrams that give rise to polarization effects, as discussed by Woll and Rose [27], should also be included. The very good results obtained however suggest the possibility that these terms might cancel against higher order diagrams in a similar way to the cancellations obtained in Carbotte's thesis [14] for the diagrams of the conduction theory in simple metals.

In conclusion the questions posed earlier may now be

answered. It seems evident that the general positron annihilation theory derived by Kahana and Carbotte gives good results both in metals, and with some slight modifications, in general. At least non-ionic insulators can definitely be described by it and with a further extension as suggested above the theory should be able to explain the experimental results to within five to ten per cent.

APPENDIX A

CARBOTTE-KAHANA THEORY OF POSITRON ANNIHILATION[17]

In order to make the thesis complete and self contained the following appendix, which is a synopsis of the paper by Carbotte[17], is included.

In the non-relativistic limit of quantum electrodynamics the Hamiltonian operator, that produces a two-photon final state of total momentum $\hbar\,\underline{p}$ is proportional to

$$\sum_{\underline{k}_1} \sum_{\underline{k}_2} a_{\underline{k}_1}\, b_{\underline{k}_2}\, \delta_{\underline{k}_1 + \underline{k}_2,\, \underline{p}} \qquad (1)$$

where $a_{\underline{k}_1}$ and $b_{\underline{k}_2}$ are annihilation operators for the electron of momentum $\underline{k}_1$ and the positron of momentum $\underline{k}_2$ respectively[6]. The corresponding point annihilation operators $\Phi(\underline{x}_1)$ and $\Psi(\underline{x}_2)$ can be introduced by means of the relations

$$a_{\underline{k}_1} = \frac{1}{\sqrt{V}} \int d^3\underline{x}_1\, e^{-i\underline{k}_1 \cdot \underline{x}_1}\, \Phi(\underline{x}_1)$$

$$b_{\underline{k}_2} = \frac{1}{\sqrt{V}} \int d^3\underline{x}_2\, e^{-i\underline{k}_2 \cdot \underline{x}_2}\, \Psi(\underline{x}_2) \qquad (2)$$

where V is the volume of quantisation. Substituting (2) into

(1) and performing the summation over $\underline{k}_2$ yields

$$\frac{1}{V} \sum_{\underline{k}_1} \int d^3\underline{x}_1 \, d^3\underline{x}_2 \, e^{-i\underline{p}\cdot\underline{x}_2} \, e^{-i\underline{k}_1\cdot(\underline{x}_1-\underline{x}_2)} \, \Phi(\underline{x}_1) \, \Psi(\underline{x}_2) \quad .$$

Summing over $\underline{k}_1$ and integrating over $\underline{x}_2$ yields

$$\int d^3\underline{x}_1 \, e^{-i\underline{p}\cdot\underline{x}_1} \, \Phi(\underline{x}_1) \, \Psi(\underline{x}_1) \quad . \tag{3}$$

The partial annihilation rate is easily obtained by taking the matrix element of equation (3) between the initial and final states, squaring the absolute value, and summing over all final states i.e.

$$R(\underline{p}) \propto < \int d^3\underline{x} \, d^3\underline{y} \, e^{-i\underline{p}\cdot(\underline{x}-\underline{y})} \, \Phi(\underline{x}) \, \Phi^+(\underline{y}) \, \Psi(\underline{x}) \, \Psi^+(\underline{y}) > \quad . \tag{4}$$

It is possible to relate equation (4) to a contraction of the zero temperature electron positron correlation or Green's function. The latter is defined as

$$G_{ep}(xy;x'y') = i^2 < T \, \Psi(x) \, \Phi(y) \, \Phi^+(y') \, \Psi^+(x') > \tag{5}$$

where $x = (\underline{x}, t_x)$ and T is the Wick time ordering operator. Using this (4) becomes

$$R(\underline{p}) = \frac{(-i)^2\lambda}{V} \int d^3\underline{x}\, d^3\underline{y}\, e^{-i\underline{p}\cdot(\underline{x}-\underline{y})}\, G_{ep}(x,x;y^+,y^+) \qquad (6)$$

where $x = (\underline{x},t)$ and $y^+ = (\underline{y},t^+)$. The proportionality constant λ in equation (6) can conveniently be fixed by reference to the known properties of singlet positronium. The electron density at the positron in the positronium ground state is $1/(8\pi a_o^3)$ and the annihilation rate is $4\lambda_o$ with $\lambda_o \simeq 2.01 \times 10^4\ \text{sec}^{-1}$. Since annihilation into two quanta can only occur from a singlet spin state, the correct proportionality constant for a metal is $\lambda = 4\lambda_o\ (8\pi a_o^3)\frac{1}{4}$ where the factor $\frac{1}{4}$ is just the probability for a given electron-positron pair in a metal to be in a singlet state.

Equation (6) is not only a mathematical expression for $R(\underline{p})$ but also a physical one, since the G_{ep} term diagrammatically contains all of the interactions between the annihilating pair. Solving for this in the ladder approximation i.e. summing all the ladder diagrams yields the integral equation

$$G_{ep}(x,x';y,y') = G_e^o(x;y)G_p^o(x';y') - i\int d^4z\, d^4z' U(z;z') G_e^o(x;z)$$

$$G_p^o(x';z')\, G_{ep}(z,z';y,y') \qquad (7)$$

where

$$U(z;z') = U_s(\underline{z};\underline{z}')\ \delta(t_z - t_{z'})$$

$U_s(\underline{z};\underline{z}')$ is the screened Coulomb force of an electron-gas theory[12], i.e. only the conduction electrons are assumed to play a significant role in the screening. The functions G_e^o and G_p^o are respectively the zeroth order electron and positron propagators.

The positron Bloch state will be denoted by $\Phi_{\underline{m}}(\underline{x})$ and the positron propagator is then given by

$$G_p^o(x;x') = \sum_{\underline{m}} \Phi_{\underline{m}}(\underline{x}) \; \Phi^*_{\underline{m}}(\underline{x}') \int \frac{d\omega}{2\pi} e^{-i\omega(t_x - t_{x'})} \; G_p^o(\underline{m};\omega) \qquad (8)$$

with

$$G_p^o(\underline{m};\omega) = \frac{\theta_p^{u.o.}(\underline{m})}{E_{\underline{m}}^p - \omega - io^+} + \frac{\theta_p^o(\underline{m})}{E_{\underline{m}}^p - \omega + io^+} \qquad (9)$$

where $E_{\underline{m}}^p$ is the energy of the positron in the state $\Phi_{\underline{m}}(\underline{x})$, while $\theta_p^{u.o.}(\underline{m})$ is a theta function equal to 1 for all unoccupied states and equal to zero otherwise. The function $\theta_p^o(\underline{m}) = 1 - \theta_p^{u.o.}(\underline{m})$.

The electron wavefunction will be denoted by $\Psi_{\underline{m}}(\underline{x})$, where the Bloch label $\underline{m}$ stands for the usual $(n\ell m_s)$ if it is a core state, or for any momentum value in an extended zone scheme (or the equivalent) if it is a conduction state. G_e^o can be written in a similar form changing all the positron labels in (8) and (9) to electron ones.

In equation (7) the variables y and y' do not get coupled in the integration. Since the two body potential is assumed to be static the electron-positron Green's function $G_{ep}(z,z';y,y')$ need only be known for $t_z = t_{z'}$. Henceforth in this appendix for any pair of variables x and x' it is always understood that $t_x = t_{x'}$.

In order to simplify expression (7) the Bethe-Goldstone amplitude $\Omega(x,x';y,y')$ is introduced as follows

$$G_{ep}(x,x';y,y') = \int d^4z\, d^3z'\, \Omega(x,x';z,z')\, G_e^o(z;y)\, G_p^o(z';y'). \tag{10}$$

Introducing equation (10) into equation (7) yields

$$\int d^4z\, d^3z'\, \Omega(x,x';z,z')\, G_e^o(z;y)\, G_p^o(z';y') = G_e^o(x;y)\, G_p^o(x';y') -$$

$$i \int d^4z\, d^4z'\, G_e^o(x;z)\, G_p^o(x';z')\, U(z;z') \int d^4r\, d^3r$$

$$\Omega(z,z';y,y')\, G_e^o(r;y)\, G_p^o(r';y') \quad . \tag{11}$$

On interchanging dummy symbols and introducing delta functions this expression can be rewritten as

$$\int d^4z\, d^4z'\, G_e^o(z;y)\, G_p^o(z';y')[\Omega(x,x';z,z') - \delta^4(x-z)\, \delta^3(\underline{x}'-\underline{z}') +$$

$$i \int d^4r\, d^3\underline{r}'\, G_e^o(x;r) G_p^o(x';r') U(r;r')\, \Omega(r,r';z,z')] = 0. \tag{12}$$

which implies that

$$\Omega(x,x';y,y') = \delta^4(x-y)\ \delta^3(\underline{x}'-\underline{y}') - i \int d^4z\ d^3\underline{z}'\ G_e^o(x;z)\ G_p^o(x';z')$$

$$U(z;z')\ \Omega(z,z';y,y') \quad . \tag{13}$$

Because of the translational invariance in time, $\Omega(x,x';y,y')$ can depend only on the time difference t_x-t_y. Thus, the generalized Fourier transform, can be introduced for Ω i.e.

$$\Omega(x,x';y,y') = \sum_{\underline{m},\underline{n};\underline{m}',\underline{n}'} \Psi_{\underline{m}}(\underline{x})\ \Phi_{\underline{n}}(\underline{x}') \int \frac{d\omega}{2\pi}\ e^{-i\omega(t_x-t_y)}$$

$$\Omega_{\underline{m},\underline{n};\underline{m}',\underline{n}'}(\omega)\ \Psi^*_{\underline{m}'}(\underline{y})\ \Phi^*_{\underline{n}'}(\underline{y}') \quad . \tag{14}$$

Using this result to Fourier transform (13) yields

$$\sum_{\underline{m},\underline{n};\underline{m}',\underline{n}'} \Psi_{\underline{m}}(\underline{x})\ \Phi_{\underline{n}}(\underline{x}') \int \frac{d\omega}{2\pi}\ e^{-i\omega(t_x-t_y)}\ \Omega_{\underline{m},\underline{n};\underline{m}',\underline{n}'}(\omega)\Psi^*_{\underline{m}'}(y)\Phi^*_{\underline{n}'}(\underline{y}')$$

$$= \frac{1}{2\pi}\int e^{i\underline{k}\cdot(\underline{x}-\underline{y})}d\underline{k} \int \frac{d\omega}{2\pi}\ e^{-i\omega(t_x-t_y)}\ \frac{1}{2\pi}\int d\underline{k}_2\ e^{i\underline{k}_2\cdot(\underline{x}'-\underline{y}')}$$

$$- i \int dt_z\ d^3\underline{z}\ d^3\underline{z}'\ \frac{1}{V}\sum_{\underline{p}_1} e^{i\underline{p}_1\cdot(\underline{z}-\underline{z}')}\ U_s(\underline{p}_1)\ \sum_{\underline{p}_2}\int \frac{d\omega_2}{2\pi}\ \Psi_{\underline{p}_2}(\underline{x})\Psi^*_{\underline{p}_2}(\underline{z})$$

$$e^{i\omega_2(t_x-t_z)}\ G_e^o(\underline{p}_2;\omega_2)\ \sum_{\underline{p}_3}\int\frac{d\omega_3}{2\pi}\ \Phi_{\underline{p}_3}(\underline{x}')\ \Phi^*_{\underline{p}_3}(\underline{z}')\ e^{-i\omega_3(t_{x'}-t_{z'})}$$

$$G_p^o(\underline{p}_3;\omega_3)\ \sum_{\underline{m},\underline{n};\underline{m}',\underline{n}'}\Psi_{\underline{m}'}(\underline{z})\Phi_{\underline{n}}(\underline{z}')\int\frac{d\omega}{2\pi}\ e^{-i\omega(t_z-t_y)}\Omega_{\underline{m},\underline{n};\underline{m}',\underline{n}'}(\omega)$$

$$\Psi^*_{\underline{m}'}(\underline{y})\ \Phi^*_{\underline{n}'}(\underline{y}') \quad . \tag{15}$$

where $U_s(\underline{p}_1)$ is the usual Fourier transform of the static effective potential $U_s(\underline{x},\underline{x}')$. Carrying out the trivial integrals and summations and interchanging dummy variables yields

$$\sum_{\underline{p}_2,\underline{p}_3;\underline{m}',\underline{n}'} \Psi_{\underline{p}_2}(\underline{x})\ \Phi_{\underline{p}_3}(\underline{x}') \int \frac{d\omega}{2\pi} e^{-i\omega(t_x-t_y)}\ \Psi^*_{\underline{m}'}(\underline{y})\ \Phi^*_{\underline{n}'}(\underline{y}')$$

$$[\Omega_{\underline{p}_2,\underline{p}_3;\underline{m}',\underline{n}'}(\omega) - \delta_{\underline{p}_2,\underline{m}'}\ \delta_{\underline{p}_3,\underline{n}'} + i \sum_{\underline{k},\underline{k}'} \{\frac{1}{V} \sum_{\underline{p}_1} U_s(\underline{p}_1)$$

$$\int \Psi_{\underline{m}}(\underline{z})\ e^{i\underline{p}_1\cdot\underline{z}}\ \Psi^*_{\underline{k}}(\underline{z}) \int \Phi_{\underline{n}}(\underline{z}')\ e^{-i\underline{p}_1\cdot\underline{z}'}\ \Phi_{\underline{k}'}(\underline{z}')d^3\underline{z}'\}$$

$$\int \frac{d\omega_2}{2\pi}\ \Omega_{\underline{p}_2,\underline{p}_3;\underline{m}',\underline{n}'}(\omega)\ \ G^o_e(m,\omega_2)\ \ G^o_p(p_3;\omega_3-\omega)] \qquad (16)$$

which implies that

$$\Omega_{\underline{m},\underline{n};\underline{m}',\underline{n}'}(\omega) = \delta_{\underline{m},\underline{m}'}\ \delta_{\underline{n},\underline{n}'} - i \sum_{\underline{k},\underline{k}'} H_{\underline{m},\underline{n};\underline{k},\underline{k}'}$$

$$\int \frac{d\varepsilon}{2\pi}\ \Omega_{\underline{k},\underline{k}';\underline{m}',\underline{n}'}(\omega)\ G^o_e(\underline{m};\varepsilon)\ G^o_p(\underline{n};\omega-\varepsilon) \qquad (17)$$

where

$$H_{\underline{m},\underline{n};\underline{k},\underline{k}'} = \frac{1}{V} \sum_{\underline{q}} U_s(\underline{q})\ [\underline{m}\ |\underline{q}|\ \underline{k}]^e\ [\underline{n}\ |-\underline{q}|\ \underline{k}']^p \qquad (18)$$

and

$$[\underline{m}\,|\underline{q}|\,\underline{k}]^{e} = \int \Psi_{\underline{m}}(\underline{x})\; e^{i\underline{q}.\underline{x}}\; \Psi^{*}_{\underline{k}}(\underline{x})\; d^{3}\underline{x} \tag{19}$$

$$[\underline{n}\,|-\underline{q}|\,\underline{k}']^{p} = \int \Phi_{\underline{n}}(\underline{x})\; e^{-i\underline{q}.\underline{x}}\; \Phi^{*}_{\underline{k}'}(\underline{x})\; d^{3}\underline{x} \quad . \tag{20}$$

Substituting equation (10) into (6) results in

$$R(\underline{p}) = \frac{(-i)^{2}\lambda}{V} \int d^{3}\underline{x}\; d^{3}\underline{y}\; e^{-i\underline{p}.(\underline{x}-\underline{y})} \int d^{4}z\; d^{3}\underline{z}'\; \Omega(\underline{x},\underline{x};\underline{z},\underline{z}')$$

$$G^{o}_{e}(\underline{z};\underline{y})\; G^{o}_{p}(\underline{z}';\underline{y}) \tag{21}$$

Fourier analysing the right hand side of this equation gives

$$R(\underline{p}) = \frac{(-i)^{2}\lambda}{V} \int d^{3}\underline{x}\; d^{3}\underline{y}\; e^{-i\underline{p}.(\underline{x}-\underline{y})} \int dt_{z}\; d^{3}\underline{z}\; d^{3}\underline{z}'$$

$$\sum_{\underline{m},\underline{n};\underline{m}',\underline{n}'} \Psi_{\underline{m}}(\underline{x})\; \Phi_{\underline{n}}(\underline{x}) \int \frac{d\omega}{2\pi}\; e^{-i\omega(t_{x}-t_{z})}\; \Omega_{\underline{m},\underline{n};\underline{m}',\underline{n}'}(\omega)$$

$$\Psi^{*}_{\underline{m}'}(\underline{z})\; \Phi^{*}_{\underline{n}'}(z') \sum_{\underline{\ell}} \Psi_{\underline{\ell}}(\underline{z})\; \Psi^{*}_{\underline{\ell}}(\underline{y}) \int \frac{d\omega_{1}}{2\pi}\; e^{-i\omega_{1}(t_{z}-t_{y})}\; G^{o}_{e}(\underline{\ell};\omega_{1})$$

$$\sum_{\underline{\ell}'} \Phi_{\underline{\ell}'}(\underline{z}')\; \Phi^{*}_{\underline{\ell}'}(\underline{y}) \int \frac{d\omega_{2}}{2\pi}\; e^{-i\omega_{2}(t_{z}-t_{y})}\; G^{o}_{p}(\underline{\ell}';\omega_{2}) \quad . \tag{22}$$

On rearranging terms

$$R(\underline{p}) = \frac{(-i)^2\lambda}{V} \sum_{\underline{m},\underline{n};\underline{\ell},\underline{\ell}'} \int \Psi_{\underline{m}}(\underline{x})\ e^{-i\underline{p}.\underline{x}}\ \Phi_{\underline{n}}(\underline{x})\ d^3\underline{x}$$

$$\int \Psi^*_{\underline{\ell}}(\underline{y})\ e^{i\underline{p}.\underline{y}}\ \Phi^*_{\underline{\ell}'}(\underline{y})\ d^3\underline{y} \int \frac{d\omega}{2\pi}\frac{d\omega_1}{2\pi}\frac{d\omega_2}{2\pi} \int dt_z\ e^{-it_x(\omega-\omega_1-\omega_2)}$$

$$e^{it_z(\omega-\omega_1-\omega_2)} \sum_{\underline{m}',\underline{n}'} \Omega_{\underline{m},\underline{n};\underline{m}',\underline{n}'}(\omega)\ G^o_e(\underline{\ell};\omega_1)\ G^o_p(\underline{\ell}';\omega_2)$$

$$\int d^3\underline{z}\ d^3\underline{z}'\ \Psi^*_{\underline{m}'}(\underline{z})\ \Psi_{\underline{\ell}}(\underline{z})\ \Phi_{\underline{\ell}'}(\underline{z}')\ \Phi^*_{\underline{n}'}(\underline{z}') \quad . \tag{23}$$

Carrying out the integral over dt_z, $d^3\underline{z}$, $d^3\underline{z}'$and subsequent summations over $\underline{m}'$, $\underline{n}'$ gives

$$R(\underline{p}) = \frac{(-i)^2\lambda}{V} \sum_{\underline{m},\underline{n};\underline{\ell},\underline{\ell}'} I_{\underline{m},\underline{n}}(\underline{p})\ I^*_{\underline{\ell},\underline{\ell}'}(\underline{p})$$

$$\int \frac{d\omega}{2\pi}\ \frac{d\omega_1}{2\pi}\ \frac{d\omega_2}{2\pi}\ e^{i\omega o^+}\ \delta(\omega-\omega_1-\omega_2)\ \Omega_{\underline{m},\underline{n};\underline{\ell},\underline{\ell}'}(\omega)$$

$$G^o_e(\underline{\ell};\omega_1)\ G^o_p(\underline{\ell}';\omega_2) \tag{24}$$

where the rotation

$$I_{\underline{m},\underline{n}}(\underline{p}) = \int \Psi_{\underline{m}}(\underline{x})\ e^{-i\underline{p}.\underline{x}}\ \Phi_{\underline{n}}(\underline{x})\ d^3\underline{x} \tag{25}$$

has been introduced. Doing the integral over ω_2 and changing dummy variables yields

$$R(\underline{p}) = \frac{(-i)^2\lambda}{V} \sum_{\underline{m},\underline{n};\underline{m}',\underline{n}'} I_{\underline{m},\underline{n}}(\underline{p})\ I^*_{\underline{m}',\underline{n}'}(\underline{p})$$

$$\int \frac{d\omega}{2\pi} \int \frac{d\varepsilon}{2\pi}\ e^{i\omega o^+}\ \Omega_{\underline{m},\underline{n};\underline{m}',\underline{n}'}(\omega)\ G^o_e(\underline{m}';\varepsilon) G^o_p(\underline{n}';\omega-\varepsilon). \quad (26)$$

The ε integration can now easily be done with the help of equation (9) by contour integration i.e.

$$\int \frac{d\varepsilon}{2\pi}\ G^o_e(\underline{m}';\varepsilon)\ G^o_p(\underline{n}';\omega-\varepsilon)$$

$$= \int \frac{d\varepsilon}{2\pi} \left| \frac{\theta^{u.o.}_e(\underline{m}')}{E^e_{\underline{m}',-\varepsilon-io^+}} + \frac{\theta^o_e(\underline{m}')}{E^e_{\underline{m}',-\varepsilon+io^+}} \right| \left| \frac{\theta^{u.o.}_p(\underline{n}')}{E^p_{\underline{n}',-\omega+\varepsilon-io^+}} + \frac{\theta^o_p(\underline{n}')}{E^p_{\underline{n}',-\omega+\varepsilon+io^+}} \right|$$

$$= i \left| \frac{\theta^{u.o.}_e(\underline{m}')\ \theta^{u.o.}_p(\underline{n}')}{E^p_{\underline{n}',+E^e_{\underline{m}',-\omega-io^+}}} - \frac{\theta^o_e(\underline{m}')\ \theta^o_p(\underline{n}')}{E^e_{\underline{m}',+E^p_{\underline{n}',-\omega+io^+}}} \right|$$

$$= i\ [P^+_{\underline{m}',\underline{n}'}(\omega) + P^-_{\underline{m}',\underline{n}'}(\omega)] \quad (27)$$

where the functions

$$P^+_{\underline{m}',\underline{n}'}(\omega) = \frac{\theta^{u.o.}_e(\underline{m}')\ \theta^{u.o.}_p(\underline{n}')}{E^p_{\underline{n}',+E^e_{\underline{m}',-\omega-io^+}}} \quad (28)$$

and

$$P^{-}_{\underline{m}',\underline{n}'}(\omega) = - \frac{\theta^{o}_{e}(\underline{m}')\ \theta^{o}_{p}(\underline{n}')}{E^{p}_{\underline{n}'}+E^{e}_{\underline{m}'}-\omega+i\sigma^{+}} \quad . \tag{29}$$

Hence equation (26) becomes

$$R(\underline{p}) = \frac{-i\lambda}{V} \sum_{\underline{m},\underline{n};\underline{m}',\underline{n}'} I_{\underline{m},\underline{n}}(\underline{p})\ I^{*}_{\underline{m}',\underline{n}'}(\underline{p})$$

$$\int \frac{d\omega}{2\pi}\, e^{i\omega\sigma^{+}}\, \Omega_{\underline{m},\underline{n};\underline{m}',\underline{n}'}(\omega)\,[P^{+}_{\underline{m}',\underline{n}'}(\omega) + P^{-}_{\underline{m}',\underline{n}'}(\omega)] \,. \tag{30}$$

The result of equation (27) can also be applied to equation (17) to give

$$\Omega_{\underline{m},\underline{n};\underline{m}',\underline{n}'}(\omega) = \delta_{\underline{m},\underline{m}'}\ \delta_{\underline{n},\underline{n}'} + [P^{+}_{\underline{m},\underline{n}}(\omega) + P^{-}_{\underline{m},\underline{n}}(\omega)]$$

$$\sum_{\underline{k},\underline{k}'} H_{\underline{m},\underline{n};\underline{k},\underline{k}'}\ \Omega_{\underline{k},\underline{k}';\underline{m}',\underline{n}'}(\omega) \quad . \tag{31}$$

In order to further simplify equation (30) a simple matrix notation is introduced. In this notation (30) reads

$$R(\underline{p}) = \frac{-i\lambda}{V} \sum_{\underline{m},\underline{n};\underline{m}',\underline{n}'} I_{\underline{m},\underline{n}}(\underline{p})\ I^{*}_{\underline{m}',\underline{n}'}(\underline{p})$$

$$\int \frac{d\omega}{2\pi}\, e^{i\omega\sigma^{+}} \langle\, \underline{m}\ \underline{n} \mid\ \Omega(\omega)\,[P^{+}(\omega) + P^{-}(\omega)] \mid \underline{m}'\ \underline{n}' \rangle \tag{32}$$

and (31) becomes

$$\Omega(\omega) = 1 + [P^{+}(\omega) + P^{-}(\omega)]\, H\Omega(\omega) \quad . \tag{33}$$

The whole integral of equation (32) can be easily performed by treating the integrals that arise when $\Omega(\omega)$ is expanded with the help of (33) separately. The first term in the expansion is

$$\int \frac{d\omega}{2\pi}\, e^{i\omega o^{+}}\, [P^{+}_{\underline{m},\underline{n}}(\omega) + P^{-}_{\underline{m},\underline{n}}(\omega)]\, \delta_{\underline{m},\underline{m}'}\, \delta_{\underline{n},\underline{n}'} \quad . \tag{34}$$

Using the definitions of $P^{+}(\omega)$ and $P^{-}(\omega)$ this integral can easily be performed by contour integration, and closing the contour in the upper half plane $P^{+}(\omega)$ can be neglected since there are no poles. Hence

$$i\, \theta^{o}_{e}(\underline{m})\, \theta^{o}_{p}(\underline{n})\, \delta_{\underline{m},\underline{m}'}\, \delta_{\underline{n},\underline{n}'} \tag{35}$$

results. Other possible members in the expansion are of the type

$$e^{i\omega o^{+}}\, (P^{+} + P^{-})\, H\, (P^{+} + P^{-}) \ldots H\, (P^{+} + P^{-}) \tag{36}$$

which reduce to

$$P^+ H P^+ H \ldots\ldots P^+ \qquad (37)$$

$$P^- H P^- H \ldots\ldots P^- \qquad (38)$$

$$P^- H P^+ H \ldots\ldots P^+ \qquad (39)$$

$$P^+ H P^- H \ldots\ldots P^+ \qquad (40)$$

$$P^+ H P^- H \ldots\ldots P^- \qquad (41)$$

$$\ldots\ldots\ldots\ldots\ldots ,$$

the exponential factor being dropped as the contour can now be defined unambigously. Neither (37) or (38) contribute as the integration contour encloses a perfectly analytic function in one of the half-planes. Terms with two or more P^- can also be discarded for the following simple reason. For each P^- in a term there exists a theta function of the type $\theta^o_p(\underline{n})$. These can be used to eliminate one of the intermediate summations over the positron states (cf equation (43) below), so that the remaining expression is of the order of $\frac{1}{V}$, which vanishes in the limit of infinite volume since the rest of the expression remains finite. Hence the only remaining terms are those with at least one P^- and any number of P^+. These can simply be treated by introducing the intermediate amplitude Ω^o defined by

$$\Omega^o = 1 + P^+ H \Omega^o \quad .$$

Then clearly all the remaining terms as well as (34) above are included in $\Omega^o P^- \Omega^{o\dagger}$. Hence equation (32) now reduces to

$$R(\underline{p}) = \frac{-i\lambda}{V} \sum_{\underline{m},\underline{n};\underline{m}',\underline{n}'} I_{\underline{m},\underline{n}}(\underline{p})\ I^*_{\underline{m}',\underline{n}'}(\underline{p})\ .$$

$$\int \frac{d\omega}{2\pi}\, e^{i\omega o^+} \langle \underline{m},\underline{n} \mid \Omega^o(\omega)\ P^-(\omega)\ \Omega^{o\dagger}(\omega) \mid \underline{m}'\ \underline{n}' \rangle\ . \quad (42)$$

Introducing a set of intermediate states into this equation gives

$$R(\underline{p}) = \frac{-i\lambda}{V} \sum_{\underline{m},\underline{n};\underline{m}',\underline{n}'} I_{\underline{m},\underline{n}}(\underline{p})\ I^*_{\underline{m}',\underline{n}'}(\underline{p})$$

$$\int \frac{d\omega}{2\pi}\, e^{i\omega o^+} \sum_{\underline{s},\underline{t};\underline{s}',\underline{t}'} \langle \underline{m}\ \underline{n} \mid \Omega^o(\omega) \mid \underline{s}\ \underline{t} \rangle$$

$$\langle \underline{s}\ \underline{t} \mid P^-(\omega) \mid \underline{s}'\ \underline{t}' \rangle \quad \langle \underline{s}'\ \underline{t}' \mid \Omega^{o\dagger}(\omega) \mid \underline{m}'\ \underline{n}' \rangle . \quad (43)$$

Noting that all the singularities of the Ω's are in the lower half plane, the contour is closed above, picking up the P^- contribution to yield

$$R(\underline{p}) = \frac{\lambda}{V} \sum_{\underline{s},\underline{t}} \theta^o_e(\underline{s})\ \theta^o_p(\underline{t})\ \Big[\sum_{\underline{m},\underline{n}} I_{\underline{m},\underline{n}}(\underline{p})\ \Omega^o{}_{\underline{m},\underline{n};\underline{s},\underline{t}}(E^e_{\underline{s}}+E^p_{\underline{t}}) \Big]$$

$$\Big[\sum_{\underline{m}',\underline{n}'} I^*_{\underline{m}',\underline{n}'}(\underline{p})\ \Omega^{o\dagger}{}_{\underline{s},\underline{t};\underline{m}',\underline{n}'}(E^e_{\underline{s}}+E^p_{\underline{t}}) \Big] \quad (44)$$

which can be rewritten as

$$R(\underline{p}) = \frac{\lambda}{V} \sum_{\underline{m}',\underline{n}'} \theta_e^o(\underline{m}')\ \theta_p^o(\underline{n}')$$

$$\left| \sum_{\underline{m},\underline{n}} I_{\underline{m},\underline{n}}(\underline{p})\ \Omega^o_{\underline{m},\underline{n};\underline{m}',\underline{n}'}(E^p_{\underline{n}'}+E^e_{\underline{m}'}) \right|^2 \qquad (45)$$

Since the positron is thermalized on annihilating[7,8] the summation over $\underline{n}'$ is equivalent to setting $\underline{n}' = 0$ since all other states are empty. Finally equation (45) can be put in a more physical form by making the transformation

$$\Omega^o_{\underline{m},\underline{n};\underline{m}',o} = \delta_{\underline{m},\underline{m}'}\ \delta_{\underline{n},o} + \chi^o_{\underline{m},\underline{n};\underline{m}',o} \qquad (46)$$

and substituting into equation (31)

$$\delta_{\underline{m},\underline{m}'}\ \delta_{\underline{m},o} + \chi^o_{\underline{m},\underline{n};\underline{m}',o} = \delta_{\underline{m},\underline{m}'}\ \delta_{\underline{n},o} +$$

$$P^+_{\underline{m},\underline{n}}(\omega) \sum_{\underline{k},\underline{k}'} H_{\underline{m},\underline{n};\underline{k},\underline{k}'} \left[\delta_{\underline{k},\underline{m}'}\ \delta_{\underline{k},o} + \chi^o_{\underline{k},\underline{k}';\underline{m}',o}\right] . \qquad (47)$$

This implies that

$$\chi^o_{\underline{m},\underline{n};\underline{m}',o} = P^+_{\underline{m},\underline{n}}(\omega) \left[H_{\underline{m},\underline{n};\underline{m}',o} + \sum_{\underline{k},\underline{k}'} H_{\underline{m},\underline{n};\underline{k},\underline{k}'} \chi^o_{\underline{k},\underline{k}';\underline{m}',o}\right] \qquad (48)$$

and

$$R(\underline{p}) = \frac{\lambda}{V} \sum_{\underline{m}'} \theta_e^o(\underline{m}') \left| I_{\underline{m}',o}(\underline{p}) + \sum_{\underline{m},\underline{n}} I_{\underline{m},\underline{n}}(\underline{p}) \chi^o_{\underline{m},\underline{n};\underline{m}',o}(E_o^p + E_{\underline{m}'}^e) \right|^2. \tag{49}$$

This equation was obtained by Carbotte in reference 17 and is of basic importance to this thesis. In the form (49) it is completely general within the ladder framework and no approximations have as yet been made. It can easily be applied to describe both the core and conduction electron annihilation and hence a complete physical interpretation is given in the appropriate section of the thesis. However a mere glance shows that the rate $R(\underline{p})$ is proportional to the absolute square of the sum of two terms. The first gives the I.P.M. result and is the pth Fourier component of the core electron and positron single particle wavefunction overlap. The second term is a correction which describes in an approximate way the correlation in the relative motion of the annihilating pair.

APPENDIX B

CORE ANNIHILATION FORMULA

Expression (A-49) is now further reduced to deal with core annihilation in simple metals. It is important to bear this in mind because some of the approximations, that will be made, only hold for simple metals but not in general e.g. the case of solid Argon treated in chapter 3.

In order to evaluate equation (A-48) the following simplifying approximation has to be made. In a Wigner Seitz cell a core state is highly localized about the centre, while a conduction state extends appreciably throughout the cell. Hence the matrix element $[\underline{m} \,|\underline{q}|\, \underline{k}]$, where $\underline{k}$ is a core state and $\underline{m}$ is a conduction electron or positron wavefunction, is very sensitive to the deviations of $\underline{m}$ from a plane wave. Thus band effects are of tantamount importance in the evaluation of such matrix elements. This point is clearly seen from figure 1 where a plot of the overlap between core and conduction matrix element is shown for Sodium. In such evaluations the mesh for the integration has to be carefully chosen. However if $\underline{k}$ is also a conduction state, then it is quite reasonable, at least for simple cases

like Sodium, to set

$$[\underline{m} \,|\underline{q}|\, \underline{k}] = \delta_{\underline{m}+\underline{q}-\underline{k},o} \quad . \tag{1}$$

That this is a good approximation can be inferred by examining figure 5, where it is seen that the major portion of the curves are plane-wave like. This point can perhaps be seen more clearly by looking at the expansion of a conduction state in reciprocal space i.e.

$$\Psi_{\underline{k}}(\underline{x}) = \frac{1}{\sqrt{V}} e^{i\underline{k}.\underline{x}} \sum_{\underline{a}} e^{i\underline{a}.\underline{x}} u_{\underline{k}}(\underline{a}) \quad . \tag{2}$$

For the simple metals the $u_{\underline{k}}(\underline{a} = o)$ term dominates and is approximately equal to one. As a result the $\Psi_{\underline{k}}(\underline{x})$ are nearly plane waves. However figure 16 suggests that this is not the case for Argon. The $\underline{a} = o$ term does not dominate the expansion (2) and several of the $\underline{a}$ terms have to be included. Hence this approximation, whilst good for simple metals, is not good for non-metals such as Argon. In fact this is the very reason why the calculations for Argon are only carried to Born approximation in chapter 3.

Applying (1) to (A-18) yields

$$H_{\underline{m},\underline{n};n\ell m_s,o} \simeq \frac{1}{V} U_s(\underline{n}) \; [\underline{m}|\underline{n}|n\ell m_s]^e \tag{3}$$

and

$$H_{\underline{m},\underline{n};\underline{k},\underline{k}'} \simeq \frac{1}{V} U_s(\underline{n}-\underline{k}') \; \delta_{\underline{m}+\underline{n},\underline{k}+\underline{k}'} \tag{4}$$

where it should be clearly noted that in (3) the corresponding positron matrix element does not appear since it is treated as a plane wave. Hence (A-48) can be written as

$$\chi^{o}_{\underline{m},\underline{n};n\ell m_s,o}(\omega) = P^{+}_{\underline{m},\underline{n}}(\omega) \; \frac{1}{V} U_s(\underline{n}) \; [\underline{m}|\underline{n}|n\ell m_s]^{e} +$$

$$P^{+}_{\underline{m},\underline{n}}(\omega) \sum_{\underline{k}} \frac{1}{V} U_s(\underline{k}-\underline{m}) \chi^{o}_{\underline{k},\underline{n}+\underline{m}-\underline{k};n\ell m_s,o}(\omega) \quad . \tag{5}$$

Since the $\underline{m}$ and $\underline{n}$ momenta refer to excited states, on account of $P^{+}_{\underline{m},\underline{n}}(\omega)$, the quadratic approximation for $E^{e}_{\underline{m}}$ and $E^{p}_{\underline{n}}$ can be made. This measures the electronic energies from the bottom of the 3s band and positron energies from the 1s band.

Also $I_{\underline{m},\underline{n}}(\underline{p})$ can be replaced by $\delta_{\underline{m}+\underline{n},\underline{p}}$ where $\underline{m}$ and $\underline{n}$ refer to unoccupied states as in (A-49). Hence

$$\chi^{o}_{\underline{m},\underline{p}-\underline{m};n\ell m_s,o}(\omega) = J^{1}_{\underline{m},\underline{p}-\underline{m}}(\omega) [\underline{m} \; |\underline{p}-\underline{m}| \; n\ell m_s]^{e} +$$

$$\sum_{\underline{k}} J^{2}_{\underline{m},\underline{p}-\underline{m};\underline{k}}(\omega) \; \chi^{o}_{\underline{k},\underline{p}-\underline{k};n\ell m_s,o}(\omega) \tag{6}$$

where

$$J^{1}_{\underline{m},\underline{p}-\underline{m}}(\omega) = \frac{1}{V} P^{+}_{\underline{m},\underline{p}-\underline{m}}(\omega) \; U_s(\underline{p}-\underline{m})$$

and

$$J^2_{\underline{m},\underline{p}-\underline{m};\underline{k}}(\omega) = \frac{1}{V} P^+_{\underline{m},\underline{p}-\underline{m}}(\omega)\ U_s(\underline{k}-\underline{m}) \quad . \tag{7}$$

In order to solve (6) the trial solution

$$\chi^o_{\underline{m},\underline{p}-\underline{m};n\ell m_s,o}(\omega) = \sum_{\underline{k}} \Phi_{\underline{m},\underline{p}-\underline{m};\underline{k}}(\omega)\ J^1_{\underline{k},\underline{p}-\underline{k}}(\omega)$$

$$[\underline{k}\ |\underline{p}-\underline{k}|\ n\ell m_s]^e \tag{8}$$

is taken. Substituting into (6) yields

$$\sum_{\underline{k}} \Phi_{\underline{m},\underline{p}-\underline{m};\underline{k}}(\omega)\ J^1_{\underline{k},\underline{p}-\underline{k}}(\omega)\,[\underline{k}\ |\underline{p}-\underline{k}|\ n\ell m_s]^e$$

$$= J^1_{\underline{m},\underline{p}-\underline{m}}(\omega)\ [\underline{m}\ |\underline{p}-\underline{m}|\ n\ell m_s]^e +$$

$$\sum_{\underline{k}'} J^2_{\underline{m},\underline{p}-\underline{m};\underline{k}'}(\omega) \sum_{\underline{k}} \Phi_{\underline{k}';\underline{p}-\underline{k}';\underline{k}}(\omega)$$

$$J^1_{\underline{k},\underline{p}-\underline{k}}(\omega)\ [\underline{k}\ |\underline{p}-\underline{k}|\ n\ell m_s]^e \quad .$$

Rearranging terms

$$\sum_{\underline{k}} J^1_{\underline{k},\underline{p}-\underline{k}}(\omega)\ [\underline{k}\ |\underline{p}-\underline{k}|\ n\ell m_s]^e\ [\Phi_{\underline{m},\underline{p}-\underline{m};\underline{k}} - \delta_{\underline{m},\underline{k}}$$

$$\sum_{\underline{k}'} J^2_{\underline{m},\underline{p}-\underline{m}';\underline{k}'}(\omega)\ \Phi_{\underline{k}',\underline{p}-\underline{k}';\underline{k}}(\omega)\,]$$

which implies that

$$\Phi_{\underline{m},\underline{p}-\underline{m};\underline{k}}(\omega) = \delta_{\underline{m},\underline{k}} + \sum_{\underline{k}'} J^2_{\underline{m},\underline{p}-\underline{m};\underline{k}'}(\omega)\ \Phi_{\underline{k}',\underline{p}-\underline{k}';\underline{k}}(\omega). \qquad (9)$$

Summing both sides over $\underline{m}$ and introducing the notation

$$\chi_{\underline{p}}(\underline{k};\omega) = \sum_{\underline{m}} \Phi_{\underline{m},\underline{p}-\underline{m};\underline{k}}(\omega) \qquad (10)$$

yields

$$\chi_{\underline{p}}(\underline{k};\omega) = \sum_{\underline{m}} \delta_{\underline{m},\underline{k}} + \sum_{\underline{m}} \sum_{\underline{k}'} \frac{1}{V} P^{+}_{\underline{m},\underline{p}-\underline{m}}(\omega)\ U_s(\underline{k}'-\underline{m})\Phi_{\underline{k}',\underline{p}-\underline{k}';\underline{k}}(\omega). \qquad (11)$$

Interchanging dummies on the right hand side and using (10)

$$\chi_{\underline{p}}(\underline{k};\omega) = 1 + \frac{1}{V}\sum_{\underline{m}} \chi_{\underline{p}}(\underline{m};\omega)\ P^{+}_{\underline{m},\underline{p}-\underline{m}}(\omega)\ U_s(\underline{k}-\underline{m}) \quad . \qquad (12)$$

Introducing the notation

$$J^{n\ell m s}_{\underline{p}} = \sum_{\underline{m}} \chi^{o}_{\underline{m},\underline{p}-\underline{m};n\ell m s,o}(E^{p}_{o} + E^{e}_{n\ell m s})$$

equation (8) becomes

$$J^{n\ell m s}_{\underline{p}} = \sum_{\underline{k}} \sum_{\underline{m}} \Phi_{\underline{m},\underline{p}-\underline{m};\underline{k}}(E^{p}_{o} + E^{e}_{n\ell m s})\ J^{1}_{\underline{k},\underline{p}-\underline{k}}(E^{p}_{o} + E^{e}_{n\ell m s})$$

$$[\underline{k}\ |\underline{p}-\underline{k}|\ n\ell m s]^{e} \quad . \qquad (13)$$

This is the second expression of the square in (A-49) which on using (10) becomes

$$J_{\underline{p}}^{n\ell m\underline{s}} = \frac{1}{V} \sum_{\underline{k}} \chi_{\underline{p}}(\underline{k}; E_o^p + E^e_{n\ell m\underline{s}}) P^+_{\underline{k},\underline{p}-\underline{k}}(E_o^p + E^e_{n\ell m\underline{s}}) U_s(\underline{p}-\underline{k}). \quad (14)$$

Using the energy convention introduced above it now follows that $E_o^p = 0$ and $E^e_{n\ell m\underline{s}} = -\Delta_{n\ell}$ where $\Delta_{n\ell}$ is the band gap between the core level $(n\ell m\underline{s})$ and the bottom of the 3s band. Equation (14) finally becomes

$$J_{\underline{p}}^{n\ell m\underline{s}} = \frac{1}{V} \sum_{\underline{k}} E_{\underline{p}}^{n\ell}(\underline{k}) \; [\underline{k} \; |\underline{p}-\underline{k}| \; n\ell m\underline{s}]^e \quad (15)$$

where

$$E_{\underline{p}}^{n\ell} = \chi_{\underline{p}}(\underline{k}; -\Delta_{n\ell}) \; P^+_{\underline{k},\underline{p}-\underline{k}}(-\Delta_{n\ell}) \; U_s(\underline{p}-\underline{k}) \quad . \quad (16)$$

This is the required result.

FIGURE CAPTIONS

FIGURE 1

The Hartree-Fock-Slater core wavefunctions for Sodium as given by Taylor[19]. Superimposed on these is the zero momentum O.P.W. This clearly shows that the core wavefunctions are greatest where the O.P.W. are smallest and vice versa.

FIGURE 2

The O.P.W. orthogonalization coefficients $A_{n\ell}(k)$ defined by equation (I-17) and the normalization constant A(k) defined by equation (I-19) for the Sodium core wavefunctions. Only momentum values greater than p_F are of interest.

FIGURE 3

The equivalent of figure 2 for Aluminum.

FIGURE 4

Solution of the integral equation (I-43) for the

amplitude $\chi^{n\ell}(\gamma,k)$ as a function of momentum k and for a number of γ values. Notice that $\chi^{n\ell}(\gamma,k)$ is defined only for $k > 1$, i.e., above the Fermi surface.

FIGURE 5

The k dependence of the quantity $G(k_F k,r)$ entering equation (I-41). The complex structure from the orthogonalization parts smooths out for sufficient large k.

FIGURE 6

The function $S^{n\ell}(o;r)$ for the 2p and 2s shell.

FIGURE 7

The γ dependence of the function $S^{n\ell}(\gamma;r)$ for the 2p shell. The lack of oscillations implies that the correlation corrections have much the same variation with r as the I.P.M. term.

FIGURE 8

The overlap integrals $J^{\pm}_{2s}(k)$ for the 2s electronic shells showing the similarity of the J^- to the J^+ term.

FIGURE 9

The equivalent of figure 8 for the 2p electronic shell.

FIGURE 10

The contribution of the core electrons to the two-photon counting rate for both Na and Al. The enhanced curves are nearly simple multiples of the I.P.M. curves.

FIGURE 11

The two-photon counting rate for Na. The experimental data have not been corrected for background effects.

FIGURE 12

The two-photon counting rate for Al.

FIGURE 13

The reciprocal transform of the O.P.W.-positron wavefunction overlap as given by equation (2-12). As can be seen the momentum dependence only introduces an appreciable

error in the first and second shells otherwise it could be neglected.

FIGURE 14

The unenhanced lattice contribution to the annihilation rate. The units are such to allow easy comparison with figure 15.

FIGURE 15

The full enhanced lattice contribution to the annihilation rate. A bulging of the parabola is seen on comparison to figure 14 but both the central distribution and tails are equally enhanced.

FIGURE 16

The equivalent of figure 5 for Argon. The extra oscillation in the O.P.W. forces a first order calculation of the core theory.

FIGURE 17

The positron wavefunction for Argon. This is very similar to that given in reference 35.

FIGURE 18

The overlap integrals $J^{\pm}_{3s}(k)$ for the 3s electronic shells in Argon. These are not as closely matched as the Na case of figure 8.

FIGURE 19

The equivalent of figure 18 for the 3p electronic shell in Argon.

FIGURE 20

The annihilation rate for Argon. A rough fit was applied to the experimental points as given in reference 27. The units were chosen for easy reference to 27.

FIGURE 1

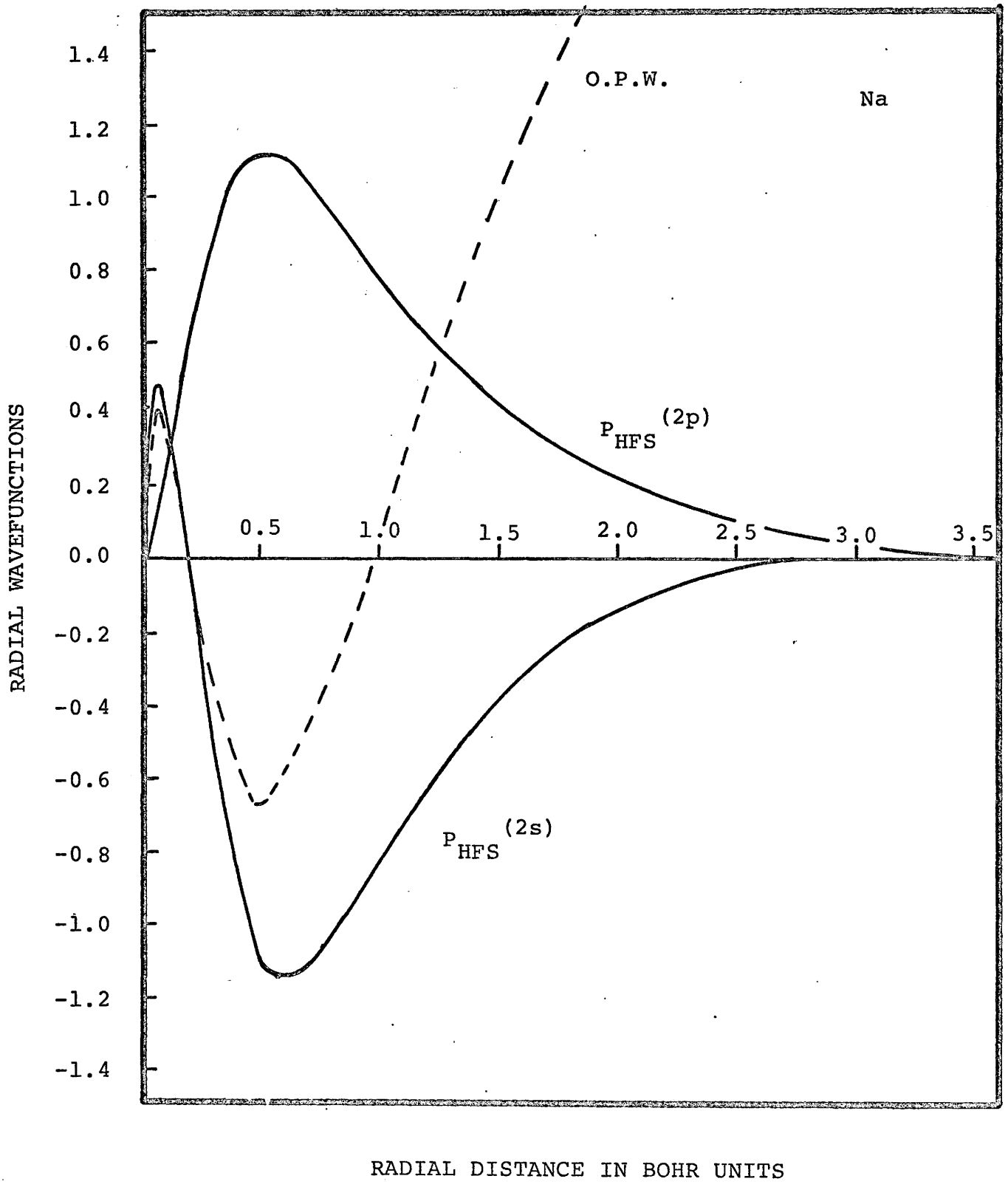
1.4
1.2
1.0
0.8
0.6
0.4
0.2
0.0
-0.2
-0.4
-0.6
-0.8
-1.0
-1.2
-1.4
0.5
1.0
1.5
2.0
2.5
3.0
3.5
O.P.W.
Na
$P_{HFS}(2p)$
$P_{HFS}(2s)$
RADIAL WAVEFUNCTIONS
RADIAL DISTANCE IN BOHR UNITS

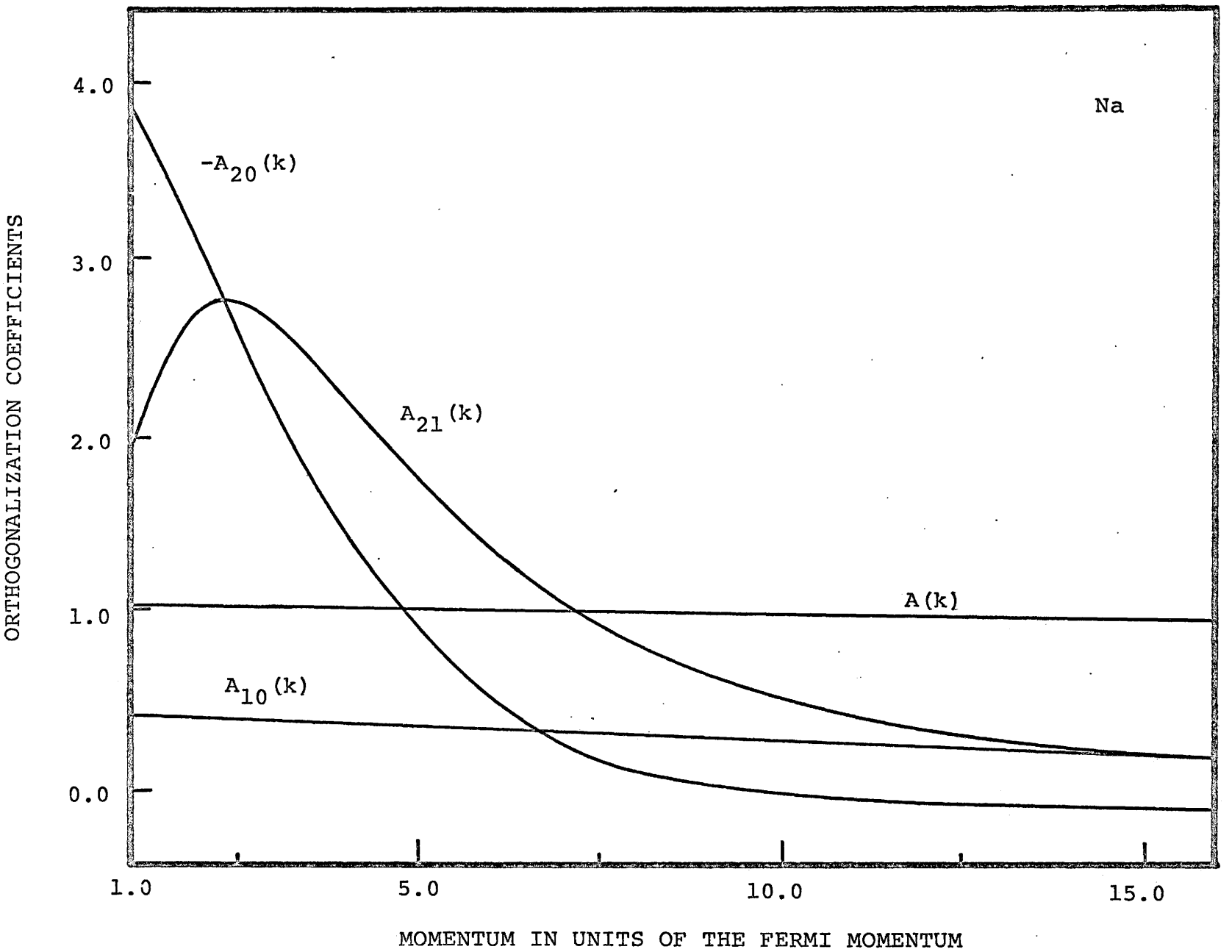
Na
$-A_{20}(k)$
$A_{21}(k)$
$A(k)$
$A_{10}(k)$
4.0
3.0
2.0
1.0
0.0
1.0
5.0
10.0
15.0
ORTHOGONALIZATION COEFFICIENTS
MOMENTUM IN UNITS OF THE FERMI MOMENTUM

FIGURE 2

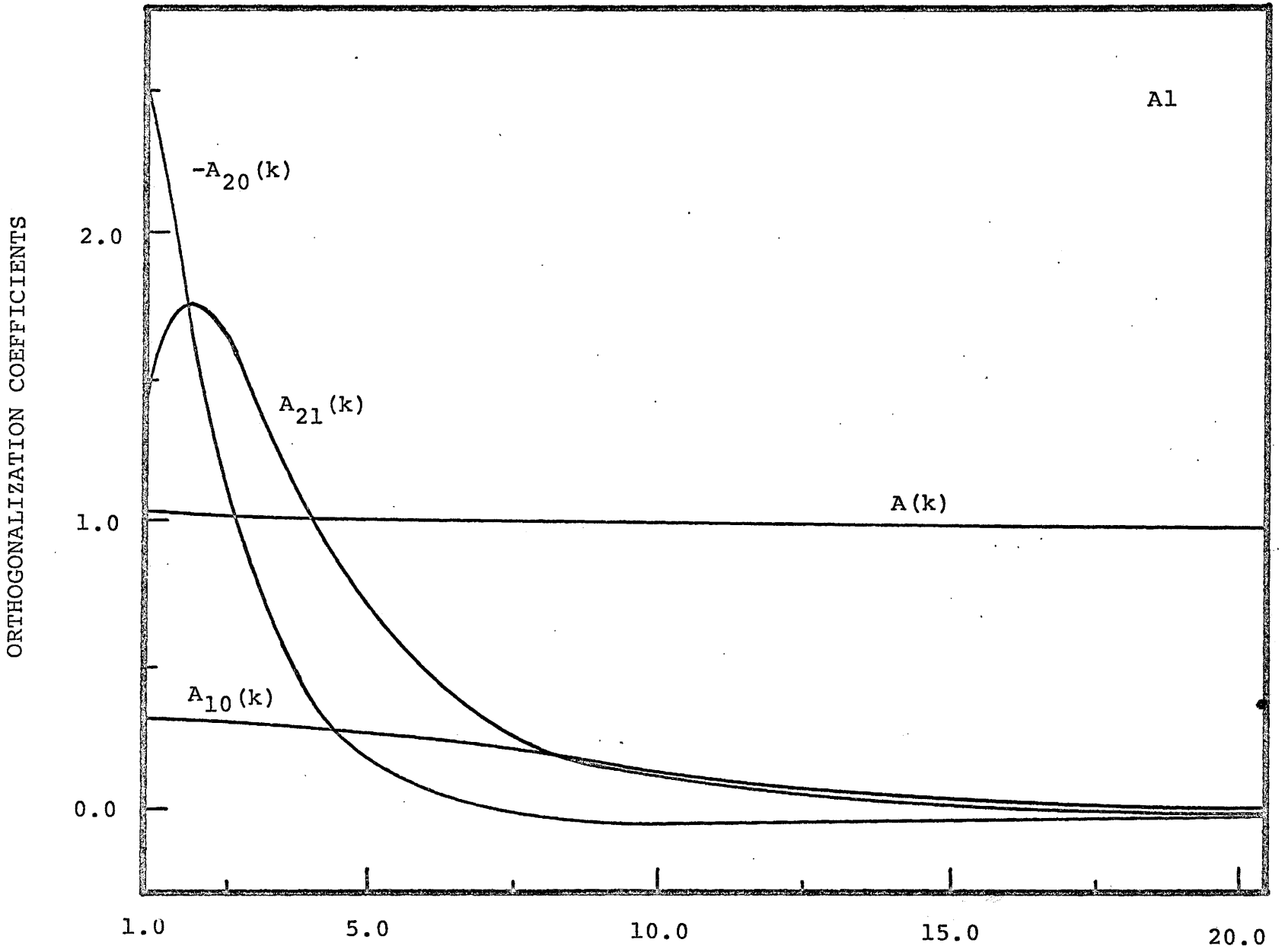
Al
$-A_{20}(k)$
$A_{21}(k)$
A(k)
$A_{10}(k)$
2.0
1.0
0.0
1.0
5.0
10.0
15.0
20.0
ORTHOGONALIZATION COEFFICIENTS
MOMENTUM IN UNITS OF THE FERMI MOMENTUM

FIGURE 3

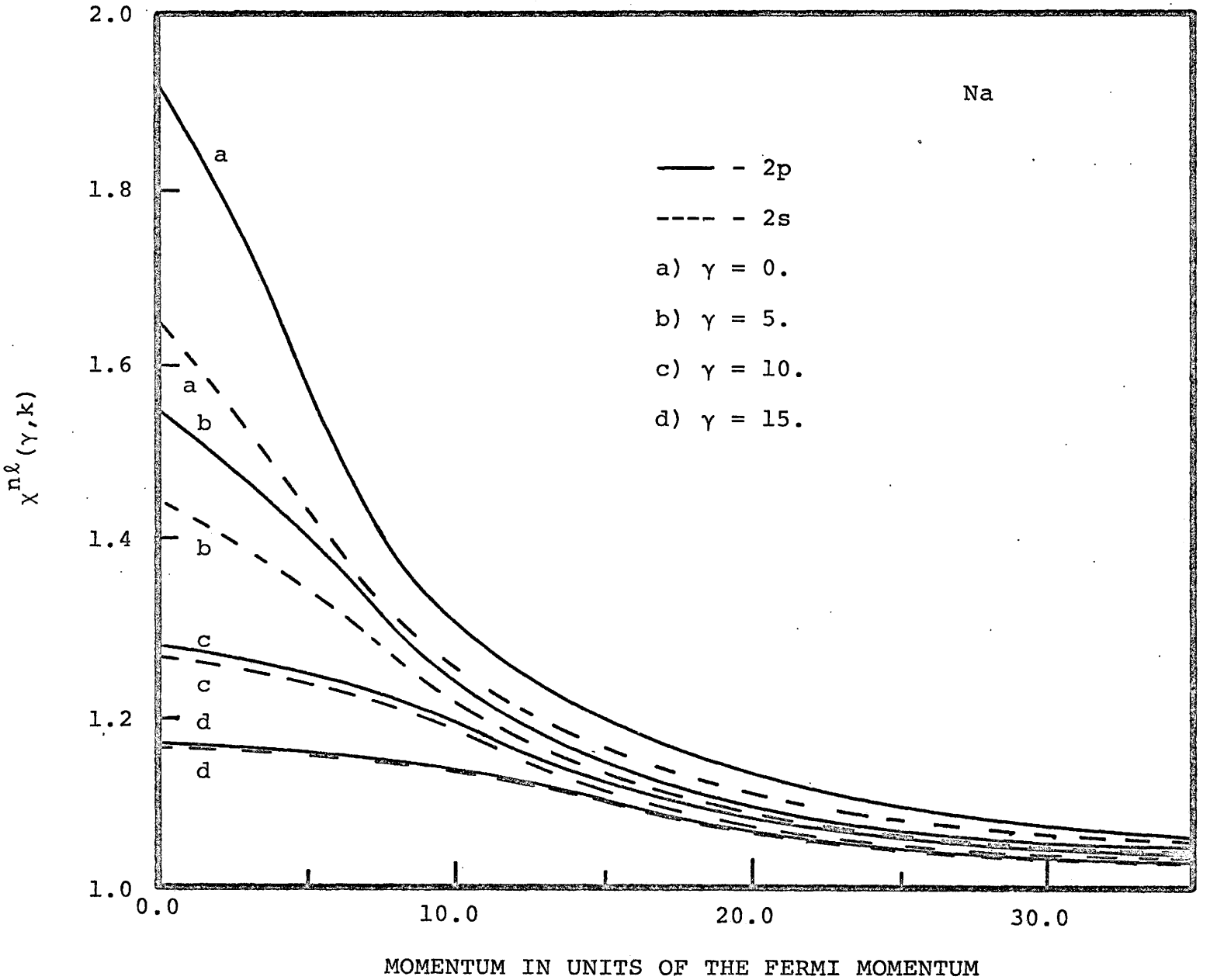
Na
—— - 2p
---- - 2s
a) γ = 0.
b) γ = 5.
c) γ = 10.
d) γ = 15.
$\chi^{n\ell}(\gamma,k)$
2.0
1.8
1.6
1.4
1.2
1.0
0.0
10.0
20.0
30.0
MOMENTUM IN UNITS OF THE FERMI MOMENTUM

FIGURE 4

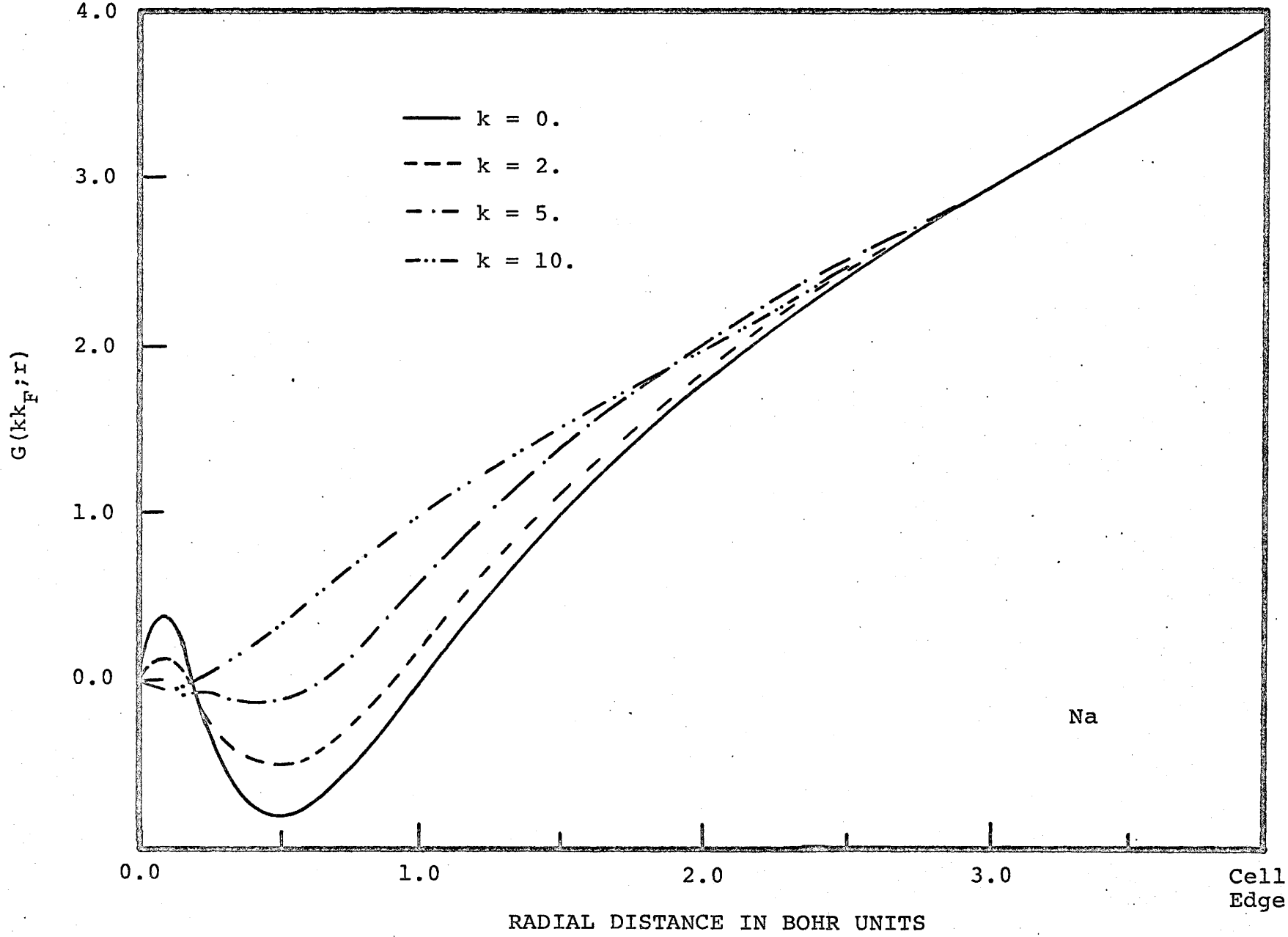
4.0
3.0
2.0
1.0
0.0
k = 0.
k = 2.
k = 5.
k = 10.
Na
G(kk_F;r)
0.0
1.0
2.0
3.0
Cell Edge
RADIAL DISTANCE IN BOHR UNITS

FIGURE 5

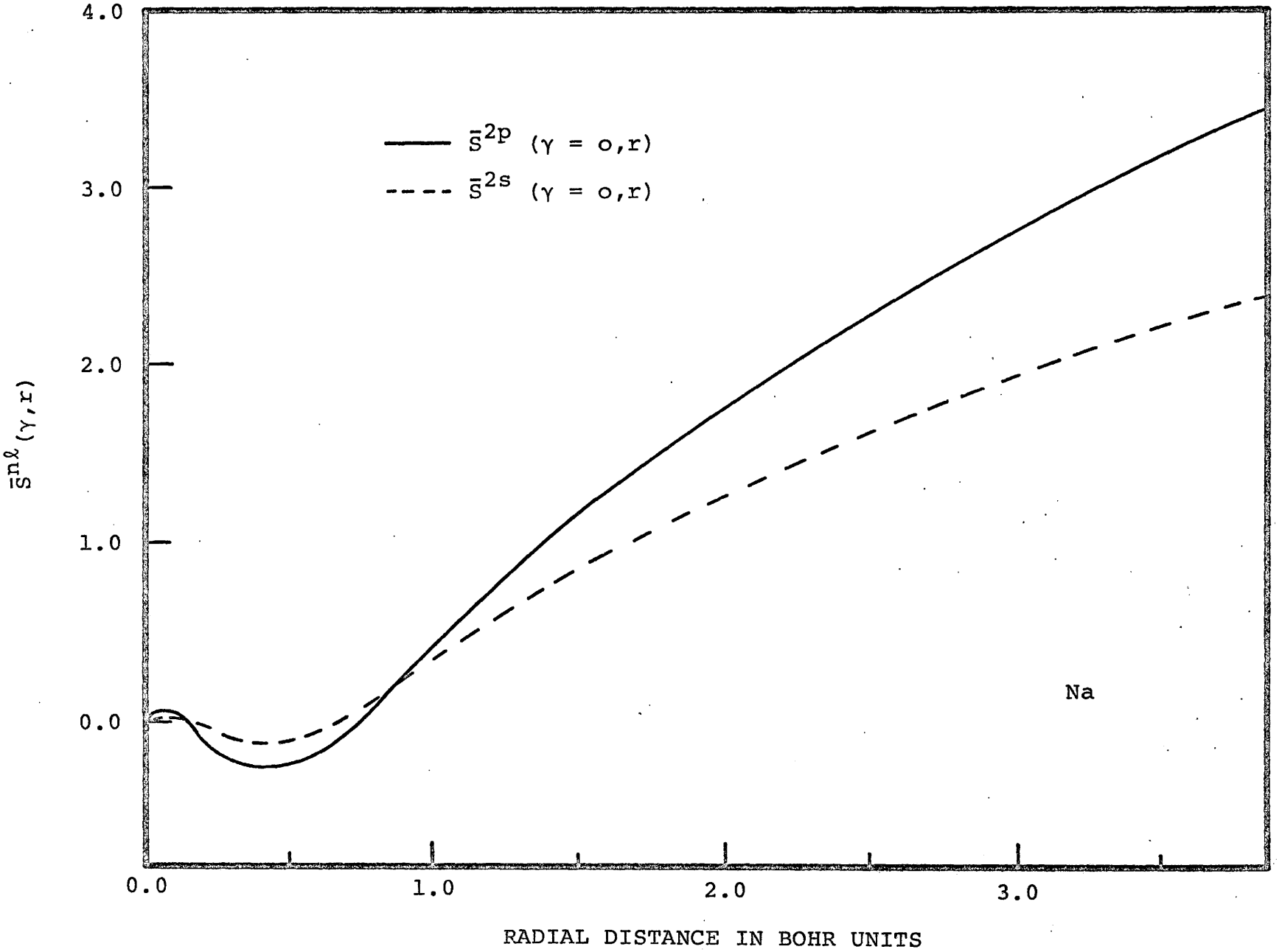
4.0
3.0
2.0
1.0
0.0
$\bar{s}^{2p}$ (γ = o,r)
$\bar{s}^{2s}$ (γ = o,r)
Na
$\bar{s}^{n\ell}(\gamma,r)$
0.0
1.0
2.0
3.0
RADIAL DISTANCE IN BOHR UNITS

FIGURE 6

FIGURE 7

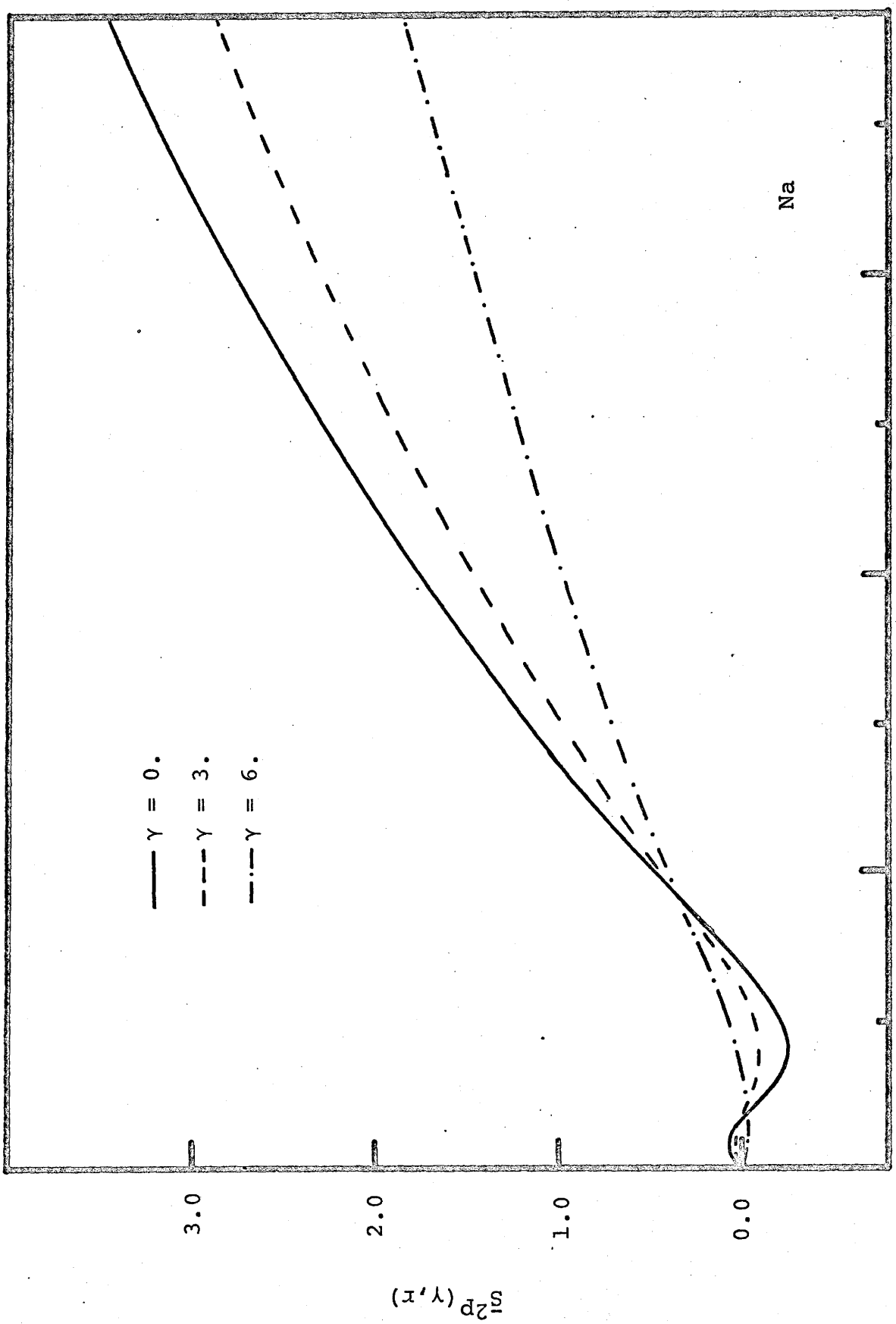

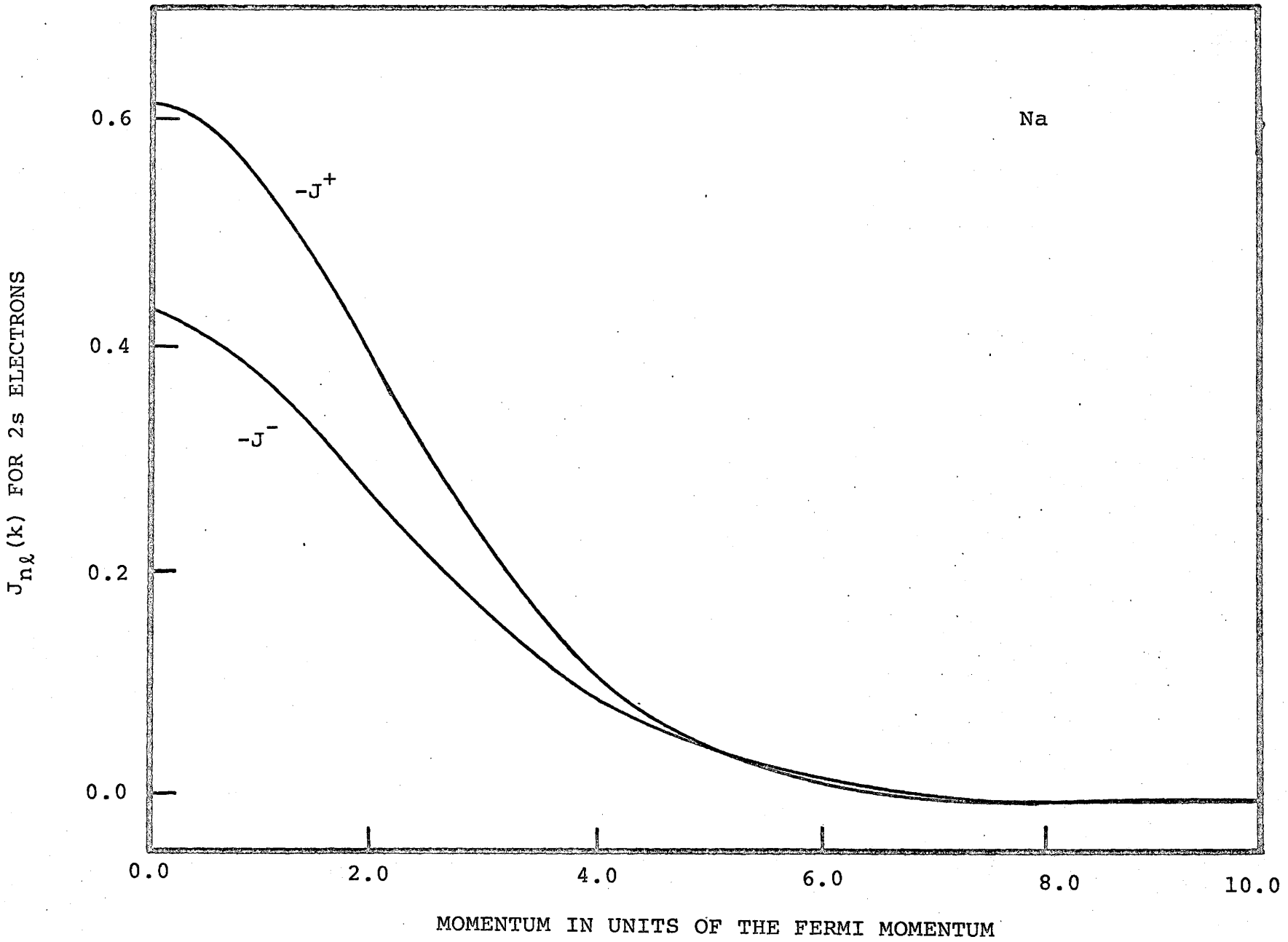
Na
$-J^+$
$-J^-$
0.6
0.4
0.2
0.0
0.0
2.0
4.0
6.0
8.0
10.0
$J_{n\ell}(k)$ FOR 2s ELECTRONS
MOMENTUM IN UNITS OF THE FERMI MOMENTUM

FIGURE 8

FIGURE 9

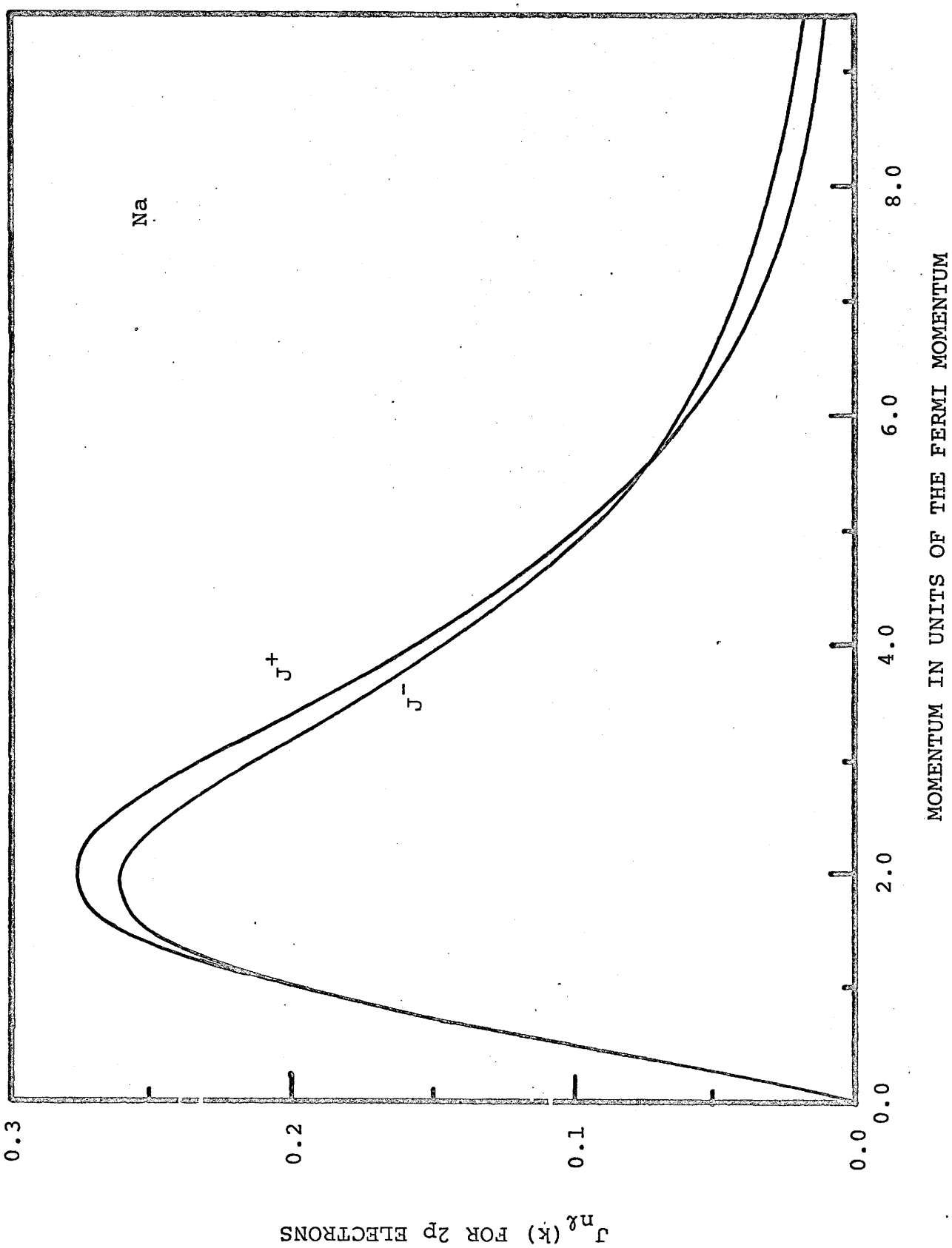
Na
J^+
J^-
0.3
0.2
0.1
0.0
0.0
2.0
4.0
6.0
8.0
$J_{n\ell}(k)$ FOR 2p ELECTRONS
MOMENTUM IN UNITS OF THE FERMI MOMENTUM

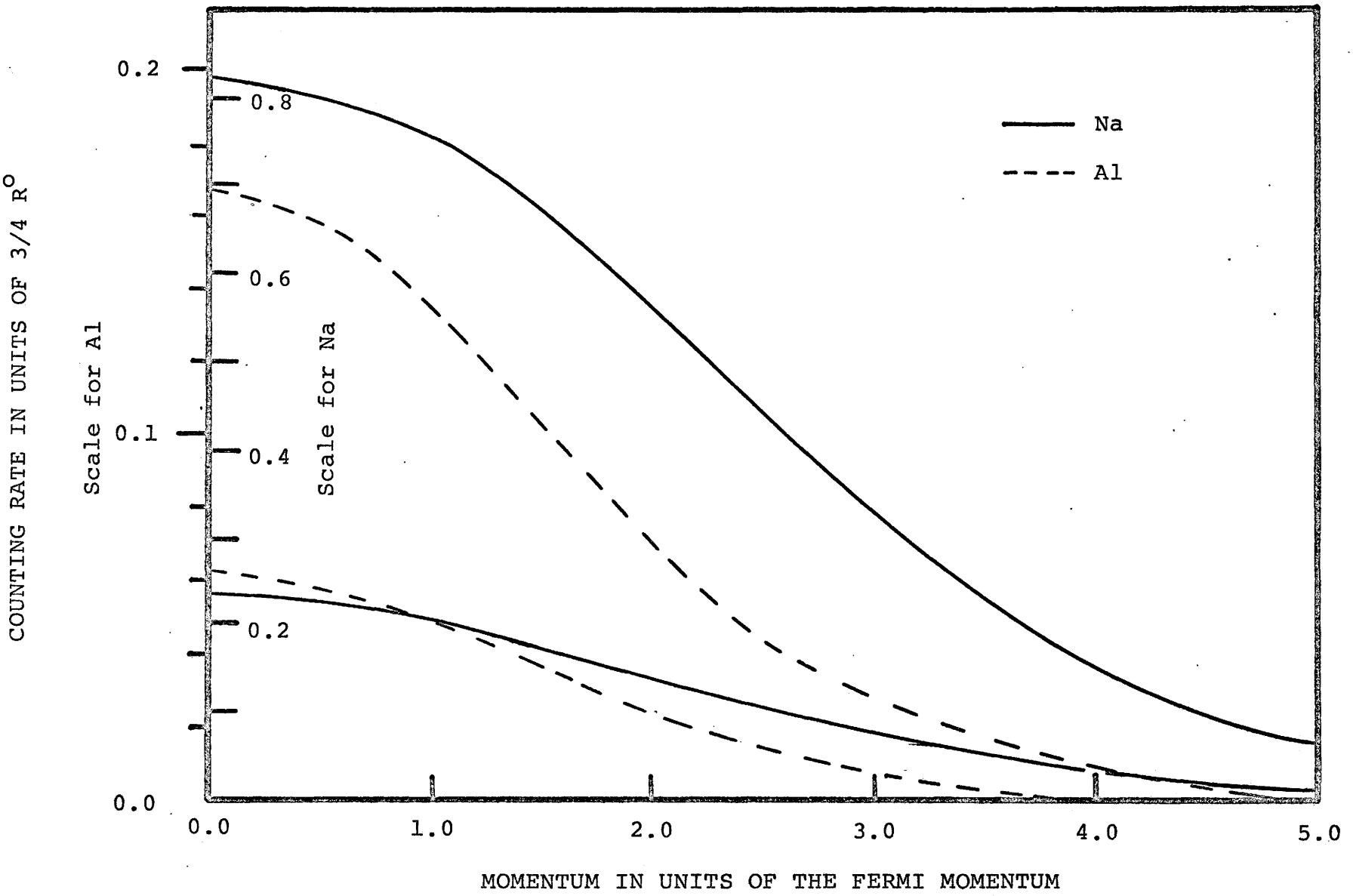
COUNTING RATE IN UNITS OF 3/4 R°
Scale for Al
Scale for Na
0.2
0.1
0.0
0.8
0.6
0.4
0.2
Na
Al
0.0
1.0
2.0
3.0
4.0
5.0
MOMENTUM IN UNITS OF THE FERMI MOMENTUM

FIGURE 10

FIGURE 11

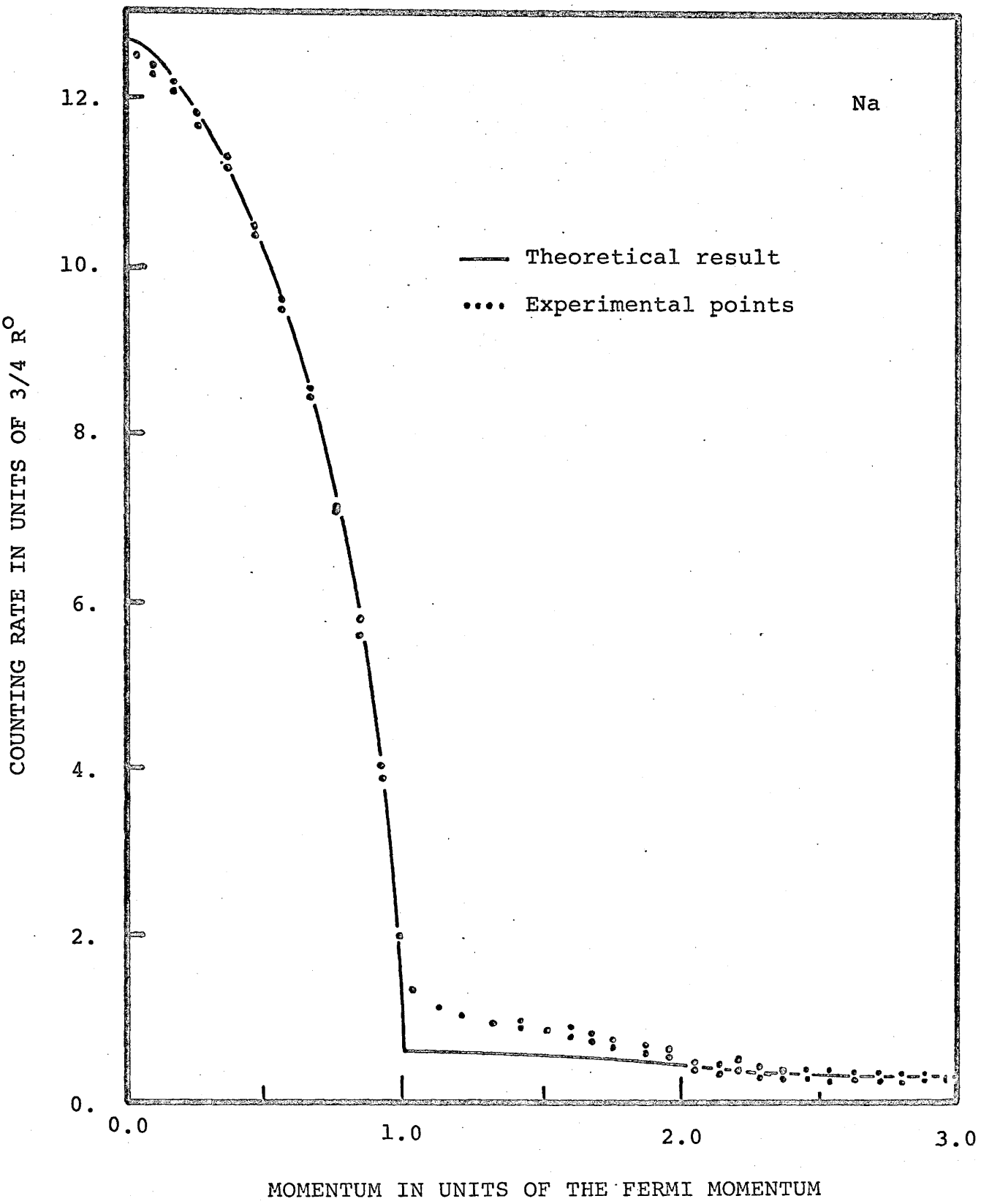
Na
Theoretical result
Experimental points
COUNTING RATE IN UNITS OF 3/4 R°
0.
2.
4.
6.
8.
10.
12.
0.0
1.0
2.0
3.0
MOMENTUM IN UNITS OF THE FERMI MOMENTUM

FIGURE 12

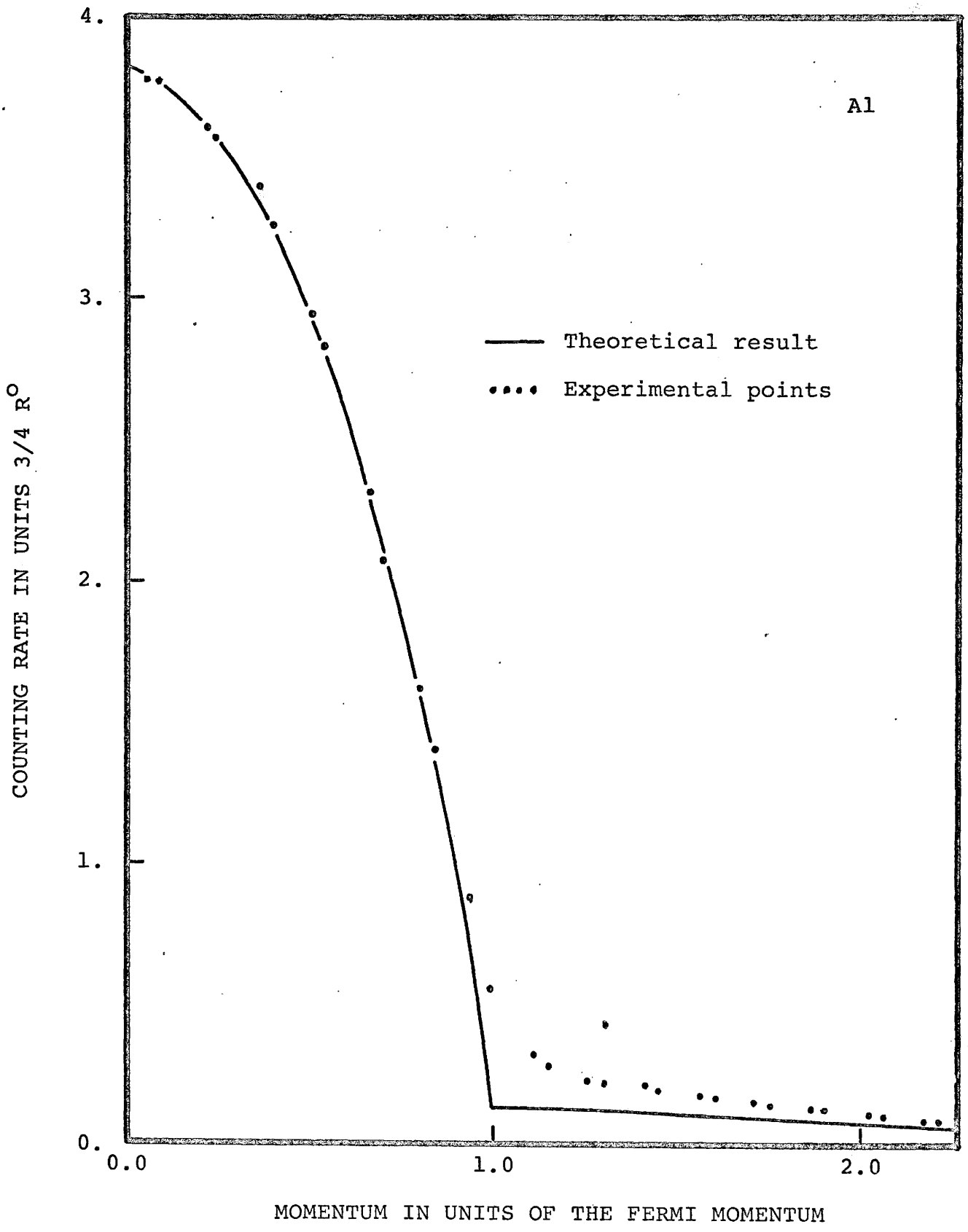
4.
3.
2.
1.
0.
Al
Theoretical result
Experimental points
COUNTING RATE IN UNITS 3/4 R°
0.0
1.0
2.0
MOMENTUM IN UNITS OF THE FERMI MOMENTUM

RECIPROCAL TRANSFORM OF THE O.P.W.-POSITRON OVERLAP WAVEFUNCTION
1.0
0.0
-.02
-.04
-.06
Na
+ x = 0.
X x = 5.
O x = 10.
0
2
4
6
8
10
12
SHELL NUMBER

FIGURE 13

FIGURE 14

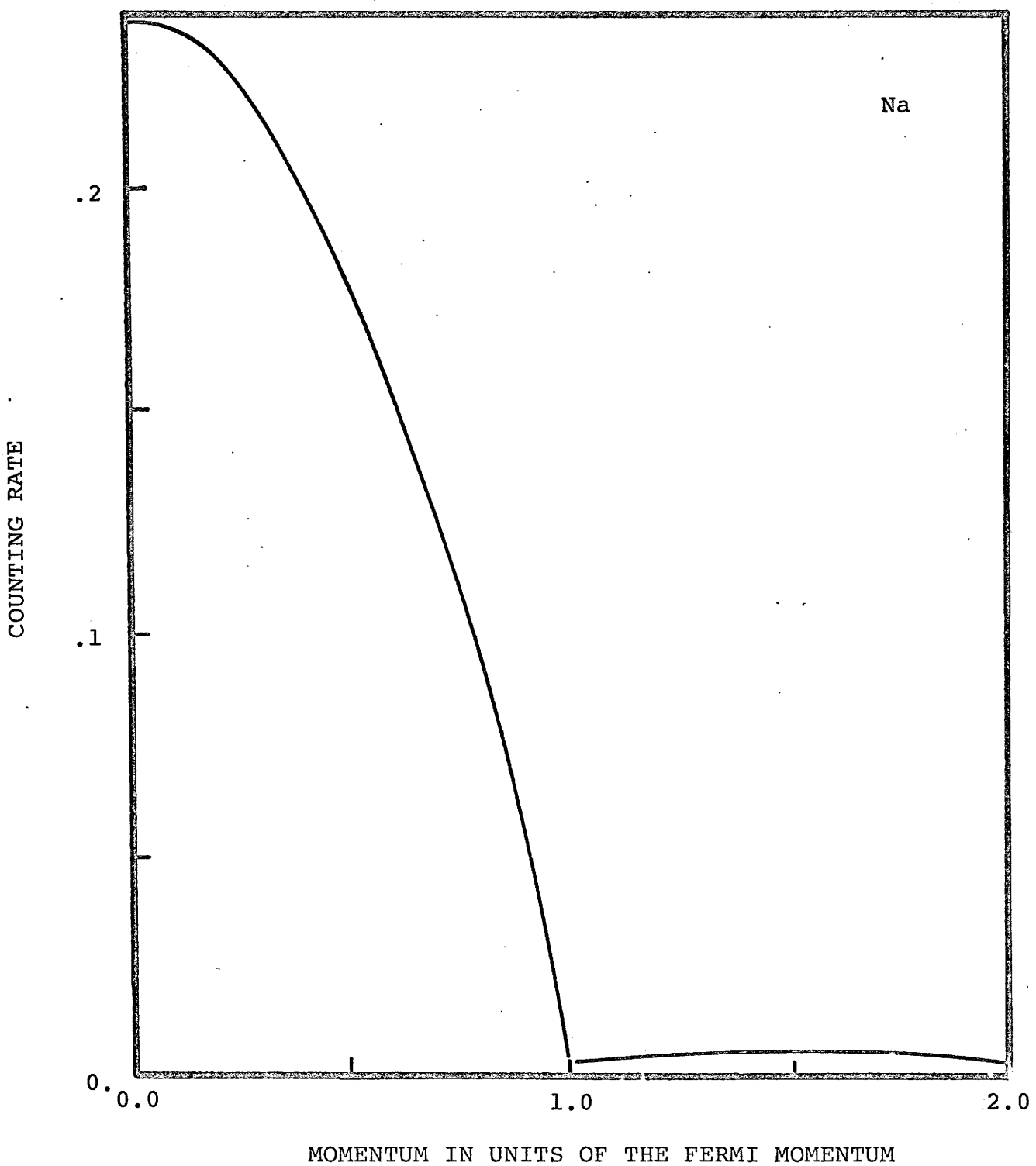
Na
.2
.1
0.
0.0
1.0
2.0
COUNTING RATE
MOMENTUM IN UNITS OF THE FERMI MOMENTUM

FIGURE 15

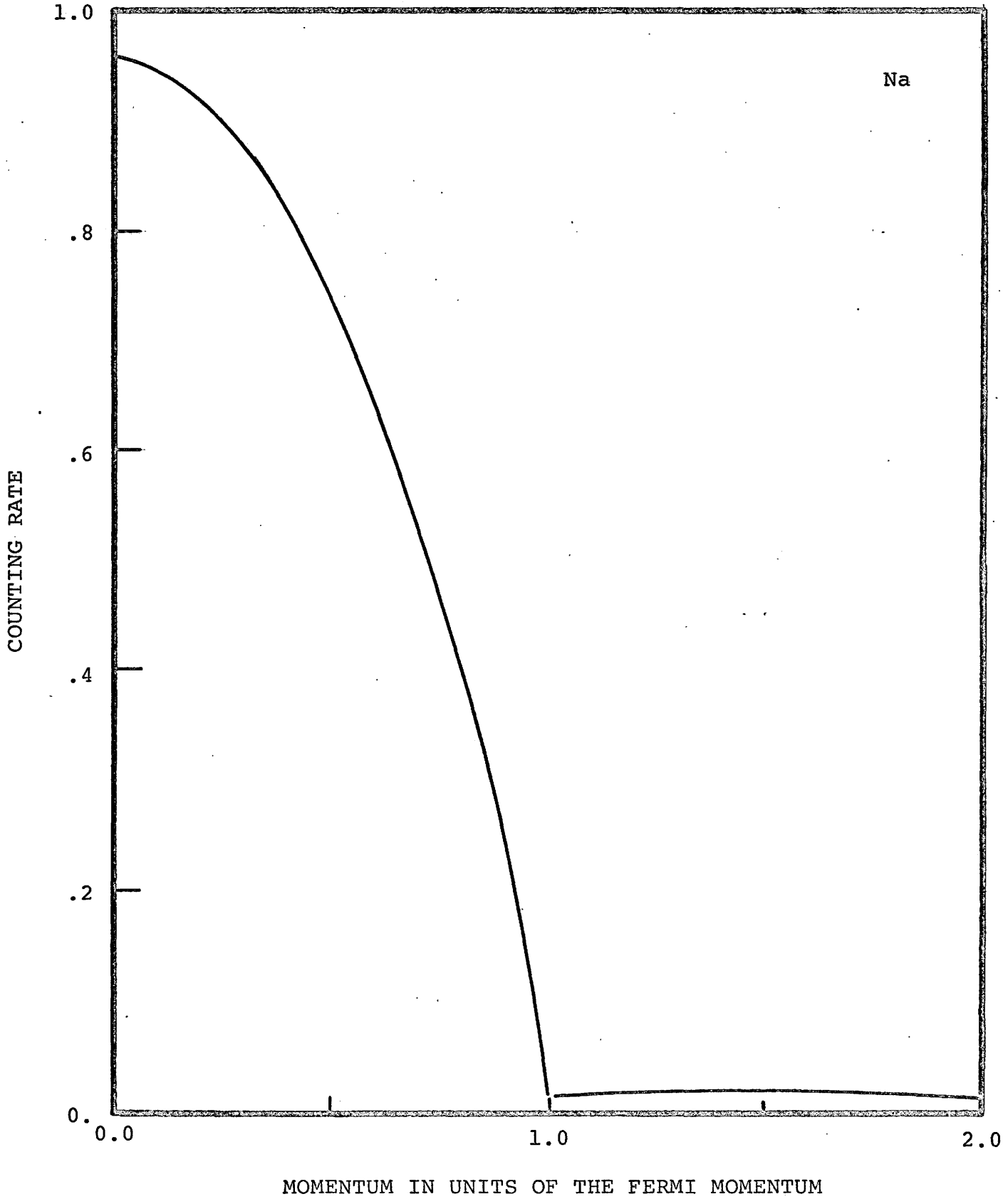
1.0
.8
.6
.4
.2
0.
Na
COUNTING RATE
0.0
1.0
2.0
MOMENTUM IN UNITS OF THE FERMI MOMENTUM

FIGURE 16

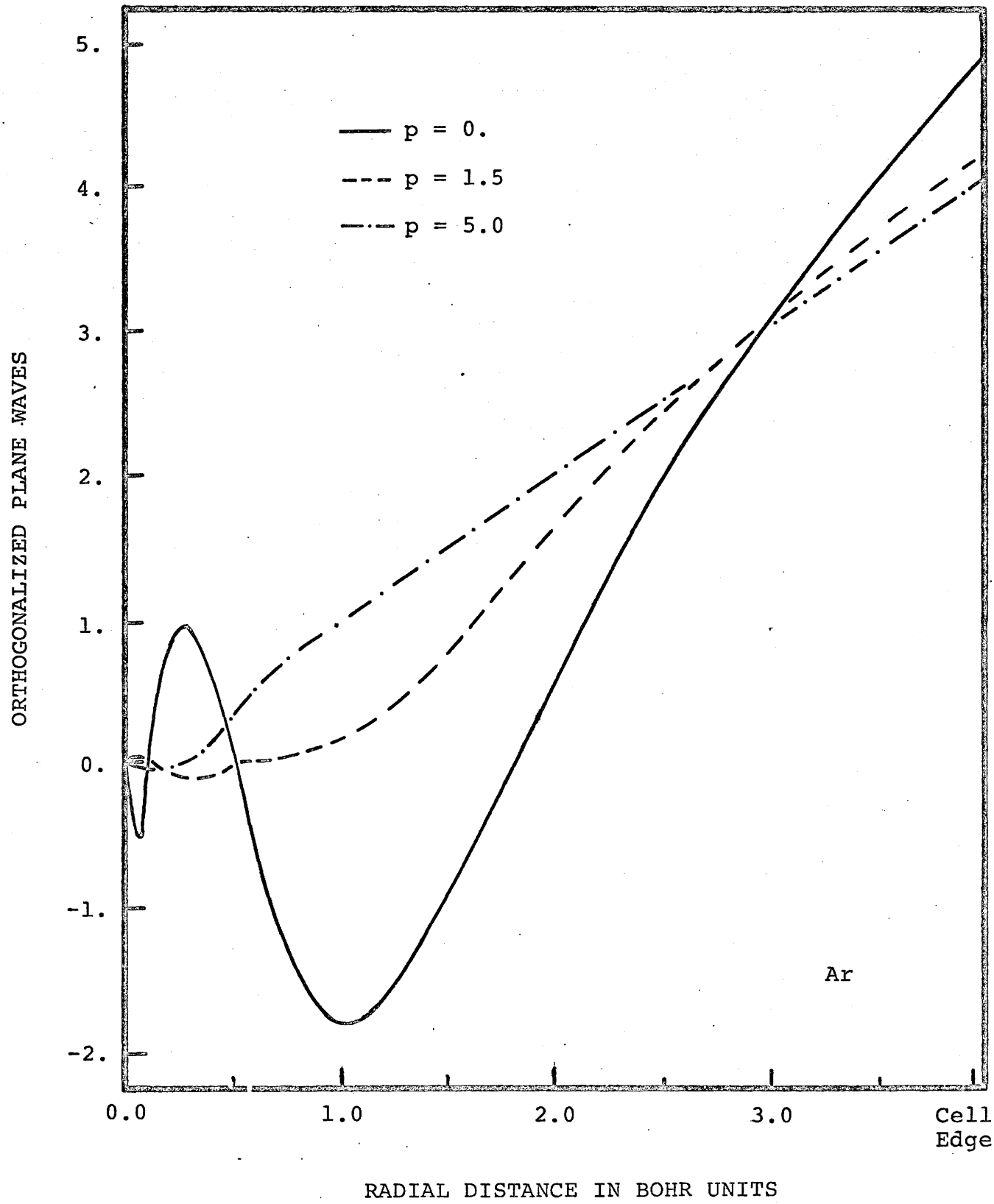
5.
4.
3.
2.
1.
0.
-1.
-2.
p = 0.
p = 1.5
p = 5.0
Ar
0.0
1.0
2.0
3.0
Cell Edge
ORTHOGONALIZED PLANE WAVES
RADIAL DISTANCE IN BOHR UNITS

FIGURE 17

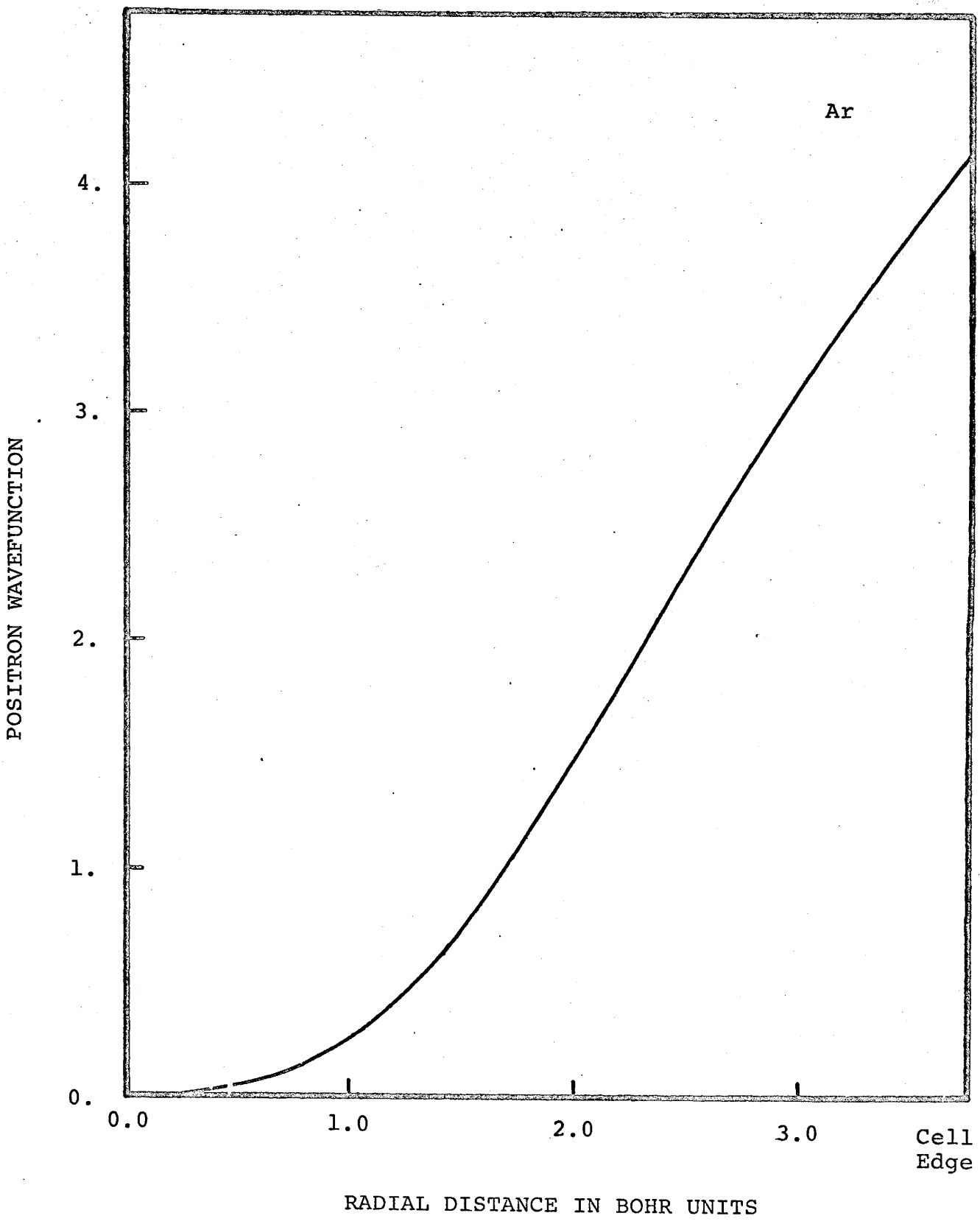
Ar
4.
3.
2.
1.
0.
POSITRON WAVEFUNCTION
0.0
1.0
2.0
3.0
Cell Edge
RADIAL DISTANCE IN BOHR UNITS

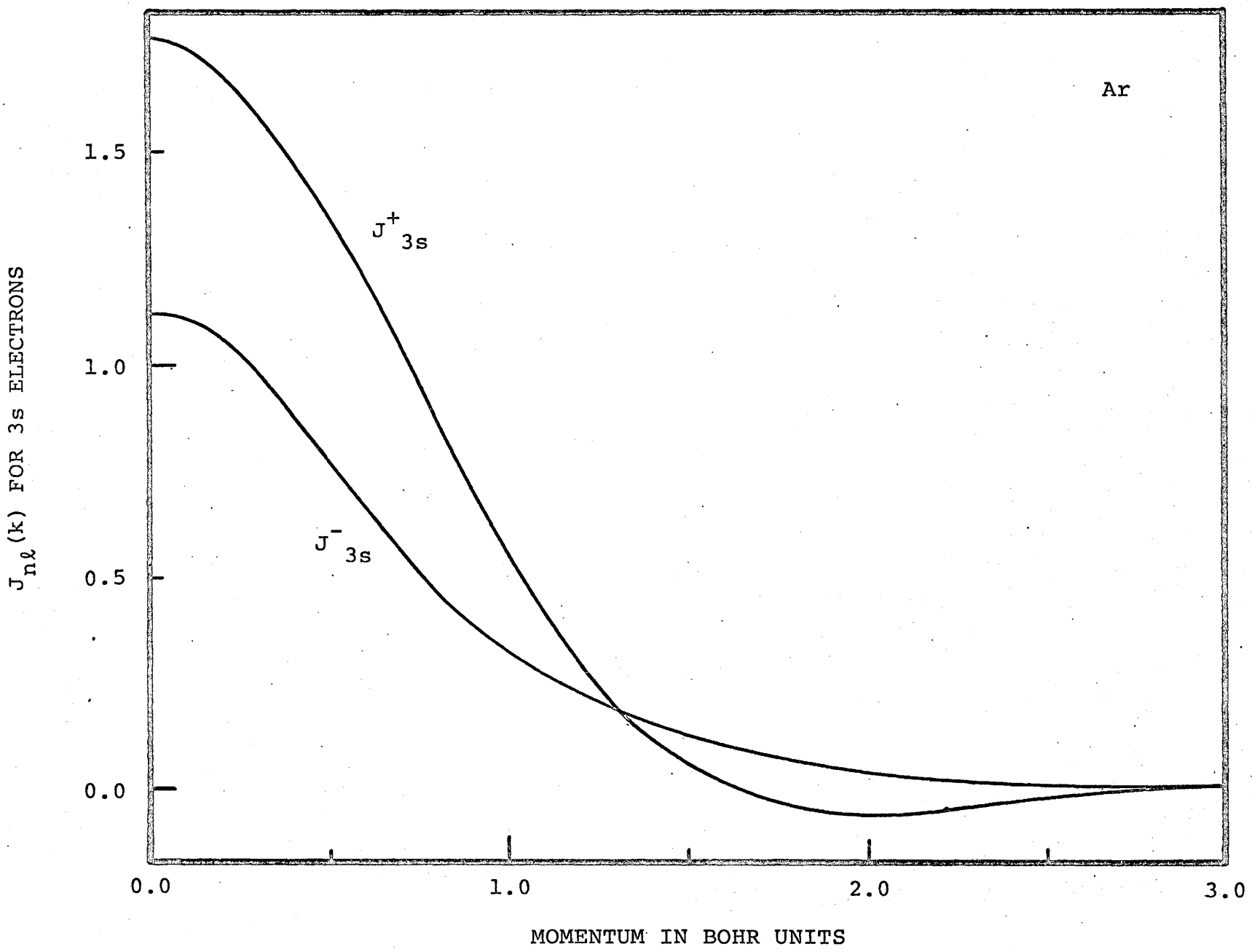
Ar
1.5
1.0
0.5
0.0
J^+_{3s}
J^-_{3s}
$J_{n\ell}(k)$ FOR 3s ELECTRONS
0.0
1.0
2.0
3.0
MOMENTUM IN BOHR UNITS

FIGURE 18

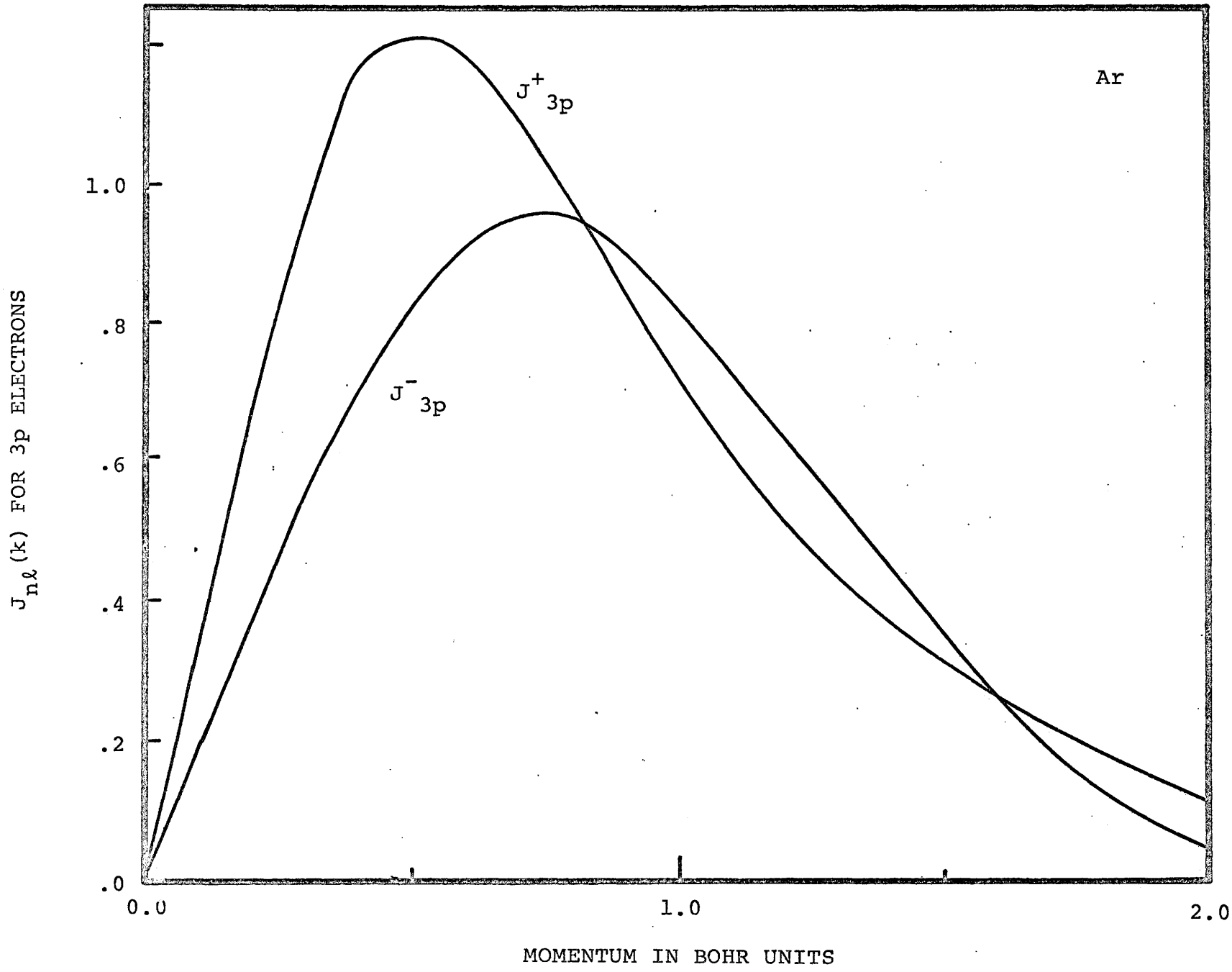
Ar
J^+_{3p}
J^-_{3p}
1.0
.8
.6
.4
.2
.0
0.0
1.0
2.0
$J_{n\ell}(k)$ FOR 3p ELECTRONS
MOMENTUM IN BOHR UNITS

FIGURE 19

FIGURE 20

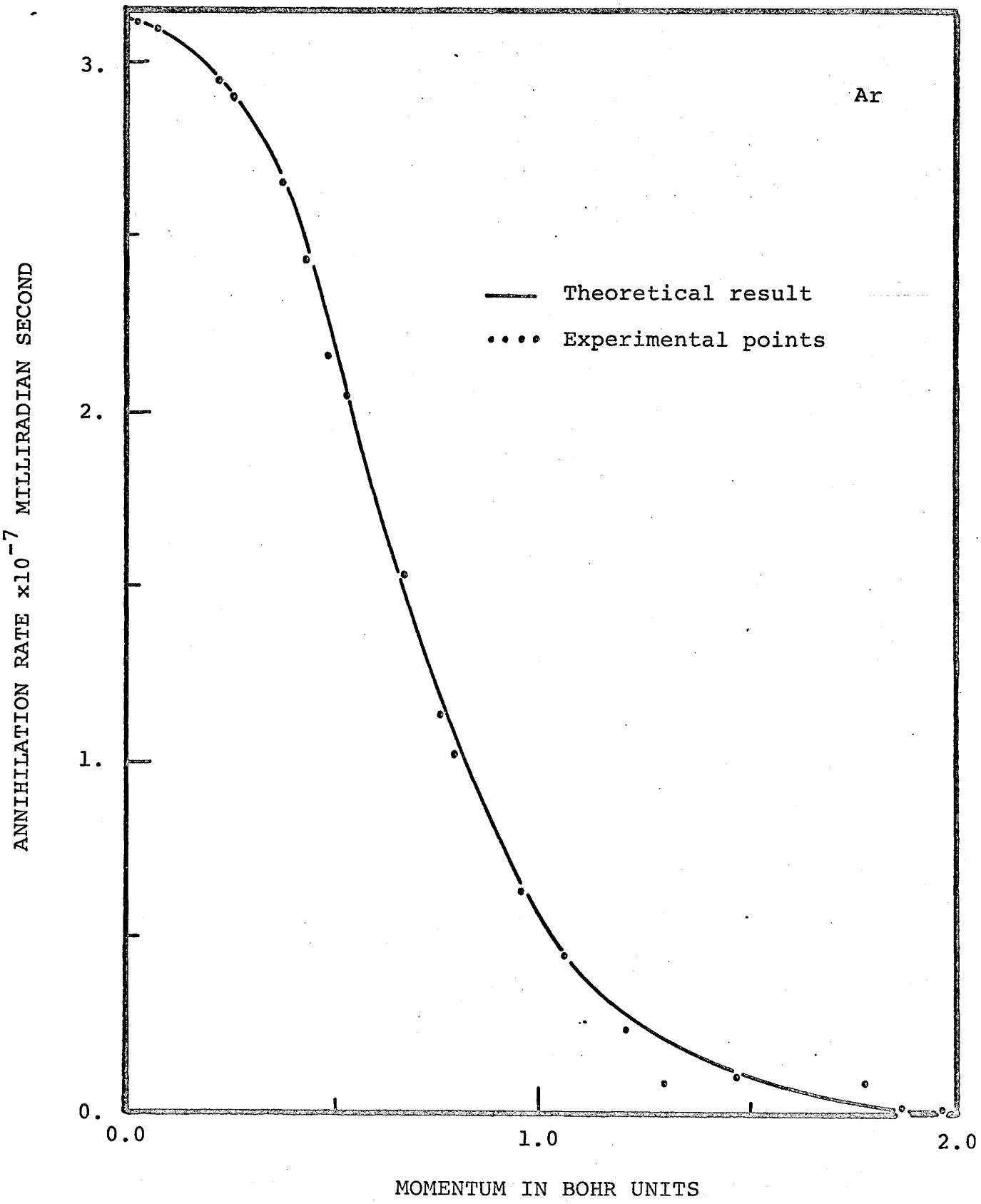
Ar
Theoretical result
Experimental points
ANNIHILATION RATE x10^{-7} MILLIRADIAN SECOND
3.
2.
1.
0.
0.0
1.0
2.0
MOMENTUM IN BOHR UNITS

TABLE 1

The radial core wavefunctions after Taylor[19]

Sodium			Aluminum		
r	P_{2s}	P_{2p}	r	P_{2s}	P_{2p}
0.0000	0.0000	0.0000	0.0000	0.0000	0.0000
0.0149	0.2234	0.0087	0.0094	0.2005	0.0060
0.0299	0.3756	0.0322	0.0188	0.3530	0.0228
0.0498	0.4915	0.0805	0.0282	0.4644	0.0482
0.0796	0.5284	0.1763	0.0377	0.5408	0.0808
0.1095	0.4576	0.2865	0.0565	0.6087	0.1615
0.1592	0.2149	0.4749	0.0753	0.5915	0.2559
0.2189	-0.1410	0.6785	0.0941	0.5156	0.3569
0.2787	-0.4732	0.8409	0.1130	0.4008	0.4597
0.3981	-0.9405	1.0362	0.1883	-0.1997	0.8314
0.5175	-1.1470	1.0935	0.2636	-0.7386	1.0871
0.6768	-1.1569	1.0416	0.3389	-1.0948	1.2227
0.9156	-0.9321	0.8529	0.4895	-1.3281	1.2375
1.1545	-0.6642	0.6483	0.7154	-1.0887	0.9766
1.5525	-0.3340	0.3792	0.8660	-0.8384	0.7696
2.0303	-0.1330	0.1867	1.1672	-0.4325	0.4341
2.5080	-0.0503	0.0887	1.7697	-0.0898	0.1147
3.4634	-0.0068	0.0193	2.3721	-0.0164	0.0275
4.4188	-0.0009	0.0041	3.5770	-0.0005	0.0015
5.6927	-0.0000	0.0000	4.7819	-0.0000	0.0000

TABLE 2

Reciprocal Transforms

a	$f_{oo}(a)$	g(a)	$\omega_o(a)$
0.00000	1.00000	1.00000	0.98531
1.11044	-0.03490	-0.07635	-0.06752
1.57040	-0.01396	-0.01854	-0.02688
1.92334	-0.00220	-0.00041	-0.01075
2.22088	0.00448	0.00274	-0.00494
2.48302	0.00820	0.00160	-0.00296
2.72001	0.01014	0.00016	-0.00212
2.93795	0.01100	-0.00057	-0.00151
3.14080	0.01119	-0.00065	-0.00092
3.33132	0.01098	-0.00039	-0.00039
3.51152	0.01054	-0.00007	0.00002
3.68291	0.00996	0.00017	0.00030
3.84668	0.00932	0.00028	0.00044
4.00375	0.00864	0.00027	0.00050
4.30072	0.00729	0.00009	0.00046
4.44176	0.00663	-0.00001	0.00043
4.57846	0.00600	-0.00007	0.00041
4.71120	0.00541	-0.00010	0.00040
4.84030	0.00585	-0.00009	0.00040
4.96604	0.00434	-0.00006	0.00041
5.08868	0.00387	-0.00003	0.00042
5.20843	0.00345	0.00002	0.00042
5.32549	0.00305	0.00005	0.00041
5.44002	0.00269	0.00007	0.00040
5.55220	0.00237	0.00009	0.00039

TABLE 3

Matrix elements of the integral (2-27)

c ↓ \ b →											
	.978	.680	.522	.444	.430	.380	.359	.330	.331	.317	.279	.267
	.896	.582	.504	.471	.382	.381	.328	.342	.307	.314	.268	.281
	.819	.613	.437	.401	.406	.330	.324	.294	.320	.307	.249	.276
	.755	.516	.444	.451	.352	.345	.300	.319	.283	.291	.250	.292
	.732	.494	.463	.476	.339	.368	.298	.345	.283	.304	.255	.291
	.688	.619	.470	.377	.444	.345	.381	.293	.310	.267	.297	.233
	.673	.646	.408	.337	.464	.306	.355	.264	.347	.294	.253	.238
	.621	.441	.407	.444	.312	.331	.273	.317	.260	.279	.237	.298
	.612	.579	.423	.352	.440	.316	.368	.271	.302	.254	.285	.231
	.646	.531	.443	.369	.379	.365	.327	.320	.380	.415	.246	.245
	.543	.433	.340	.348	.319	.271	.261	.252	.257	.255	.213	.285
	.588	.491	.385	.339	.359	.317	.298	.285	.355	.383	.223	.249

BIBLIOGRAPHY

1. Anderson,C.D., Science 76, 238 (1932).
2. Dirac,P.A.M., Proc. Cambridge Phil. Soc. 26, 361 (1930).
3. Beringer,R., and Montgomery,C.G., Phys. Rev. 61, 222 (1942).
4. Stewart,A.T., Proc. of the Positron annihilation conference Academic Press,New York (1967).
5. Wallace,P.R., in Solid State Physics 10, Academic Press, New York (1960).
6. Ferrell,R.A., Rev. Mod. Phys. 28, 308 (1956).
7. Lee-Whiting,G.E., Phys. Rev. 97, 1557 (1955).
8. Carbotte,J.P., and Arora,H.L., Can. Jour. Phys. 45, 387 (1967).
9. e.g. Stewart,A.T., and Green,R.E., Phys. Rev. 98, 232 (1955); ibid 486 (1955); Gustafson,D.R., Mackintosh,A.R., Zaffarano,D.J., Phys. Rev. 130, 1455 (1963).
10. Bell,R.E., and Jørgensen,M.H., Can. Jour. Phys. 38, 652 (1960).
11. Berko,S., and Plaskett,J.S., Phys. Rev. 112, 1877 (1958).
12. Carbotte,J.P., Phys. Rev. 155, 197 (1967).
13. Kahana,S., Phys. Rev. 129, 1622 (1963).
14. Carbotte,J.P., Ph.D. Thesis McGill (unpublished); also Carbotte,J.P., and Kahana,S., Phys. Rev. 139, A213 (1965).
15. Bergersen,B., Ph.D. Thesis Brandeis University (1964) unpublished.
16. Berko,S., Phys. Rev. 128, 2166 (1962).
17. Carbotte,J.P., Phys. Rev. 144, 309 (1966).

18. For the details in deriving these formulae cf the first of ref. 13.

19. Taylor,R., Ph.D. Thesis McMaster (1966).

20. Hartree,D.R., and Hartree,W., Proc. Roy. Soc. (London) A166, 450 (1938).

21. For a complete review of the O.P.W. method and its applications see Woodruff,T.O., The Orthogonalized Plane-Wave Method, Solid State Physics 4, 367 (1965).

22. Herman,F., and Skillman,S., Atomic Structure Calculations, Prentice-Hall Inc. (1963).

23. Values for these parameters may be obtained in Bearden,J.A., and Burr,A.F., Rev. Mod. Phys. 39,(1967).

24. Callaway,J., Phys. Rev. 123, 1255 (1961).

25. Carbotte,J.P., and Salvadori,A., Phys. Rev. 162, 290 (1967).

26. Berko,S., and Terrell,J.H., Optical properties and electronic structure of metals and alloys, Abeles,F., editor, John Wiley and Sons, Inc. (1966) Page 210.

27. Woll, E.J., and Rose,K.L., Phys. Rev. 145, 268 (1966).

28. McKenzie,I., (private communication).

29. Only the central parabola was used in the least-square fit. This was thought to be the most reasonable procedure since lattice effects in the conduction-electron gas not included in the theoretical curves must certainly make an additive contribution in the tails. The comparison is therefore not unambiguous and the agreement can be changed somewhat by using a different criterion for the least-squares fit.

30. Kim,S.M., and Stewart,A.T., (private communication).

31. These results are presented in figure 4 of an article by Terrell,J.H., Weisberg,H.L. and Berko,S., Proc. of Positron annihilation converence Academic Press, New York (1967).

32. Kusmiss,J.H., and Stewart,A.T., (private communication).

33. A further argument to justify this will be pointed out later.

34. Hammersley,J.M., and Handscomb,A., Monte Carlo Methods, Methuen and Co., Page 55.

35. Rose,K., and DeBenedetti,S., Phys. Rev. 138, A927 (1965).

36. Figure 5 of reference 27.

37. Liu,D.C., and Roberts,W.K., Phys. Rev. 132, 1633 (1963).

38. Berko,S., and Erskine,J.C., Phys. Rev. Letters 19, 307 (1967).

39. MacKenzie,I.K., McKee,B.T.A., and Bird,A.M.B., Phys. Rev. Letters (in press).